

1.0 INTRODUCTION

The “Maurepas” is an extensive zone of second-growth swamp forest that surrounds Lake Maurepas in the upper reaches of the Pontchartrain estuary. This estuary occupies a deltaic basin between the Mississippi River and Pleistocene age uplands north of New Orleans in Louisiana (Figure 1.1). Although it is tidally influenced, the swamp ecosystem is dominated by cypress (*Taxodium distichum*) and tupelo (*Nyssa aquatica*) with little tolerance for prolonged exposure to estuarine salinity. The Maurepas swamp ecosystem has been profoundly affected over the past 200 years by artificial levee building to contain the Mississippi River and by clear-cutting of the virgin cypress forest. Now, it is facing new threats from sea level rise and the increased severity of salt water intrusion that has accompanied that rise (Lee Wilson & Assoc. 2001). Here, we discuss investigations conducted by researchers at Louisiana State University (LSU) between April 2002 and May 2004 to support design of an artificial diversion project that will reconnect the Mississippi River in a controlled way with 20,000 ha of the Maurepas lying south of the lake (Figure 1.2). It is a continuation of reconnaissance work conducted in 2000 and 2001 (Lee Wilson & Assoc. 2001). Planning has focused on a gated diversion in the vicinity of Garyville with a maximum discharge capacity of between 1,500 and 2,500 cubic feet per second (cfs) (Lee Wilson & Assoc. 2001). Mississippi River water would enter the swamp south of Lake Maurepas through a small existing channel optimistically named Hope Canal (Figure 1.2).

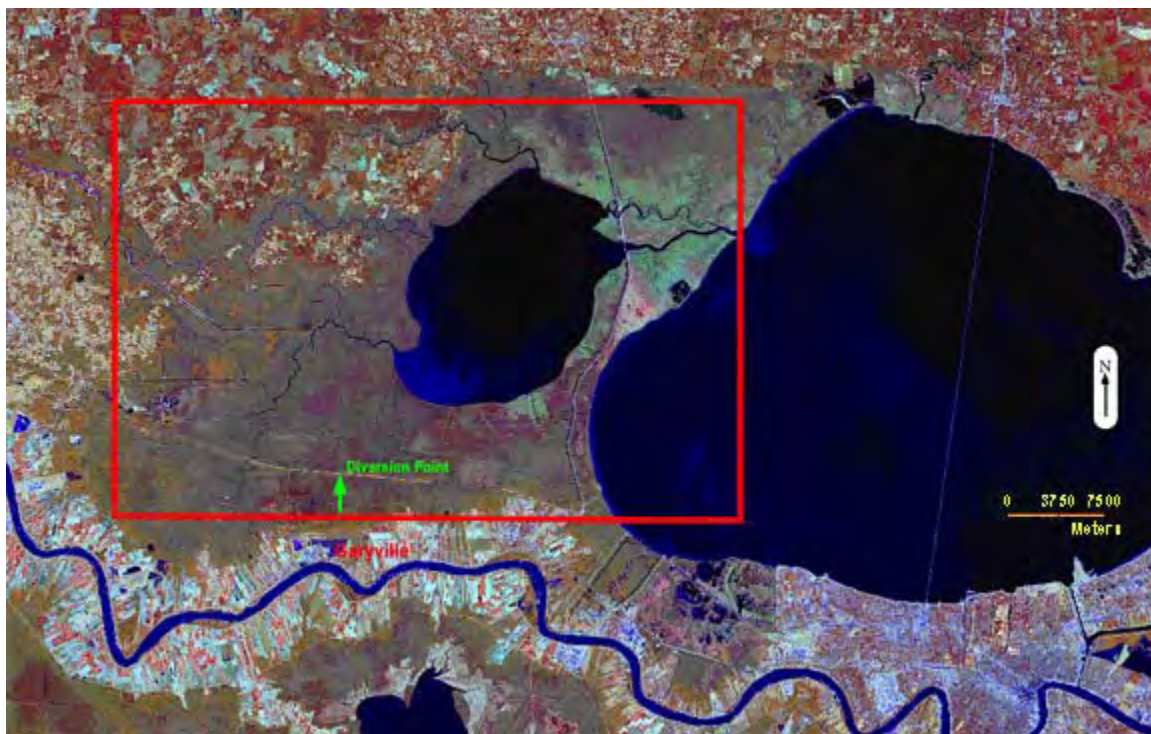


Figure 1.1 Pontchartrain Basin showing location of the Maurepas study area



Figure 1.2 Proposed alignment for a diversion at Hope Canal

Engineering design work (Phase 1) for the Maurepas Project was authorized in July 2001 under the Coastal Wetlands Planning, Protection and Restoration Act (CWPPRA). The project has since been jointly managed by the U.S. Environmental Protection Agency (EPA) and the Louisiana Department of Natural Resources (LDNR). After a one-year hiatus, EPA approved continuation of ecologically oriented investigations at Southeastern Louisiana University (SLU) as well as the LSU work discussed here in mid-2002. Another year later, LDNR contracted with the URS Corporation (URS) in mid-2003 for more traditional engineering design services, and with LSU for additional gaging stations. SLU completed its characterization of the ecosystem health of the Maurepas swamp last year (Shaffer et al. 2003). The LSU project was extended at no cost to provide technical continuity between the original project team and later participants. This LSU report is the second to be finished under the Phase 1 authorization.

1.1 Study Objectives

The investigations reported here have four objectives:

- (1) Establish a representative baseline of pre-diversion water quality for suspended sediments, salinity, nitrogen, phosphorus and chlorophyll *a* by repeating a monthly synoptic water quality sampling program conducted originally during the drought period of April 2000 to June 2001 for a more normal rainfall period and for the full year from April 2002 to May 2003.

- (2) Acquire hydrographic information in the Maurepas sufficient to calibrate and validate hydrodynamic models constructed for complementary purposes by LSU and URS.
- (3) Construct, calibrate and validate hydrodynamic and water quality models for the Maurepas with sufficient resolution to capture those processes important to swamp enhancement and sustainability that will be affected by the proposed diversion.
- (4) Develop model-based techniques for predicting long-term ecological benefits and impacts of the Maurepas diversion to the swamp and lake.

1.2 River Diversion Science

Spring crevassing and overbank flooding were critical to the formation and maintenance of the Mississippi delta wetlands prior to construction of artificial levees (Viosca, 1928; Hatton et al., 1983; Kesel, 1988; Kesel, 1989; Day et al., 2000). These floods provided a source of mineral sediments, which contribute directly to vertical accretion of wetlands affected by relative sea level rise (RSLR). Nutrients in river water, particularly dissolved inorganic nitrogen, have been shown to further promote vertical accretion and soil aggradation by enhancing root growth and litter production (Delaune et al., 1983, Rybczyk et al. 1998, Rybczyk et al. 2002). Any stimulation of aggradation helps to maintain wetland elevation with respect to sea level and prolongs wetland survival.

RSLR is the sum of the eustatic sea-level rise observed globally (1 to 2 mm yr⁻¹) in the world ocean (Gornitz et al., 1982), and a locally varying land subsidence. The local sinking component is estimated at 3 to 6 mm-y⁻¹ in the Maurepas (Penland and Ramsey 1990, Shaffer et al. 2003).

Although the height and reliability of artificial flood control levees increased through the 19th century, crevasses continued to vex residents by periodically breaching the Mississippi River levees in the vicinity of the Maurepas and elsewhere (Davis 2000). Since the flood of 1927, however, levees constructed by the U.S. Army Corps of Engineers (USACE) have entirely prevented river flooding, and, thus, have severed the Maurepas swamp from nourishment by the River (Mossa, 1996; Boesch et al. 1994).

The purpose of a diversion from the Mississippi River at Garyville is to introduce sufficient sediment and nutrients to increase swamp productivity, tree recruitment and aggradation of organic soils, while reducing the likelihood of severe intrusions of high salinity waters (> 5 ppt) (Lee Wilson & Assoc., 2001; Wilson et al., 2002). Suspended sediments introduced from the Mississippi River freshwater diversions are rapidly trapped in receiving wetlands (Lane et al., 1999; 2001; 2002). Current velocity and competence to transport sediment diminishes abruptly when flow leaves the confined channel and moves into vegetated and quiescent deltaic basins (Gleason et al., 1979).

DeLaune et al. (1979) found the mineral fraction in coastal Louisiana tidal marsh soils to range from 0.2 to 0.4 g cm⁻³, with the remainder of the soil matrix -- and the vast majority of soil volume -- consisting of locally generated organic material from root growth and gas- or water-filled void space. Swamp soils are more organic than those of tidal marshes (Kosters et al. 1987). Shaffer et al. (2003) reported a range of organic matter content in Maurepas swamp soils ranging from 30 to 80 percent, but bulk soil densities were also much lower than for marsh soils, ranging from 0.05 to 0.15 g cm⁻³. This suggests that the Maurepas swamps persist with about half the mineral sediment supply of tidal marshes.

1.2.1 The Nutrient Issue. Since 1990, the USACE has constructed relatively large diversions into wetlands of the Breton Sound (Caernarvon) and Barataria Basins (Davis Pond) downstream of the proposed Maurepas diversion point. A larger flood relief structure closer to the Maurepas at Bonnet Carre has been operated occasionally since the 1930s to shunt flood waters for a month or more at rates up to 300,000 cfs into Lake Pontchartrain. It was most recently operated in 1997. Smaller siphons have been managed on the lower Mississippi since the 1950s for water supply and other purposes (Caffey and Schexnayder, 2002). The Maurepas project is one of many diversions of the Mississippi River water that have been proposed to restore wetlands by mimicking natural overbank events (Chatry and Chew, 1985; Boesch et al., 1994; Day et al., 2000).

Increase in the catch of oysters, saltwater fin fishes and penaeid shrimp have been attributed to other Mississippi River diversions (Gunter, 1953; Chew and Cali, 1981), as well as enhanced productivity and land gain in receiving wetlands (LDNR 2003). Concern remains, however, about the potential to stimulate nuisance or even hazardous algal blooms if diverted river nutrients reach open lakes and bays. Over enrichment can lead to oxygen depletion as is commonly observed in the “dead zone” offshore of the mouths of the Mississippi and Atchafalaya Rivers (Turner and Rabalais, 1991; Rabalais et al., 1994; Dortch et al., 1998). Extensive algal blooms have been documented in Lake Pontchartrain following openings of the Bonnet Carre structure, as well as in other estuaries receiving increased anthropogenic nutrient loads throughout the world (Cedarwall and Elmgren, 1990; Justic et al., 1995; Rosenberg, 1985; Cloern, 2001, Pearl et al., 1998).

When the water is clear enough to allow light penetration, phytoplankton production in estuaries like the Maurepas is usually limited by nitrogen rather than phosphorus, the other critical plant nutrient. Biologically mediated processes tend to selectively remove dissolved inorganic nitrogen more rapidly than dissolved inorganic phosphorus from the water column. These processes include denitrification, the microbial conversion of dissolved nitrate to atmospheric nitrogen, and the preferential sedimentation of nitrogen in zooplankton fecal pellets. Phosphorus, in contrast, tends to be rapidly recycled, undergoing transformations that ultimately return it to the water column (Reddy and Patrick, 1984; Howarth, 1988).

Estuarine phytoplankton production responds primarily to dissolved inorganic nitrogen, which exists as either nitrate (NO_3^-) or ammonium (NH_4^+), because nitrogen is typically more limiting than phosphorus in coastal bays and lagoons. Nitrogen associated with organic particles also contributes to total nitrogen values commonly reported, but nitrogen bound in this way is not readily available for phytoplankton assimilation or growth.

The Mississippi River receives significant inputs of fertilizer nitrogen along with runoff from the mid-west corn-belt, which remains oxidized and available while in the River. More than 90 percent of the dissolved inorganic nitrogen in the Mississippi River water occurs in the form of nitrate. There, concentrations cycle seasonally from 0.75 to 2.0 mg-N L⁻¹ (ppm), peaking in the spring together with discharge (Lane et al. 1999). Nitrate is not taken up or removed from the water column until it leaves the deep, highly oxidized and turbid river setting and moves into clearer lakes and bays or, preferably, into shallow wetland basins characterized by anoxic soils, (Mitsch et al. 2001).

A range of NO_3^- removal rates is reported from estuarine waters, and much of the reduction is generally attributed to denitrification (Khalid and Patrick, 1988; Lindau and DeLaune, 1991; Nowicki et al., 1997). Denitrification and release of nitrogen to the atmosphere typically occurs at high rates in wetlands and estuaries (Smith et al., 1983; Khalid and Patrick, 1988; Lindau and DeLaune, 1991; Nowicki et al., 1997).

Jenkins and Kemp (1984) reported that up to 50 percent of NO_3^- introduced into the Patuxent River estuary underwent denitrification. Denitrifying bacteria use nitrate to oxidize organic matter anaerobically (Koike and Hattori, 1978). Another transformation pathway of NO_3^- is assimilation into particulate organic matter by phytoplankton and vascular plants. Finally, burial of undecomposed plant material in anoxic soils is a more important loss pathway in Louisiana wetlands than elsewhere as a result of the high subsidence rates. DeLaune et al. (1981), for example, found nitrogen was buried in interior marshes of the Barataria estuary at a rate of $13.4 \text{ g-N m}^{-2}\text{y}^{-1}$, and Smith et al. (1985) measured nitrogen burial of up to $23.0 \text{ g-N m}^{-2}\text{y}^{-1}$ in wetlands surrounding the Atchafalaya River delta.

Several studies have established a relationship between the nutrient loading rate into wetlands and associated removal efficiency (Richardson and Nichols, 1985; Boustany et al., 1997; Faulkner and Richardson, 1989; Spieles and Mitsch, 2000; Mitsch et al., 2001). The focus here is on inorganic nitrogen loading, and particularly dissolved nitrate, as this is the only nutrient species that is higher in river water than in the receiving wetland. The relevant loading is the rate of addition of dissolved inorganic nitrogen on an areal basis, generally reported in $\text{g N-m}^{-2}\text{d}^{-1}$. Reilly et al. (2000) studied constructed wetlands that were used to remove nitrate from Santa Ana River water and found that at nitrate loadings from 0.25 to $1.43 \text{ g-N m}^{-2}\text{d}^{-1}$, with residence times of 9.6 to 2.1 days, respectively, nitrate removal ranged from 100 to 45 percent.

The most comprehensive studies of wetland nutrient removal efficiency have been conducted at wetland wastewater treatment systems, where NH_4^+ is the predominant form of nitrogen. Mississippi River water contains primarily NO_3^- , which is much more reactive than NH_4^+ . Boustany et al. (1997) observed that N removal efficiency was largely dependent on the $\text{NO}_3^-:\text{NH}_4^+$ ratio. When the $\text{NO}_3^-:\text{NH}_4^+$ ratio was greater than 1, average N removal efficiency ranged from 95 to 100 percent, but for ratios less than 1, average efficiencies dropped as low as 57 percent. Molar $\text{NO}_3^-:\text{NH}_4^+$ ratios in the Mississippi River average 18, with a range of 8 to 30 (Lane et al., 1999). Therefore, nitrate in Mississippi River water that enters wetlands should be removed more efficiently than wetland wastewater studies predict. Lane et al. (1999) found, for example, an 88 to 97 percent reduction of NO_3^- as Mississippi River water flowed from the Caernarvon diversion through the Breton Sound estuary, with a loading rate that ranged from 5.6 to 13.4 $\text{g-N m}^{-2}\text{y}^{-1}$ (0.02 to 0.04 $\text{g-N m}^{-2}\text{d}^{-1}$).

These studies indicate very high removal efficiencies for NO_3^- , but removal efficiencies are known to decrease at higher loading rates (Spieles and Mitsch, 2000; Boustany et al., 1997; Faulkner and Richardson, 1989; Richardson and Nichols, 1985). Spieles and Mitsch (2000) found only a 37 to 40 percent reduction in NO_3^- in wetlands receiving Olentangy River water at loading rates of 168 to 172 $\text{g-N m}^{-2}\text{y}^{-1}$ (0.46 $\text{g-N m}^{-2}\text{d}^{-1}$). In 1997, the Atchafalaya River estuarine complex, a mixture of wetlands, open bays and the near shore Gulf of Mexico, showed a 41 to 47 percent decrease in NO_3^- at loadings of 66 to 136 $\text{g-N m}^{-2}\text{y}^{-1}$ (0.18 to 0.37 $\text{g-N m}^{-2}\text{d}^{-1}$, Lane et al., 2002).

1.3 Balancing Benefit and Risk in the Maurepas

The fundamental challenge facing designers of the Maurepas diversion is to divert enough river water to stimulate significant benefits in the swamp without triggering flooding of developed areas or significant algal blooms in Lake Maurepas (Wilson et al. 2002). This balancing of swamp needs with risks to the lake and developed areas was addressed in an earlier study using a one-dimensional hydrodynamic model to drive nitrate loading and removal dynamics in the Maurepas (Lee Wilson et al. 2001; Mashriqui et al. 2002; Lane et al., 2002b; Lane et al. 2003). This preliminary analysis indicated that little Mississippi River derived nitrate should reach Lake Maurepas for a diversion of 1,500 cfs. Many assumptions are inherent in this approach that get more rigorous attention in the work reported here. Ultimately, diversion designers will seek to manage discharge rates and flow paths to ensure that nitrate concentrations reaching the lake are as close to pre-diversion background levels as possible.

Rybczyk et al. (1998, 2002) have provided a model-based approach for assessing the combined effects of adding sediment and nutrients to a subsiding and permanently flooded swamp forest system. They measured processes affecting wetland elevation including organic matter decomposition, sediment accretion, aboveground primary production and plant tissue nutrient concentrations in a 4 ha coastal forested wetland receiving nitrogen-rich, secondarily treated wastewater effluent, and in an adjacent control site, both before and after effluent applications began.

Zhang et al. (2000) estimated the inorganic nitrogen loading rate for this wetland at 0.07 to 0.11 g-N m⁻² d⁻¹. Although virtually no mineral sediment was introduced in the effluent, rates of sediment accretion increased significantly after wastewater applications began, primarily as a result of increased production of floating aquatic vegetation, to approximate a local RSLR of 12 mm-y⁻¹. Rybczyk et al. (2002) showed, however, that direct comparison between estimated RSLR rates and measured short-term sediment accretion rates is insufficient to predict the sustainability of subsiding coastal wetlands. Other factors, such as compaction and decomposition, act to reduce effective long-term accretion, and must be included. Further, such comparisons do not consider elevation feedback effects on primary production, decomposition and sediment deposition. Rybczyk et al. (1998) developed a wetland elevation model using an annual soil cohort approach tracking discrete packages of sediments through depth and time to incorporate elevation feedback mechanisms and simulate sediment dynamics over decades. Rybczyk et al. (1998) reached the following conclusion regarding the long-term potential for restoration of permanently flooded forested wetlands that is an important starting point for considering the potential to use a diversion like that proposed for the Maurepas.

“Above-ground production is low in permanently flooded wetlands relative to those that are seasonally inundated (Conner and Day 1988). In addition, Day and Megonigal (1993) have shown that below-ground production and root standing crop biomass are dramatically reduced in permanently flooded forested wetlands.

Therefore, there would be little or no autogenic response to the addition of mineral sediments until a critical elevation is reached at which there is some relief from flooding stress during the growing season. This critical point will vary by species (Phipps 1979), and by year, depending upon local hydrologic conditions. However, once a critical elevation is obtained, ecosystem response can include increased above and below-ground production, seedling establishment and forest regeneration.”

The goal of the Maurepas diversion project is not merely to improve the swamp but to save it and restore it to a sustainable condition. It is important to note that while nutrient additions alone were sufficient to increase short-term accretion rates, Rybczyk et al. (1998) determined that significant mineral addition would also be required to raise the permanently flooded forested wetland they studied to a seasonally flooded sustainable condition. Here, we adapt the modeling approach of Rybczyk et al. (1998) to predict when and where sustainability can be achieved under a range of diversion scenarios.

2.0 STUDY AREA

The Maurepas study area is a 20,000 ha swamp grading to bottomland hardwoods that is bounded on the south by the roadbed of Louisiana Highway 61 (LA 61 or Airline Highway), that skirts the developed uplands farther south on the Mississippi River natural levee (Figure 2.1). Lake Maurepas, a 3 to 4 m deep, 24,000 ha estuarine lake, exchanges tidal flow through Pass Manchac with the larger Lake Pontchartrain to the east. The lake is included in its entirety in the LSU model domain. The course of the Blind River forms the western boundary, while a north-south canal paralleling Interstate Highway 55 (I-55) is the eastern margin. The USACE maintains the only permanent tide gage within the study area at the point where I-55 crosses Pass Manchac, and both water level and salinity records are available from this station since 1951.

Interstate Highway 10 (I-10), running east-west, crosses the study area obliquely 2 to 5 km north of the Airline Highway. It encloses a triangle of higher elevation mixed bottomland hardwoods grading to swamps that widens to the west toward Blind River. The stressed swamp north of the I-10 is the primary target of the diversion project. The proposed diversion channel will extend from the Mississippi River to connect with the existing Hope Canal channel (Figure 1.2). While the area south of the I-10 is included in the LSU model domain, it is assumed that the diversion channel will be enlarged and lined with levees to the I-10 crossing so that effective input to the swamp will originate from this point (Wilson et al., 2002).



Figure 2.1 Maurepas Study Area

The Blind River and Amite River Diversion Canal come together on the western margin of the study area to flow into the lake (Figure 2.2). The Blind, and particularly the Amite, drain a large urban area to the west (Baton Rouge) and deliver most of the fresh water and sediment that today enters Lake Maurepas, averaging between 1,000 and 4,000 cfs. These tributary streams, as well as the smaller Tickfaw River that enters Lake Maurepas from the north, are flashy streams prone to brief, high-intensity floods that can occur at almost any time of the year (Figure 2.3). Mean monthly Amite River discharge did not exceed 1,000 cfs during the drought year of 2000, though it can reach 10,000 cfs in flood. Amite River flow enters Lake Maurepas through two outlets with about half through the Amite River Diversion Canal (Figure 2.1).

Several dredged channels run south to north carrying local drainage into the swamp and lake from the residential, industrial and agricultural lands of the Mississippi River levee. Hope Canal, the proposed inlet for the diversion (Figure 1.2), is the smallest and westernmost of these features, running ten km north from Airline Highway to connect with natural channels of the Tent/Dutch Bayou system (Figure 2.4). Hope Canal is a small channel today, generally less than 25 m across and 2 m deep, which was dredged almost a century ago. Like the natural bayous of the area, it is obstructed in many places by logs and fallen trees. A spoil bank on the west side once supported a small logging railway, now long gone. That levee is degraded at numerous points

permitting free exchange with the swamp on both sides whenever the water is high enough (Mashriqui et al., 2002).



Figure 2.2 Photograph of Blind River at Station 10

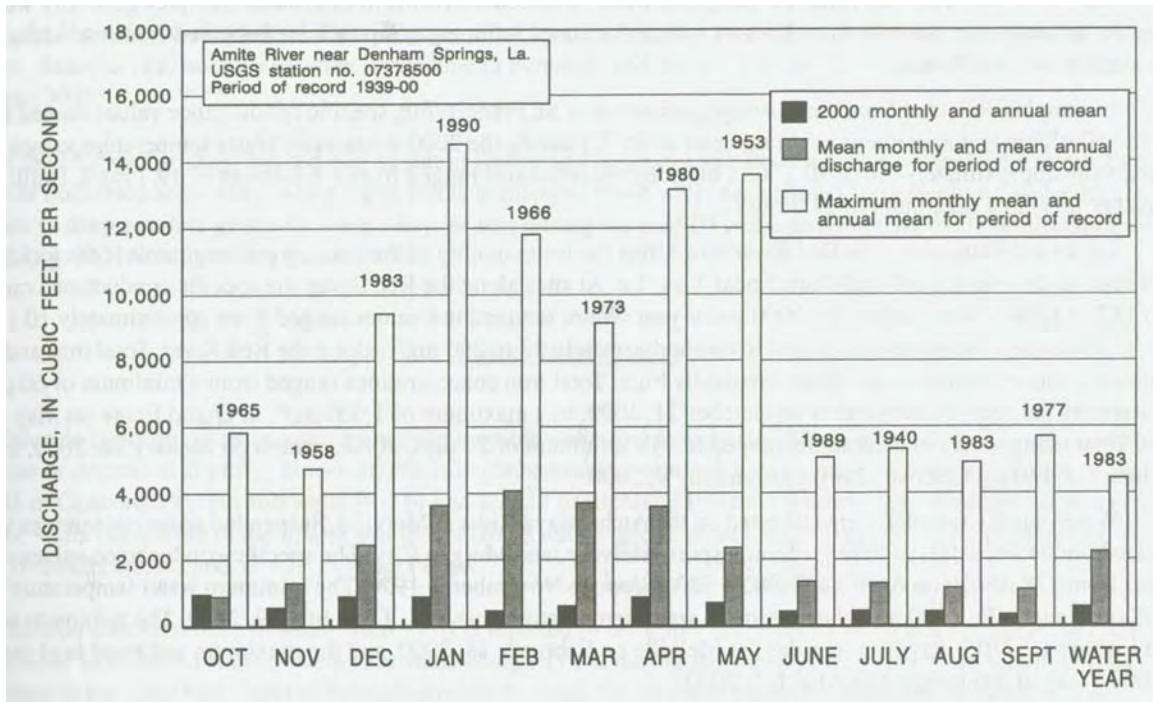


Figure 2.3 Amite River Discharge summary from USGS water resources data 2000, showing normal and drought year patterns



Figure 2.4 Photograph of Hope Canal near Station 8

Hope Canal runs into Tent Bayou, a natural waterway, which joins the Mississippi Bayou to form Dutch Bayou about 3 km south of the lake. The current restoration plan is to leave Hope Canal largely as it is north of the I-10. Hope Canal will be enlarged south of the I-10 bridge to the River at Garyville where it will also be fitted with levees and structures to accommodate local drainage (Lee Wilson & Assoc. 2001; Wilson et al., 2002)). North of the I-10, the Bourgeois Canal extends 3 km east from Blind River approaching to within a km of Hope Canal. This Canal could provide a short-circuit delivering diverted waters too quickly to Blind River, and has drawn the attention of diversion project planners.

The Reserve Relief Canal is about 8 km east of Hope Canal and runs all the way from Airline Highway to the lake, about 8 km (Figure 2.5). It is about twice the size of Hope Canal, is relatively clear of obstructions, and enjoys unhindered exchange with the lake. A few 1 to 2 km long oil well access canals extend to the east and west into the swamp. The I-55 Canal is the last large dredged channel in the study area. It parallels the route of the elevated Interstate 55 and a railroad causeway. It defines the eastern boundary of the study area and runs into Pass Manchac on the north, but contributes little freshwater to the lake.



Figure 2.5 Photograph of Reserve Relief Canal at Station USGS2

Pass Manchac is a natural tidal inlet 10 to 20 m deep through which salty water enters the study area during drought periods. Lake Maurepas salinities near Pass Manchac typically range from 0 to 3 ppt, but reached 12 ppt near the Pass and 6 ppt on the other side of the lake at the Blind River entrance, respectively, in October 2000 (Lee Wilson & Assoc. 2001; Lane et al., 2002b; Lane et al., 2003). Salinities were measured in channels and shallow wells deep within the swamp at 5 and 3 ppt, respectively, at this time, and this caused a die-off of swamp herbaceous vegetation (Lee Wilson & Assoc. 2001, Shaffer et al. 2003). While the three year rise in salinity at Pass Manchac that concluded in 2000 was unprecedented (Figure 2.6a), less prolonged incursions of high salinity waters into Lake Maurepas are more frequent in the fall, and often accompany tropical storms and hurricanes (Figure 2.6b).

Apart from Blind River, the only natural charted swamp waterways in the Maurepas study area are those of the Mississippi Bayou system, a tidal channel. It has two log-choked and shallow tributaries, 10 to 20 m wide, that begin on the natural levee between Hope and Reserve Relief Canals, join after winding separately about 4 km, and then continue as one channel to the confluence with Dutch Bayou (Figure 2.7). Mississippi Bayou enlarges below the Dutch Bayou confluence to almost 30 m wide and 3 m deep. A large, partially vegetated bar has been extending in recent years from the Blind River entrance across the mouth of Mississippi Bayou, forcing the Bayou to turn to the east and follow the shoreline for 0.5 km before entering the lake.

This feature is evidence that with development of the watershed, the Amite is supplying more sediment to the lake than it did in the past. The Mississippi Bayou system is the major conduit for tidal exchange in the Maurepas swamp study area. It is well connected to the swamp through a myriad of tiny channels, detectable only by the gaps in the trees (Figure 2.8).

Sediment entering Lake Maurepas during runoff events on the Amite has been observed penetrating deep into the swamp through these small channels on wind-forced flood tides.

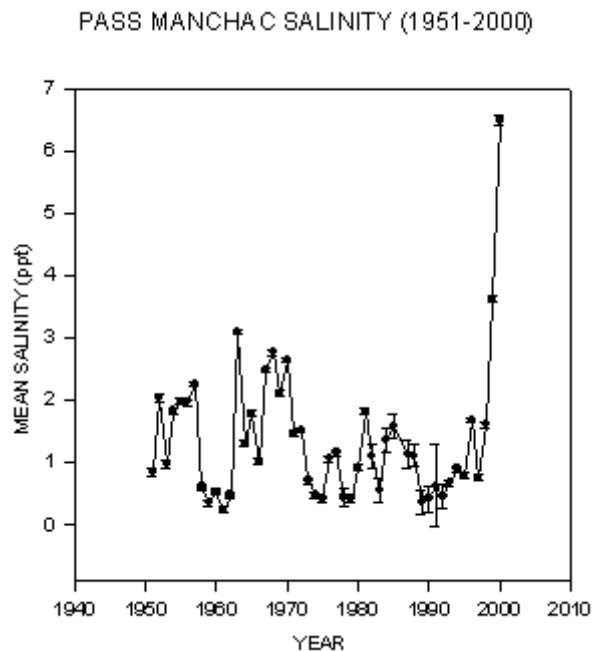


Figure 2.6(a) Mean salinity at Pass Manchac: 1951 to 2000 (from U.S. Army Corps of Engineers, New Orleans district)

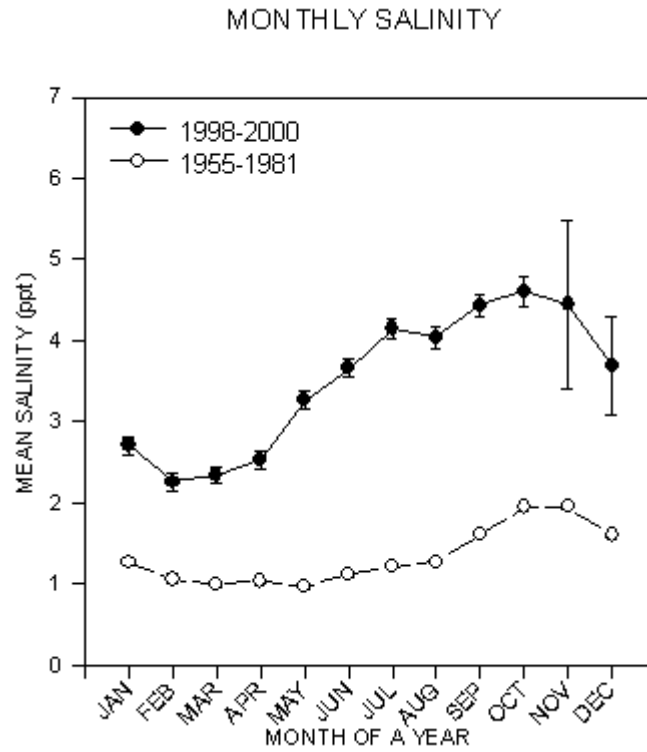


Figure 2.6(b) Mean annual and monthly salinity at Pass Manchac: 1955 to 1981, and during the 1998 to 2000 drought (from U.S. Army Corps of Engineers, New Orleans district)



Figure 2.7 Photograph of Dutch Bayou at Station 9 looking downstream with ADCP on right and WL gage on left



Figure 2.8 Photograph of North Swamp near URS N gage

2.1 Swamp Ecology

The Maurepas swamp overstory is dominated by a cypress-tupelo assemblage (*Taxodium distichum-Nyssa aquatica*) (Lee Wilson & Assoc. 2001). Shaffer et al. (2003) investigated a range of factors believed to affect the health and productivity of swamp vegetation at 20 paired plots that were monitored for three years, from February 2000 to May 2003 (Figure 2.9). Using discriminant function analysis, these 20 representative sites were divided into four categories described as throughput, lake, intermediate and interior. Throughput sites, the most productive with respect to trees in the study area, occur primarily along the Hope Canal corridor and near the Amite Diversion Canal, and Shaffer et al. (2003) characterized these sites as benefiting from externally derived inputs of sediment and nutrients. Intermediate sites were about half as productive as the throughput stations. They are generally from the inland reaches of the Reserve Relief Canal, are significantly affected by tidal exchange with the lake, but are far enough from it to escape most salinity impacts. Interior sites were significantly less productive than the intermediate sites, exhibiting about a third of the productivity of the throughput stations. They were clustered along the Blind River boundary, close enough to be flooded frequently, but too far south from the junction with the Amite Diversion Canal to receive significant sediment and nutrient inputs. Finally, the lake sites occur around the rim of Lake Maurepas and were the least productive of all stations. They tended to be more often flooded by lake waters and stressed by lake-derived salinity.

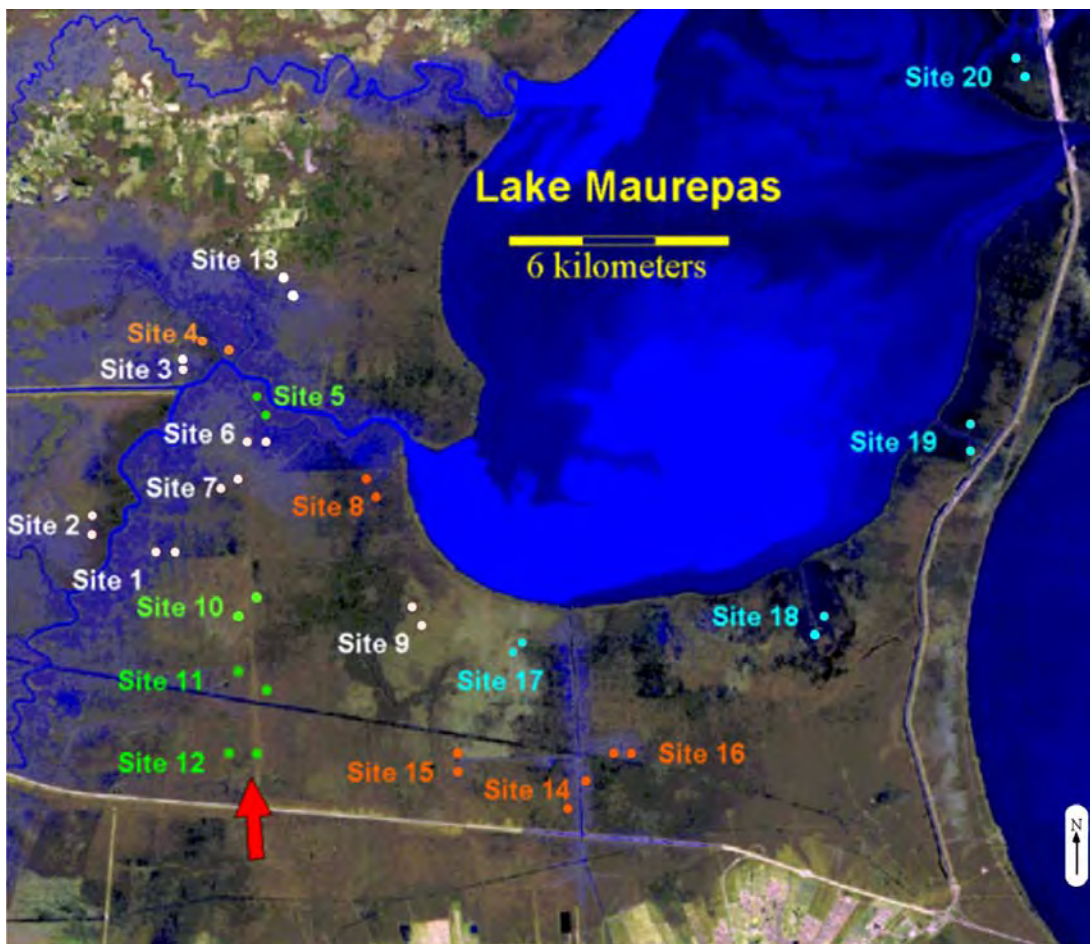


Figure 2.9 Forest monitoring sites from Shaffer et al. (2003). Lake sites are blue; intermediate stations are orange; throughput is green, and interior is white. Large red arrow indicates proposed Hope Canal diversion location.

Many smaller, less flood- and salt-tolerant trees than cypress and tupelo were found at all except the lake sites, but cypress and tupelo dominated basal area estimates everywhere. Cypress and tupelo were co-dominant with respect to basal area at the throughput and intermediate sites, where they accounted for 80 to 90 percent of the total area. Tupelo dominated at the interior sites. Conversely, cypress accounted for most of the basal area at the lake sites, although the total basal area was much lower than elsewhere.

Shaffer et al. (2003) found that only the most productive of the throughput sites are as healthy as free-flowing, periodically flooded cypress-tupelo swamps elsewhere in the southeastern U.S., though even this was not true during the drought year of 2000. Net primary productivities measured at the remainder of the swamp stations, including all of the interior, intermediate and lake sites, were comparable to values measured elsewhere only in nutrient-poor, stagnant or continuously flooded swamps. Herbaceous vegetation was increasing at these sites, suggesting a transition to marsh.

Shaffer et al. (2003) conclude that most of the Maurepas swamp study area forest is populated by relict stands. They are flooded too continuously to permit seed germination and recruitment. Salt stress was observed to kill tupelo trees preferentially over cypress at sites near the lake, but Shaffer et al. (2003) believe interior cypress-tupelo stands are more affected by prolonged flooding, nutrient deprivation and stagnant conditions than by salinity.

Wetland loss rates for the Amite/Blind River mapping unit in the 1974 to 1990 period have been reported as 0.83 percent per year for the swamps, and 0.02 percent per year for fresh marsh (Lee Wilson & Assoc. 2001). Shaffer et al. (2003) measured higher tree mortality in the study area, about 1 percent per year at the throughput sites and 2 percent per year at the interior and intermediate sites, but 10 percent per year at the lake sites. If a value of 2 percent per year is considered broadly applicable, the data presented by Shaffer et al (2003) suggest that unless conditions change, virtually all of the cypress-tupelo forest in the Maurepas study area will be lost within 60 years.

2.2 Water Quality

Lane et al. (2003) carried out an investigation of water quality in the Maurepas study area during the last year of a three-year drought, from April to October 2000. Monthly water samples were collected synoptically at 16 locations that were grouped into four regional clusters that were retained in the 2002 - 2003 study (Figure 2.10). These regions correlate well with those identified by Shaffer et al. (2003) based on forest characteristics. The Lake stations (L) of Lane et al. (2003) are just offshore of the lake forest stations, and the Reserve Canal (R) water quality stations are in the vicinity of the intermediate forest plots (Shaffer et al. 2003). Similarly, the Amite/Blind (A) stations of the water quality survey are in the vicinity of most of the interior forest sites, while the Hope Canal/Dutch Bayou (H) water quality stations occur in channels adjacent to the throughput forest stations (Shaffer et al. 2003).

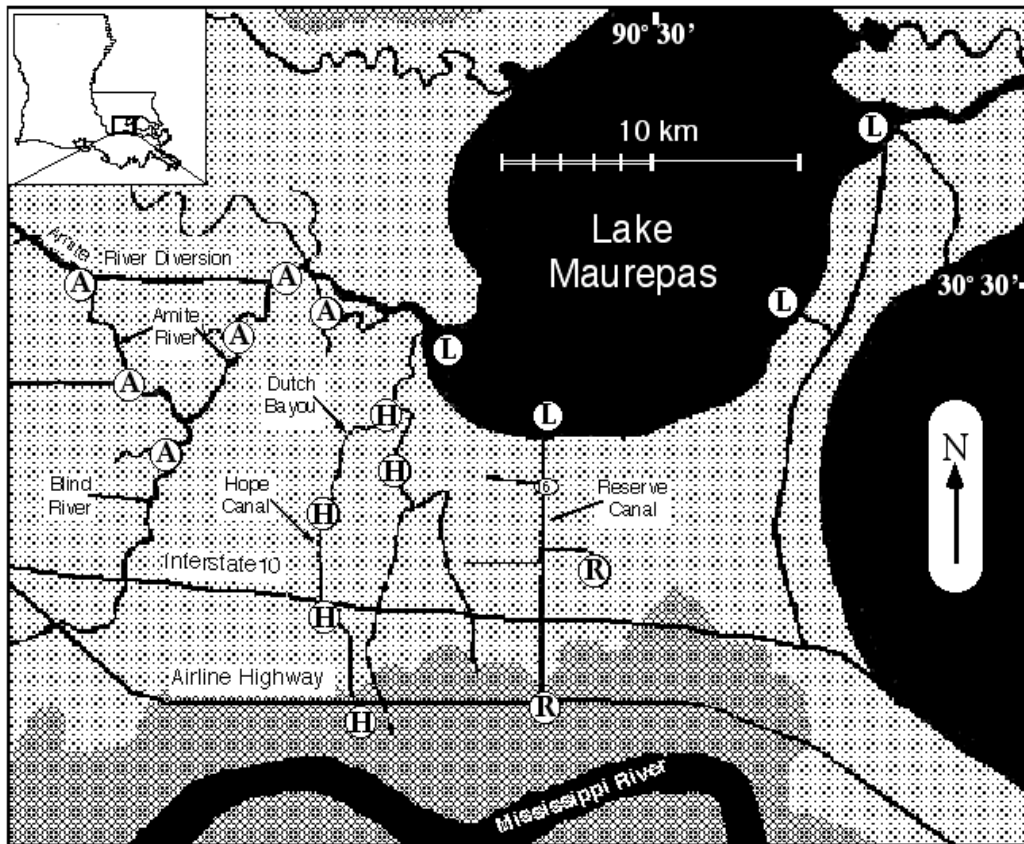


Figure 2.10 Lake (H), Amite (A), Hope (H) and Reserve (R) water quality sampling sites occupied by Lane et al. (2003) in 2000.

Salinity during the most severe drought on record averaged 3 ppt at all sites for the 7 months monitored and generally increased through the year. Lake salinities were always higher than in swamp waterways, but from April to August, a west to east salinity gradient was also present in the swamp with values decreasing from Reserve Relief Canal through Hope Canal to a minimum in the vicinity of the Amite/Blind Rivers. This gradient was maintained by discharge from the Amite River system during this period, and disappeared when flow into the lake diminished in the fall (Figure 2.3). Then, when values of 12 ppt were observed in eastern Lake Maurepas, swamp salinities rose to greater than 5 ppt in all regions (Lane et al., 2002b; Lane et al. 2003).

Suspended sediment and chlorophyll *a* concentrations were both in the low range for coastal Louisiana, generally less than 20 ppm and 20 ppb, respectively. Highest suspended sediment concentrations and lowest chlorophyll *a* values were observed in the lake, and were both attributed to wave resuspension of bottom sediments that clouded the water limiting phytoplankton growth. Suspended sediment and Chlorophyll *a* concentrations in swamp waterways did not differ significantly by region, though Chlorophyll *a* generally increased over time from spring to fall (Lane et al. 2003).

As is true of other deltaic wetlands that are not receiving the Mississippi River water, most nitrogen and phosphorus found in waters of the Maurepas study area were in the organic forms, presumably in humic substances, tannins and phytoplankton (Lane et al. 1999; 2002; 2003).

Highest concentrations of the dissolved inorganic nitrogen forms, nitrate and ammonium, though still an order of magnitude below values in the Mississippi River, were found in the Amite River region and in Lake Maurepas, indicating that the swamp itself is probably a sink. Dissolved phosphate concentrations were higher in the Hope Canal region than at other sites, but generally were similar to concentrations observed in the Mississippi River (Lane et al. 2003). The molar ratio of dissolved inorganic nitrogen to dissolved inorganic phosphorus (DIN:DIP) averaged less than 5:1 in all regions, far below the 16:1 value considered optimal for phytoplankton growth (Redfield 1958). Lane et al. (2003) interpret this to mean that the Maurepas swamp basin is severely nitrogen limited, and, therefore, would be sensitive and responsive to nitrogen introduced from the River.

2.3 Hydrology

In 2001, EPA funded development of a one-dimensional hydrodynamic model (UNET) that was used to drive nitrate loading and removal simulations in the Maurepas (Lee Wilson et al. 2001; Mashriqui et al, 2002; Lane et al., 2002b; Lane et al. 2003). A 1,500 cfs diversion with a typical river nitrate concentration of 1.5 ppm was modeled. This network model was then used to predict water levels and the rate at which diverted water would leave an unimproved Hope Canal inlet channel. Although calibrated for a dynamic tide, it was primarily operated in a steady-state configuration in which the tidal boundary was held constant, while diversion discharge was varied.

Elevations of the swamp floor had to be assumed, and swamp cells were treated as off-channel storage. Water and associated nitrate was routed from Hope Canal through a cascade of swamp “ponds” until it reached a major water body (Figure 2.11). The nitrate concentration for each cell receiving water was determined by the loading rate and associated removal in the up gradient cell. The model predicted that nitrate loadings in the swamp cells adjacent to Hope Canal could be as high as $0.24 \text{ g N}\cdot\text{m}^{-2}\cdot\text{d}^{-1}$ ($88 \text{ g N}\cdot\text{m}^{-2}\cdot\text{d}^{-1}$). The minimal reduction predicted along the shortest assumed path through the swamp was 94 percent after one month of diversion operation (Lane et al. 2003). Reductions for the longer paths that most water would follow were greater. This preliminary analysis indicated that at 1,500 cfs little Mississippi River derived nitrate should reach Lake Maurepas.

Many assumptions are inherent in this model that get more complete treatment in the work reported here. The rate of nitrogen removal is dependent on the loading rate, the form of nitrogen (e.g., NO_3^- vs. NH_4^+ ; Boustany et al., 1997), and residence time (Nixon et al., 1996; Dettmann, 2001). Residence time was difficult to evaluate with the one-dimensional model, particularly in the swamp. Although the absolute rate of nitrogen removal may be greatest at high loading, nitrogen removal is most efficient (highest percent removal) at lower loading rates (Figure 2.12) when diverted water is spread over a receiving wetland as widely as possible, increasing contact with the sediment/water interface and residence time (Richardson and Nichols, 1985; Blahnik and Day, 2000, Mitsch et al. 2001).

We are concerned in the Maurepas both with nitrogen removal efficiency and absolute rates of nitrogen removal. Ultimately, diversion designers will seek to manage discharge rates and flow paths to ensure that nitrate concentrations reaching the lake are as close to pre-diversion background levels as possible.

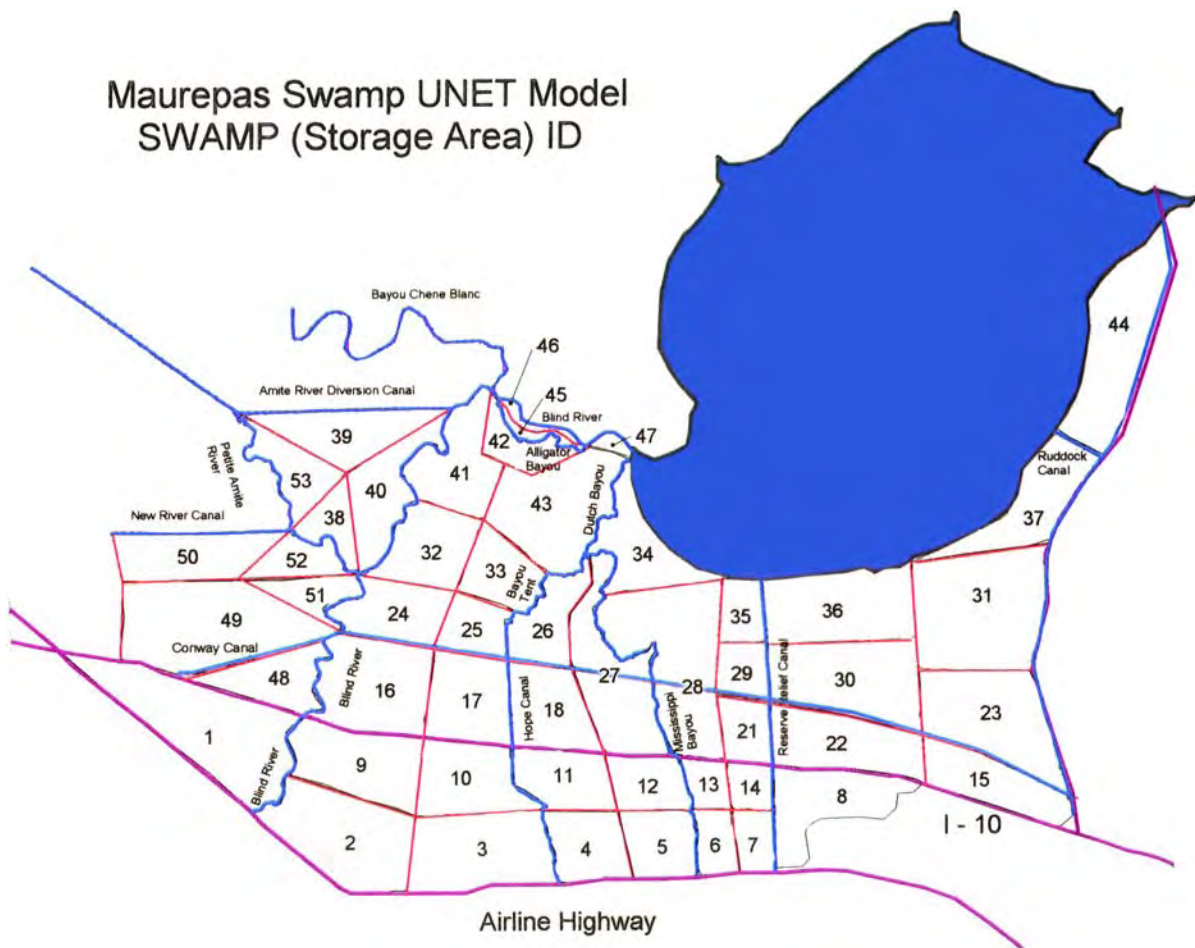


Figure 2.11 Distribution of UNET swamp cells for modeling nutrient processing by Lane et al. (2003)

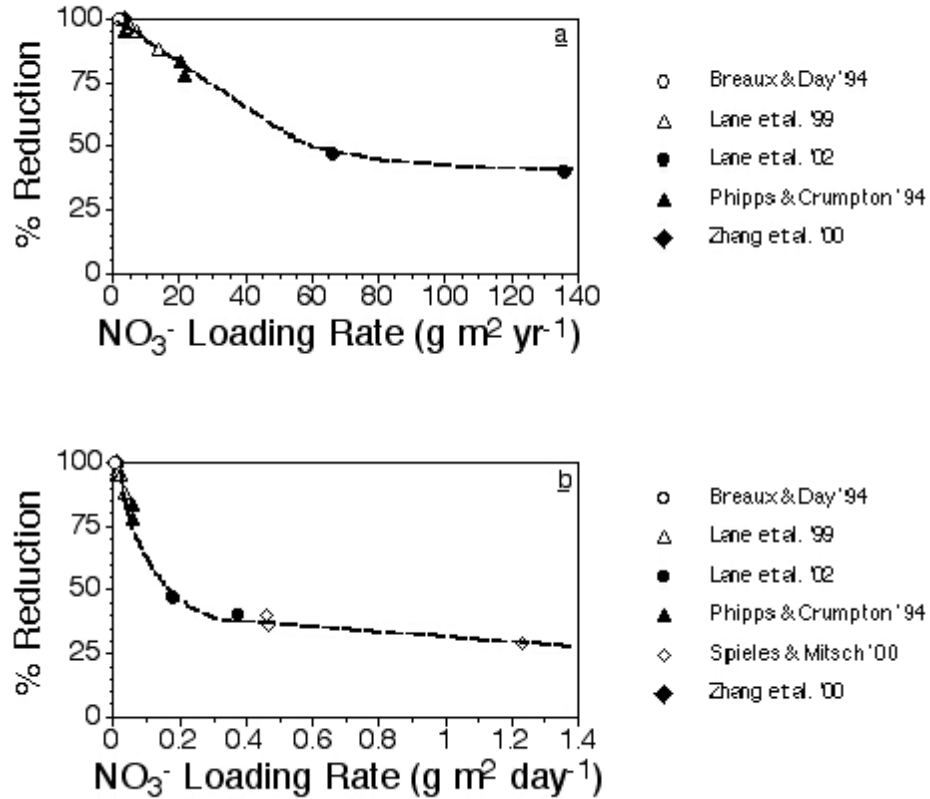


Figure 2.12 Yearly and daily nitrate loading rate versus removal efficiency for various river diversions and wetland wastewater treatment systems (Lane et al. 2003). Nitrate input sources: Breaux and Day 1994, municipal wastewater; Lane et al., 1999, Mississippi River water; Lane et al., 2002, Atchafalaya River water; Phipps & Crumpton 1994, Des Plaines River water; Spieles and Mitsch 2000, Olentangy River water; Zhang et al., 2000, municipal wastewater.

3.0 METHODS

This project was pursued along two parallel courses. A field program was deployed to satisfy the first two objectives, the acquisition of baseline water quality and hydrographic information. This was then used to establish baseline pre-diversion conditions and for calibrating and validating models. A modeling program was initiated to accomplish the last two objectives. This had two aspects. First, it was necessary to develop, calibrate and validate swamp hydrodynamic and water quality models, and, second, to establish a means of using these hydrodynamic models to enable ecological forecasting.

3.1 Field Program

The field program had two aspects. The first, water quality sampling, was initiated to collect and analyze discrete water samples from throughout the study area on a single day at monthly intervals. This was really a continuation of the program undertaken in 2000 that has been described by Lane et al. (2003). The second, hydrologic gaging, was deployed to acquire continuous information at channel stations previously surveyed, and at adjacent off-channel swamp locations.

3.1.1 Water Quality Sampling. Water sampling trips were carried out monthly from April 2002 to May 2003 to characterize current conditions in the Maurepas swamp.

The sampling trips were conducted on April 4, May 7, June 4, July 8, August 2, September 11, October 23, November 13, December 17, 2002, and January 31, March 31, and May 13, 2003. Water samples were taken at 19 locations (Figure 3.1), with the intention of covering all of the major bayous and water bodies in the Maurepas swamp. To simplify such a large data set, the stations were grouped into different regions delineated by hydrological boundaries, as was described in Lane et al. (2003). Region A comprises the Amite and Blind Rivers; region H the Hope Canal and Dutch Bayou waterways; region R the Reserve Canal sampling stations; and region L the stations in Lake Maurepas (Figure 3.1). The data were averaged for each region during each month. Stations 6 and 13, located at ends of small natural swamp drains were believed more typical of the swamp than of the larger channel system to which they were attached and were removed from this summary analysis, but all data is provided (Appendix A).

Water samples were collected in 1L acid-washed polyethylene bottles, stored on ice, and taken to the laboratory for processing. Within 24 hours, the water was subsampled into pre-acid washed bottles for total N and P analysis. Also, 60 ml from each water sample were filtered through pre-rinsed 25 mm 0.45 um Whatman GF/F glass fiber filters into pre-acid washed bottles. The total and filtered water samples, and filters, were frozen until nutrient and chlorophyll *a* analysis, respectively.

Within one week of sample collection, total suspended sediment (TSS) was determined by filtering 100-200 mL of sample water through pre-rinsed, dried and weighed 47 mm 0.45 μm Whatman GF/F glass fiber filters.

Filters were then dried for 1 hr at 105°C, weighed, dried for another 15 minutes, and reweighed for quality assurance (Greenberg et al.,1985). Salinity was determined using an Atago © S-10 hand held refractometer (accuracy: $\pm 2\%$).

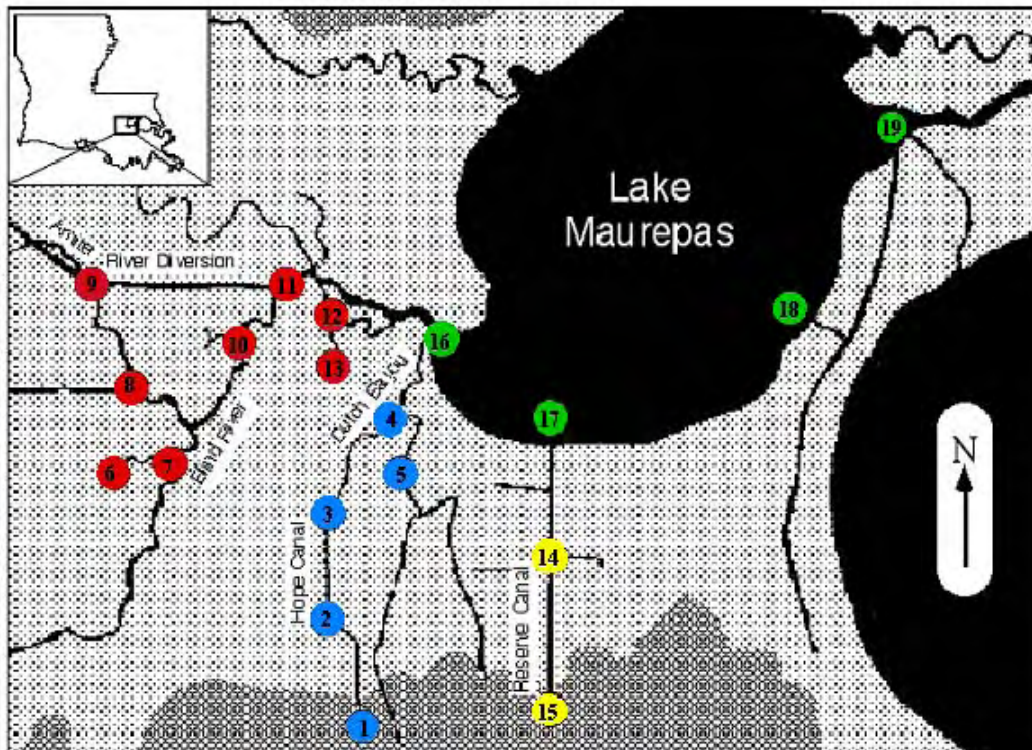


Figure 3.1 Water quality sampling stations occupied monthly from April, 2002, to May, 2003. Lake (L) is green; Reserve Canal (R) is yellow; Hope Canal (H) system is blue; Amite and Blind River (A) are red.

Within one month of sample collection, filtered samples were analyzed for chlorophyll *a*. Chlorophyll *a* was determined by a modified version of the technique suggested by Strickland and Parsons (1972). Chlorophyll pigments were extracted with a 40:60 ratio of dimethyl sulfoxide (DMSO):90% acetone as described by Burnison (1980). The extract was measured fluorometrically with a Turner Designs model 10-AU fluorometer (Greenberg et al., 1985).

Nitrate ($\text{NO}_3\text{-N}$) and nitrite ($\text{NO}_2\text{-N}$) were determined separately using the automated cadmium reduction method with an Alpkem © autoanalyzer (Greenberg et al., 1985). NO_3^- was the predominant form (>90%) of total oxidized nitrogen ($\text{NO}_3 + \text{NO}_2$), and therefore $\text{NO}_3 + \text{NO}_2$ was reported as NO_3^- . Ammonium ($\text{NH}_4\text{-N}$) was determined by the automated phenate method, and phosphate ($\text{PO}_4\text{-P}$) by the automated ascorbic acid reduction method, both with an Alpkem © autoanalyzer (Greenberg et al., 1985). Total nitrogen (TN) and total phosphorus (TP) were determined by methods described by Valderrama (1981). The accuracy of the nutrient analysis was checked every 20 samples with a known standard, and the samples were redone if the QC was off by 5%. Outliers in the data set possibly caused by sample contamination were eliminated from further analysis if: (1) the value lies outside 3.84 standard deviations from the mean; (2) the dissolved fraction of N or P is greater than total by more than 25%. Chlorophyll pigments were extracted with a 40:60 ratio of dimethyl sulfoxide (DMSO): 90% acetone as

described by Burnison (1980). The extract was measured fluorometrically with a Turner Designs model 10-AU fluorometer (Greenberg et al., 1985).

3.1.2 Hydrologic Gaging. Water level gaging stations were established in stages at 13 sites in waterways, or, in two cases, within the swamp (Figure 3.2). They are grouped in three watershed regions that correspond to regions identified by Shaffer et al (2003): the Blind and Amite Rivers (Blind/Amite), Hope Canal, Tent and Dutch Bayous (Hope/Dutch), Mississippi Bayou (MissB), and the Reserve Relief Canal (Table 3.1). Three stations are sited within the Blind/Amite system on the western margin of the study area. The majority of stations are located in either the Hope/Dutch system (7), or along Mississippi Bayou (2), the most significant tributary to Dutch Bayou. Two stations in the Reserve Relief Canal define the eastern part of the study area. Two stations at the mouths of Reserve Relief Canal and Dutch Bayou, along with the long-term USACE station at Pass Manchac provide information on the lake (Figure 3.2). All but three of these stations are located on controlled cross-sections at staff gage sites that had previously been surveyed to the NAVD88 datum (Lee Wilson & Assoc. 2001; Mashriqui et al., 2002). Vertical control for the two swamp stations, LSU A and URS N, was tied to the nearest surveyed channel staff gage, S9 and S13, respectively, less than 1 km away.

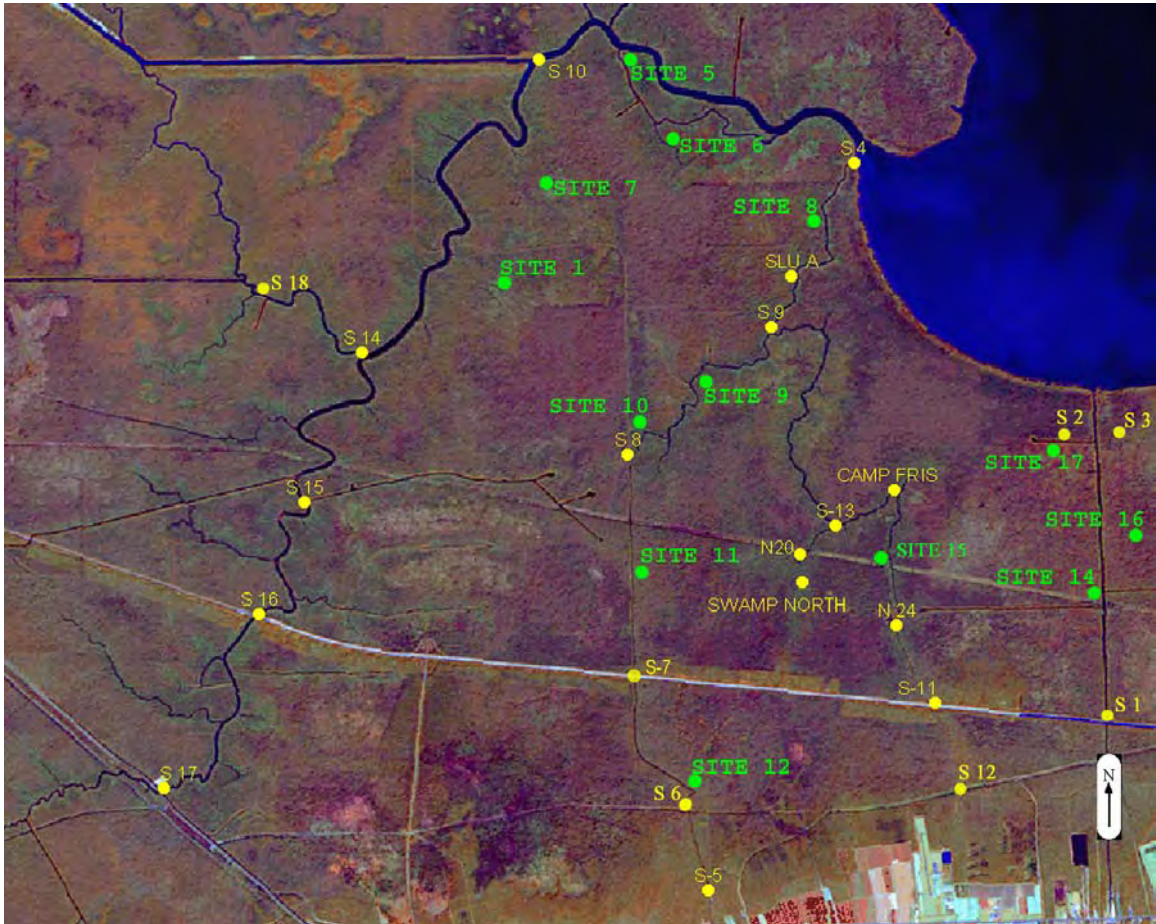


Figure 3.2 Maurepas hydrologic gages (yellow) and Shaffer et al. (2003) forest monitoring stations (green). Swamp gages located at SLU A and URS N (Swamp North)

Table 3.1 Maurepas Hydrologic Gaging Program: 2002 - 2004

Sta.	Gauge Location	Survey Sta	Watershed	Start		Record Interval (month)	Interval (hour)	Sonde	
4	<u>Dutch@Lake</u>	S4	Hope/Dutch	11/5/02	Present	19	2,0.25 (11/26/03), 0.5 (2/12/04)	RDS, YSI (11/26/03)	L,C, S
5	<u>Hope@Hy61</u>	S5	Hope/Dutch	12/10/03	Present	6	0.25	Infinities	L
6	<u>Hope@Pipeline</u>	S6	Hope/Dutch	1/20/03	3/26/03	2	2	RDS	L
7	<u>Hope@I-10</u>	S7	Hope/Dutch	12/19/03	Present	6	0.25	Infinities	L
8	<u>Hope@Tent</u>	S8	Hope/Dutch	11/21/02	12/3/03	13	2	RDS	L
								RDS, YSI (12/19/03)	
9	<u>Dutch@MissB</u>	S9	Hope/Dutch	11/4/02	Present	19	2,0.25 (12/19/03)	ADCP (10/23/03)	L,C, S,V
10	<u>Blind@AmiteD</u>	S10	Blind/Amite	11/4/02	Present	16	2,0.25 (12/4/03), 0.5 (2/12/04)	RDS, Infinities (12/4/04)	L
11	<u>MissB@I-10</u>	S11	MissB	12/18/03	Present	6	0.25	Infinities	L
16	<u>Blind@I-10</u>	S16	Blind/Amite	12/04/03	Present	6	0.25,0.5 (2/12/04)	Infinities	L
USGS 1	<u>Reserve@Lake</u>	S3	Reserve	1/9/04	Present	5	0.25,0.5 (2/12/04)	YSI	L,C, S
USGS 2	<u>Reserve@Hy61</u>	S1	Reserve	12/11/03	Present	6	0.25,0.5 (2/12/04)	Infinities	L
SLU A	<u>Swamp@S9</u>	S9	Hope/Dutch	1/31/03	Present	16	2	RDS	L
URS N	<u>Swamp@S13</u>	S13	MissB	12/15/03	Present	6	0.25	Infinities	L

* L = Water Level, C = Conductivity, S = Salinity, V = Velocity

The monitoring program evolved, as gages were added, malfunctioned or otherwise lost. Six stations were equipped with RDS resistance wire gages (Appendix B) between November 2002 and January 2003. These gages, with the exception of Station 6 ([Hope@Pipeline](#)) that was lost after 2 months and not replaced, provided water level data at 2 hour intervals for 2003. These gages were installed in slotted PVC housings and serviced monthly. The vertical position of both the physical staff gage and the recording gage were checked at least monthly against the surveyors' original witness nails so that any movement or drift could be detected and corrected.

LSU was contracted by the LDNR to install new gages in the Maurepas in the fall of 2003 under the direction of URS Corporation, the engineering contractor. Beginning in November 2003, the RDS equipment was replaced at Stations 4 ([Dutch@Lake](#)) and 9 ([Dutch@MissB](#)) with YSI 600 sondes fitted with compensated pressure sensors and conductivity/salinity probes (Appendix B). A third YSI was placed in the mouth of the Reserve Relief Canal at S3 near where it enters Lake Maurepas ([Reserve@Lake](#)). The YSI instruments were set to log data every 15 minutes (0.25 h) during the calibration period, and were then set to report every 30 minutes (0.5 h). RDS equipment that had malfunctioned in October 2003 was replaced with an Infinities compensated pressure sensor water level logger at Station 10 ([Blind@AmiteD](#)) in January 2004 (Appendix B).

Infinities gages were also installed at six new locations (Table 3.1). Except for the one remaining RDS gage at the SLU A swamp site (Swamp@S9), all data is now being acquired at 0.5 h intervals.

At the time of this report, 11 gages are monitoring water level, and three of these are logging conductivity/salinity. Water level time-series have been acquired over the past 19 months at 15 stations. Five have provided records more than a year long, nine between four and 12 months, and one for less than four months.

A Sontek acoustic Doppler current profiler (ADCP) was installed in October 2003 at an existing gage location ([Dutch@MissB](#)) just downstream of the confluence of Mississippi and Dutch Bayou (Appendix B). The profiler is in a side-looking configuration and was positioned so that it sees across the entire active cross-section (Figure 2.7). The ADCP provides an average velocity for the channel, whether positive (ebb) or negative (flood), every 15 minutes, that is computed from ensemble averages over the logging interval. Seven months of continuous ADCP record is now available. A second ADCP will be installed soon on Mississippi Bayou just upstream of the junction with Dutch Bayou, to assess the relative contributions of the two tributaries to Dutch Bayou.

3.2 Modeling Program

A modeling program was initiated to develop, calibrate and validate swamp hydrodynamic and water quality models, and, second, to establish a means of linking this model to others that will enable ecological forecasting.

3.2.1 Selection and Description of TABS Model Suite. A variety of numerical models with the capability to perform hydrodynamic and constituent transport simulations were reviewed to determine that most appropriate for this study. Moffatt & Nichol Engineers (2000) performed a comparative analysis to identify the most appropriate engineering model to characterize the hydrodynamics and salinity of Louisiana's Barataria Basin, similar in many ways to the Maurepas system. All models considered in this report have been successful in numerous applications throughout the world (Moffatt & Nichol Engineers, 2000). Moffatt & Nichol Engineers (2000) evaluated models for the following diverse characteristics: fidelity with which bathymetry is represented, computational efficiency, ease of set-up and calibration, degree of model acceptance and use, capacity to include major forcing functions and the capability to simulate cohesive and non-cohesive sediment transport. Two 2D models, TABS-MD and MIKE21, were recommended as the most suitable models for simulating the complex Barataria system, which is comparable to the Maurepas in many respects.

Forcing functions significant to the Maurepas system are discharge from the Amite and Blind, tidal exchange at Pass Manchac, winds, and waves (Lee Wilson & Assoc. 2001). Strong northerly and southerly winds substantially affect water levels and mixing during the winter and spring (van Heerden, 1980; 1983). Tides play a major role in the circulation of water and fine sediments today in the Maurepas, and will continue to be important when diverted River discharges are low.

Extremely complex natural and man-made features of the Maurepas study area challenge any numerical modeling effort. The prospective model must include discharge, salinity, high precision bathymetry, wind, tide, wave action and localized subsidence. Further, it should be expandable in the future to include sediment transport and deposition dynamics. Analyzing this complex system requires a model capable of addressing a wide range of flow conditions over a complex geometry of shallow water bodies, interspersed with intertidal swamps that alternate between wet and dry.

An accurate representation of just the most important of the small channels in the Maurepas, like Hope Canal, would require a large number of very small cells if a finite-difference (FD) model were to be selected. Alternatively, this could be accomplished using MIKE21 with a nested modeling technique, but then the usual advantage of FD over finite-element (FE) in computational efficiency would be lost.

Moffatt and Nichols (2000) recommend TABS-MD over MIKE21. TABS-MD (Thomas and McAnally, 1990) is a widely used suite of applications developed originally

by the USACE that is built around an FE hydrodynamics scheme. Perhaps the most significant reason for the popularity of TABS-MD is its ability to run on a desktop with the Surface-Water Modeling System (SMS) software that was developed at Brigham Young University in cooperation with the USACE (EMRL, 2002). The SMS software provides valuable tools for mesh generation, data interpolation, and graphical visualization.

The TABS-MD suite includes separate hydrodynamic (RMA2), water quality (RMA4) and sediment transport modules (SED2D) that are generally run in sequence.

Capps and Willson (2002) showed in preliminary work that the swamp could be modeled using a TABS FE approach. LSU proposed to develop a new TABS model for the Maurepas study area in part because it was hoped that information developed from this model would be useful in engineering the diversion project. The USACE and LDNR are experienced in reviewing TABS output, and it was thought that the current work might have more effect on design if a standard engineering model were applied.

The TABS-MD model has produced an extensive literature (Barrett, 1996; Freeman, 1992; Roig, 1994). Barrett (1996) used the TABS-MD model for wetland simulations.

Freeman (1992) conducted a review of TABS model behavior in shallow water. Roig (1994) used this tool for marsh and wetland modeling, and Capps and Willson (2002) demonstrated its suitability for the Maurepas swamp.

Three modules (GFGEN, RMA2 and RMA4) of the TABS-MD were used in this study. The module GFGEN was used to create the finite element mesh of the study area; the RMA2 module simulates hydrodynamic conditions, while RMA4 uses the output of RMA2 to simulate constituent mixing and transport. In the future, SED2D-WES, another module that again uses RMA2 output could be used to compute sediment transport, scour, and deposition and bed elevation changes within the study area.

The RMA2 program is a two-dimensional, depth-averaged, FE hydrodynamic model that is two-dimensional in the horizontal plane. Like all vertically averaged schemes, it is not recommended where vortices, vibrations or vertical accelerations are of primary interest (Donnell et al., 2000). Vertically stratified flows are similarly beyond the capability of this model (Donnell et al., 2000). The TABS-MD model assumes the fluid is well mixed vertically with a hydrostatic pressure distribution; vertical acceleration is assumed negligible.

The RMA2 hydrodynamic module solves the depth averaged two-dimensional equations of continuity and momentum transport (Donnell et al., 2000):

$$h \frac{\partial u}{\partial t} + hu \frac{\partial u}{\partial x} + hv \frac{\partial u}{\partial y} - \frac{h}{p} \left[E_{xx} \frac{\partial^2 u}{\partial x^2} + E_{xy} \frac{\partial^2 u}{\partial y^2} \right] + gh \left[\frac{\partial a}{\partial x} + \frac{\partial h}{\partial x} \right] + \frac{gun^2}{(1.486h^{1/6})^2} (u^2 + v^2)^{1/2} - \zeta V_a^2 \cos \psi - 2hv\omega \sin \Phi = 0$$

----- Equation 1

$$h \frac{\partial v}{\partial t} + hu \frac{\partial v}{\partial x} + hv \frac{\partial v}{\partial y} - \frac{h}{\rho} \left[E_{,xx} \frac{\partial^2 v}{\partial x^2} + E_{,yy} \frac{\partial^2 v}{\partial y^2} \right] + gh \left[\frac{\partial a}{\partial y} + \frac{\partial h}{\partial y} \right] + \frac{g\nu n^2}{(1.486h^{1/6})^2} (u^2 + v^2)^{1/2} - \zeta V_a^2 \sin \psi + 2hu\omega \sin \Phi = 0$$

----- Equation 2

$$\frac{\partial h}{\partial t} + h \left(\frac{\partial u}{\partial x} + \frac{\partial v}{\partial y} \right) + u \frac{\partial u}{\partial x} + v \frac{\partial h}{\partial y} = 0$$

----- Equation 3

Where

h = Water depth

u, v = Velocities in the Cartesian directions

x, y, t = Cartesian coordinates and time

ρ = Density of fluid

E = Eddy viscosity coefficient,

for xx = normal direction on x axis surface

for yy = normal direction on y axis surface

for xy and yx = shear direction on each surface

g = Acceleration due to gravity

a = Elevation of bottom

n = Manning's roughness n-value

1.486 = Conversion from SI(metric) to non-SI units

ζ = Empirical wind shear coefficient

V_a = Wind Speed

ψ = Wind direction

ω = Rate of earth's angular rotation

Φ = Local latitude

Equations 1, 2 and 3 are solved by the finite element method using the Galerkin Method of weighted residuals. The elements may be one-dimensional quadrilaterals or triangles, and may have curved (parabolic) sides. The shape (or basis) functions are quadratic for velocity and linear for depth. Integration in space is performed by Gaussian integration (Donnell et al., 2000). Derivatives in time are replaced by a nonlinear finite difference approximation. Variables are assumed to vary over each time interval with the form

$$f(t) = f(t_0) + at + bt^c \quad t_0 \leq t < t_0 + \Delta t$$

----- Equation 4

which is differentiated with respect to time, and cast in finite difference form. Letters a , b and c are constants.

At the end of simulation RMA2 produces water depth and velocity at each time within the solution domain. Water depths and velocity fields produced by the RMA2 are used by RMA4 to solve the two-dimensional advection-dispersion equation.

The basic convection-diffusion equation is presented in Ariathurai et al. (1977) and Donnell (2000),

$$\frac{\partial C}{\partial t} + u \frac{\partial C}{\partial x} + v \frac{\partial C}{\partial y} = \frac{\partial}{\partial x} \left(D_x \frac{\partial C}{\partial x} \right) + \frac{\partial}{\partial y} \left(D_y \frac{\partial C}{\partial y} \right) + \alpha_1 C + \alpha_2$$

where

C = concentration, kg/m^3

t = time, sec

u = flow velocity in x-direction, m/sec

x = primary flow direction, m

v = flow velocity in y-direction, m/sec

y = direction perpendicular to x , m

D_x = effective diffusion coefficient in x-direction, m^2/sec

D_y = effective diffusion coefficient in y-direction, m^2/sec

α_1 = a coefficient for the source term, 1/sec

α_2 = the equilibrium concentration portion of the source term, kg/m³/sec

The key coefficients or parameters necessary to set up a TABS-MD model input file are the Manning's roughness (n) and eddy viscosity coefficients (Donnell et al., 1991; Moffatt & Nichol Engineers, 2000; Roig, 1994). Manning's roughness is the most commonly used parameter for calibration of the hydrodynamic model (Donnell et al., 2000).

Manning's roughness values, n , are expected to range from 0.020 to 0.035 for channels with sand beds (Chow, 1983). The value of n depends for the most part on water depth, vegetative cover and flow conditions. For a large alluvial river, Manning's values should change during a flood event (Simons and Sentruk, 1992). For an open and tidally influenced estuary, different researchers have used different roughness numbers. In Caminada Bay, Kjerfve (1973) used a Manning's value of 0.030, while Park (1998) used the value of 0.040 for a Barataria basin study. Using a much smaller model grid, Park (2002) found that for the same Barataria area, the value of 0.020 was more appropriate. In the Atchafalaya River and delta, a range of Manning values have been applied in earlier work. Donnell et al. (1991) used lower Manning values in the main deep channel and higher n values in the shallow bays. In the lower Mississippi River, hydrodynamic model values of the roughness varied from 0.015 to 0.020 in the main channel, and from 0.025 to 0.067 in the distributaries (USACE, 1990).

Turbulence is defined as the effect of temporal variation in velocity, and the momentum exchange associated with their special gradients (Donnell et al., 2000).

Donnell et al. (2000) discusses this concept further below:

“Galerkin methods of FE modeling, like some numerical model formulations, require the addition of a minimum level of artificial diffusion in order to obtain a ‘stable’ solution that converges in the Newton-Raphson iterative scheme.

The Galerkin method of weighted residuals used by RMA2 did not include any inherent form of stabilization other than the eddy viscosity term and requires a certain amount of added turbulence to achieve stability. However, if taken in excess, the velocity distributions could be smeared in space and time. It is difficult to establish a value for an eddy viscosity for the model being developed. Turbulence exchanges depend on the momentum of the fluid and the distance over which the momentum is applied.”

Values for eddy viscosities were determined mainly from the literature and values used in earlier Louisiana studies. Eddy viscosities were assigned to each element type and size.

A preliminary finite element mesh was developed, using the SMS 8.0 software package. A finite element mesh is defined as a network of triangular and quadrilateral

elements constructed from nodes. The creation of a finite element mesh requires the user to provide bathymetric information and to define the study area extremities.

The SMS software has the capability to import aerial photographs and satellite imagery as a backdrop to delineate water and land features. In this study, the Map Module in SMS was used to define the study area boundaries and water features. Later, SMS automatically generated a mesh or grid network from the map module and then interpolated the bathymetry data onto the mesh.

3.2.1.1 Swamp Geometry. The SMS map module was used to import a satellite image acquired in 2000 to delineate model boundaries and major water features. Detailed features of the Maurepas were added from 1 m resolution color infrared aerial photographs collected by the USGS in 1998. Configuration of channels and bank breaks had been determined from surveys carried out during the reconnaissance phase (Lee Wilson & Assoc. 2001). The topography of the swamp was developed from an analysis of raw Light Detection and Ranging (LIDAR) data acquired on the nights of March 3, 1999 and March 5 and 6, 2000 (3001, Inc. 2001). This was a leaf-off period for deciduous trees like the tupelo. At all times that this data was collected, the tide at the USACE Manchac station was unusually low, between 0.54 and 0.92 ft on the gage datum (Figure 3.3). The USACE gage is reported to be set to an NGVD27 datum, but appears to be 0.2 ft below the NAVD88 datum used to set gages on the other side of the lake in the study area. The built-in interpolate command in the mesh creator module of SMS was used to assign a depth for each individual node. Later, hand editing was done to fine-tune the topography and bathymetry in the model as additional data became available (Figure 3.4). Ultimately the model mesh included about 15,000 elements.

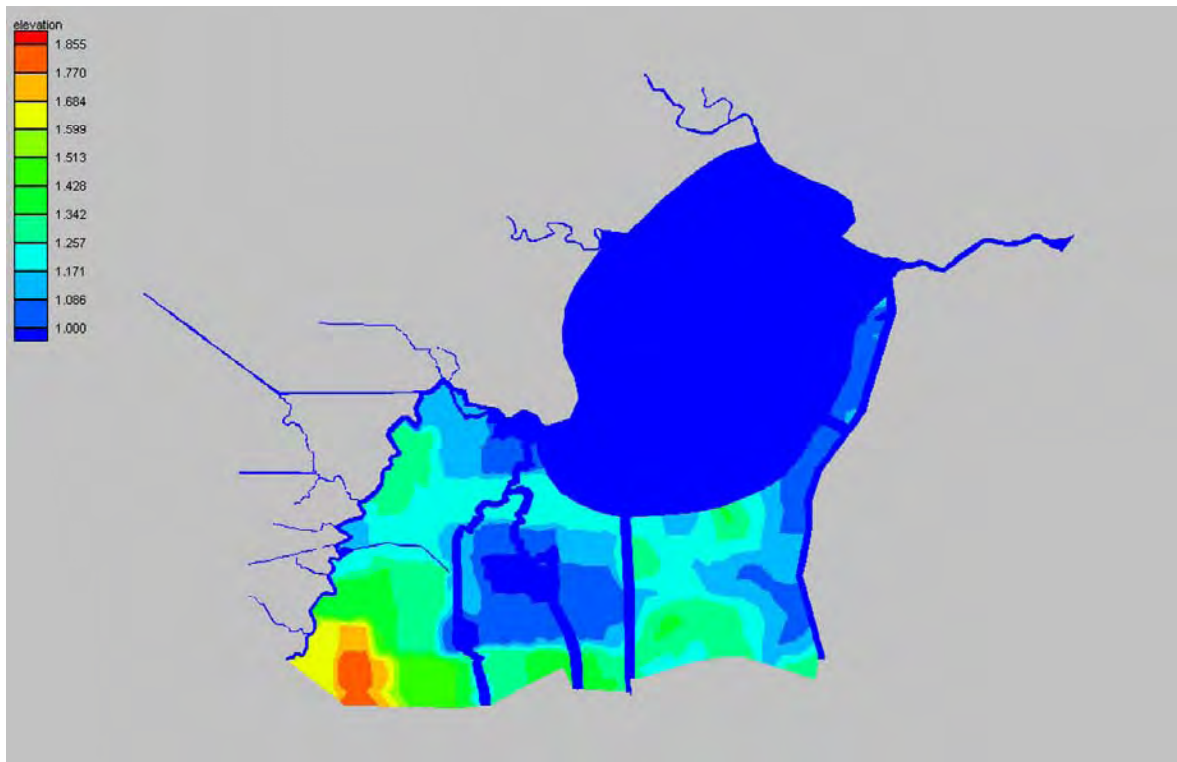


Figure 3.3 Maurepas swamp elevations (ft, NAVD88) derived from LIDAR and applied to TABS model

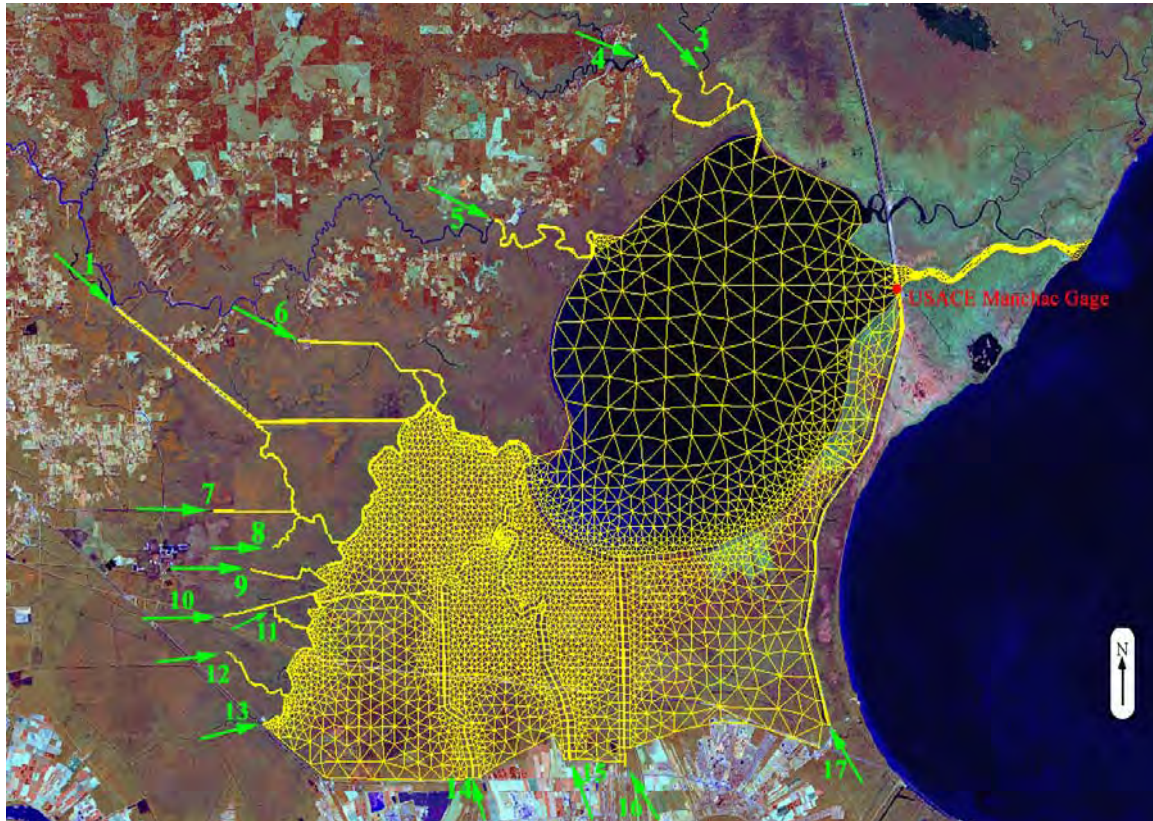


Figure 3.4 Maurepas hydrodynamic model domain showing FE grid, flow boundaries and the stage boundary at Pass Manchac.

3.2.1.2 Calibration. The model domain has 17 inflow boundaries, treated as static, corresponding to all of the streams flowing into Lake Maurepas, while Pass Manchac is specified as a dynamic tidal boundary (Figure 3.4). Once the grid was complete, water level and discharge data from December 26, 2003 to January 25, 2004 was selected for calibration. Information was available from nine water level gages for all or part of the calibration months and the ADCP was operating for the entire period. Connections between water features (rivers, canals and bayous) and swamps were simulated using an equivalent opening between swamp and channel as described in earlier reports (Lee Wilson et al. 2001; Mashriqui et al. 2002). In SMS (TABS-MD), this concept was utilized by making appropriate elements inactive (disabled). Connection within the swamp was continuous and mainly dictated by the bathymetry of the swamp floor.

Different Manning's n roughness values were used in the model, based on the type of water features and the vegetation type. A Manning's n of 0.03 was used in the lake and 0.025 was applied for the channels. The roughness values were raised in the swamp to 0.035. Roughness values were individually adjusted to achieve the closest match to water surface elevations observed at the calibration stations. An eddy viscosity of 400 lb-sec/ft^2 (19,160 Pascal-sec) was applied for all elements.

One of the most complex aspects of developing a model of swamp hydrology is the problem of realistically addressing wetting and drying of intertidal lands, and the lags and damping of the tidal signal as it is propagated through a variably flooded landscape.

Continuous stages recorded at eight stations were compared to model-simulated stages at the corresponding locations, and scatter diagrams of observed and simulated stages were also plotted, along with a perfect (1:1) match line (Figures 3.5 a - h). Beginning on the western margin of the study area in the Amite/Blind River system at S16 and S10, the model predicted peaks well, but reproduced about half the diurnal tide range, and more generally missed the lows by 0.2 ft (Table 3.2). Tide phase was captured well (Figures 3.5c, 3.5h). In the Hope Canal/Mississippi Bayou system, the model generally tracked the mean at S4, S9 and S5 and S11 (Figures 3.5c, 3.5h). The model captured the phase but underpredicted lows of the diurnal tide inland from the lake. Fidelity at the tidal frequency improved upstream from the lake (Figures 3.5a, 3.5b, 3.5e, 3.5f). Reproduction of water level and phase at the two swamp stations, SLU A and URS N was very good given that the datum of these gages has yet to be verified by survey (Figures 3.5d, 3.5g). The swamp appears to act as a low-pass filter, damping the tidal signal, and this is what the model predicts. Overpredicting the lows in the tide should not affect predicted flood duration within the swamp, because most of the missed part of the tidal frame is below the elevation of the swamp floor.

Table 3.2. Calibration Results (ft) for Maurepas Stations: December 26, 2003 to January 25, 2004

Station	Location	Obs. Range	Pred. Range	Obs. Mean	Pred. Mean	RMS Error	% Range
S16	Blind@I-10	1.43	1.00	1.13	1.38	0.34	24
S10	Blind@AmiteD	1.48	1.13	1.31	1.37	0.18	12
S4	Dutch@Lake	1.41	1.35	1.41	1.36	0.11	8
S9	Dutch@MissB	1.36	1.10	1.27	1.37	0.17	13
SLU A	Swamp@S9	0.49	1.15	1.62	1.37	0.27	56
S5	Hope@Hy61	1.12	0.99	1.37	1.38	0.13	12
URS N	Swamp@S13	0.52	1.01	1.27	1.38	0.24	46
USACE	Pass Manchac	1.66	Boundary	1.15			
USGS 1	Reserve@Lake	1.42	1.19	1.08	1.23	0.16	12
Mean				1.29	1.23	0.18*	14*
ADCP	Dutch@Miss B	76 cm-s ⁻¹	31 cm-s ⁻¹	-5 cm-s ⁻¹	-4 cm-s ⁻¹		

Mean does not include swamp stations where model predicts water level below ground elevation

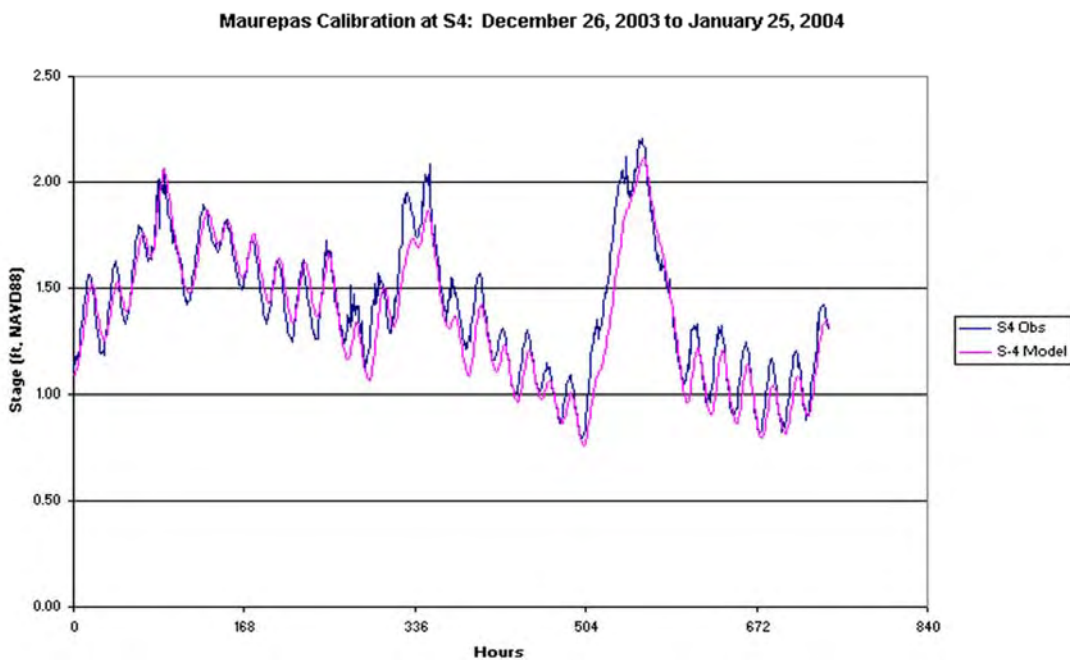


Figure 3.5(a) Calibration series: predicted and observed water level at S4 for December 26, 2003 to January 25, 2004

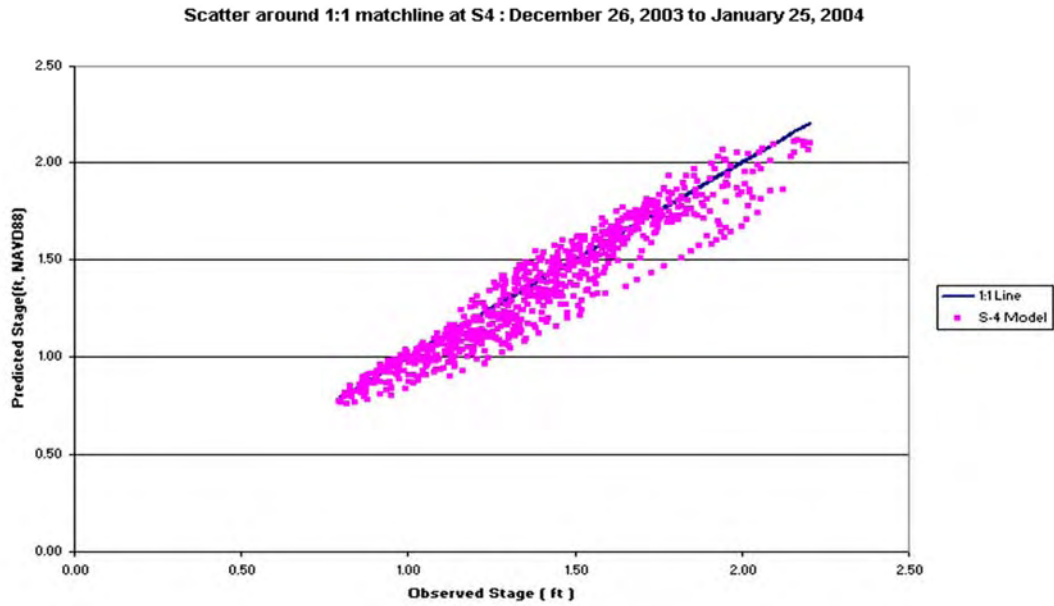


Figure 3.5(a) Calibration series: Scatter around 1:1 match line between predicted and observed water level at S4 for December 26, 2003 to January 25, 2004

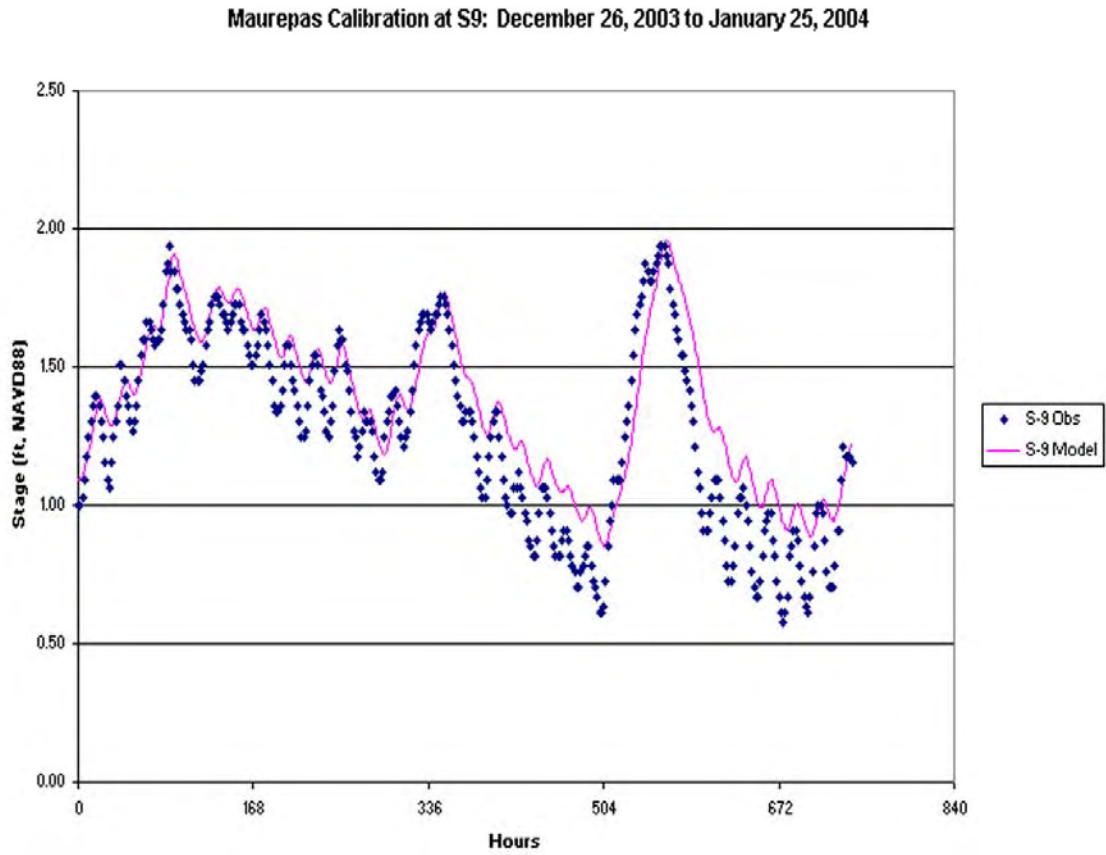


Figure 3.5(b) Calibration series: predicted and observed water level at S9 for December 26, 2003 to January 25, 2004

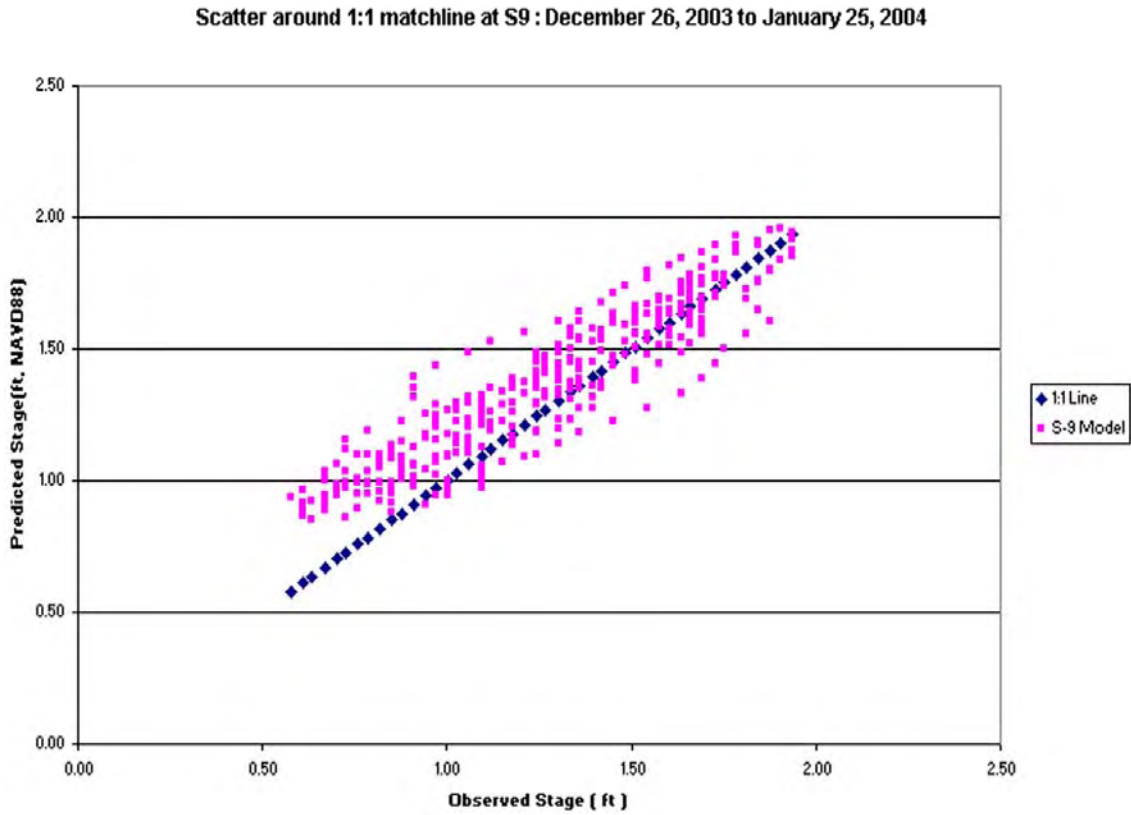


Figure 3.5(b) Calibration series: Scatter around 1:1 match line between predicted and observed water level at S9 for December 26, 2003 to January 25, 2004

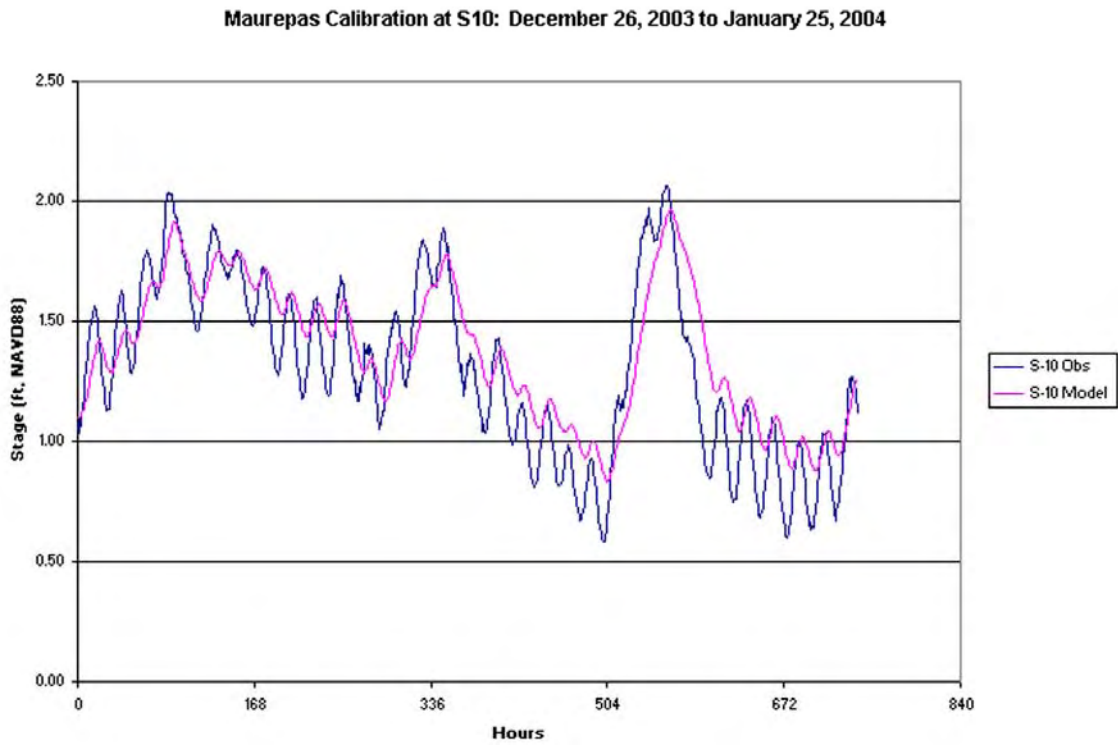


Figure 3.5(c) Calibration series: predicted and observed water level at S10 for December 26, 2003 to January 25, 2004

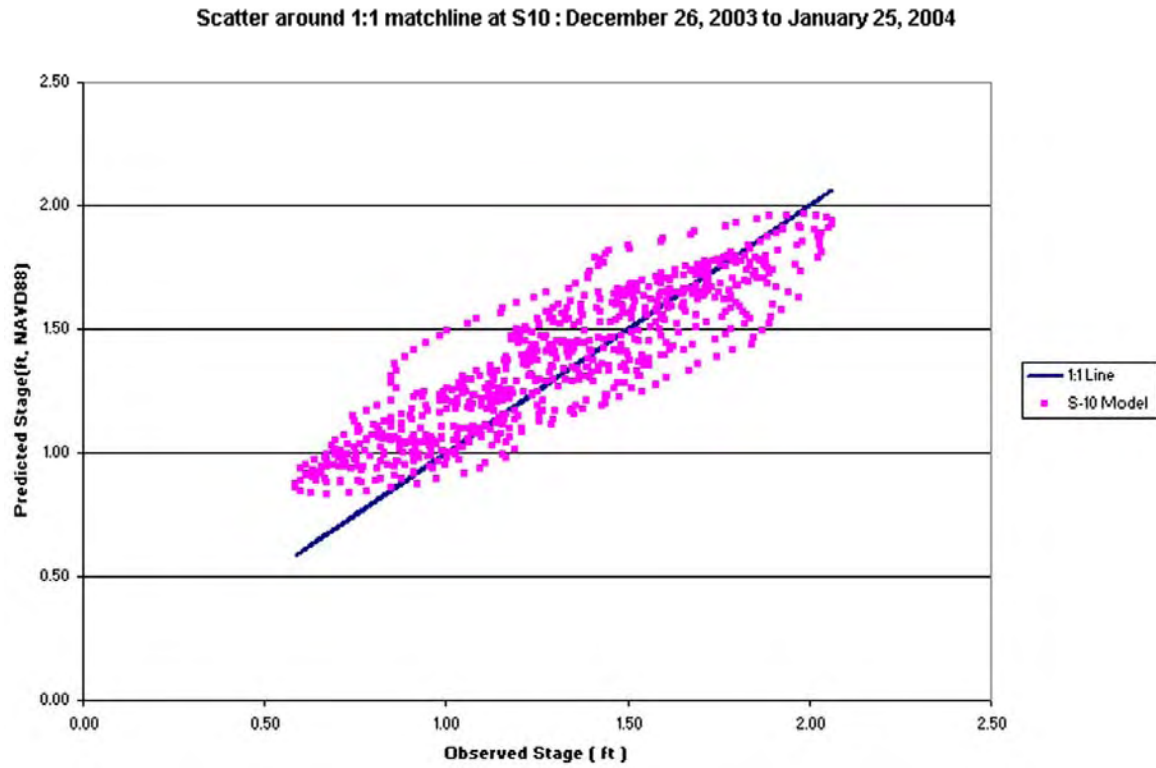


Figure 3.5(c) Calibration series: Scatter around 1:1 match line between predicted and observed water level at S10 for December 26, 2003 to January 25, 2004

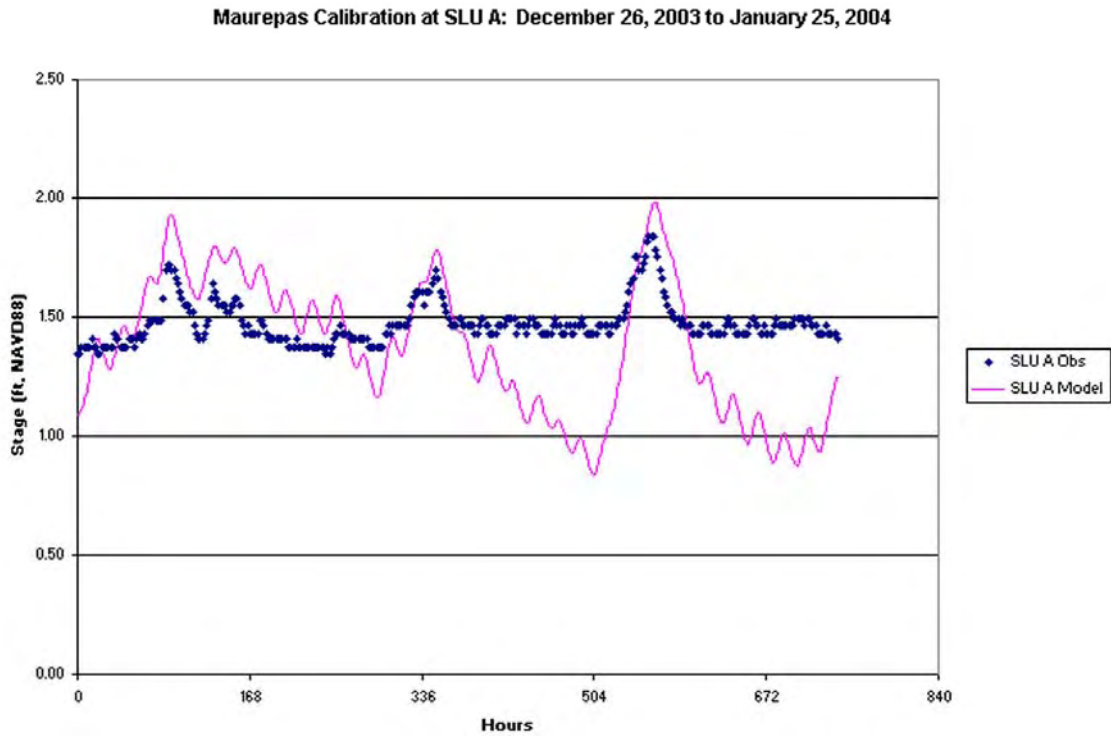


Figure 3.5(d) Calibration series: predicted and observed water level at SLUA for December 26, 2003 to January 25, 2004

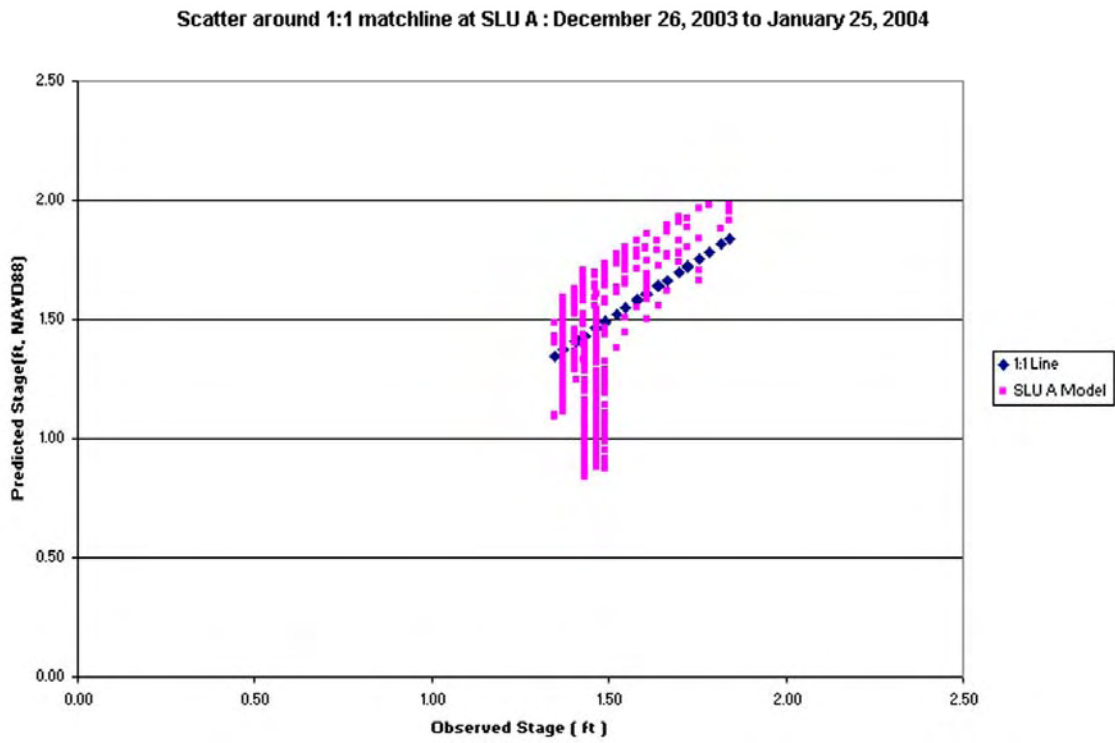


Figure 3.5(d) Calibration series: Scatter around 1:1 match line between predicted and observed water level at SLUA for December 26, 2003 to January 25, 2004

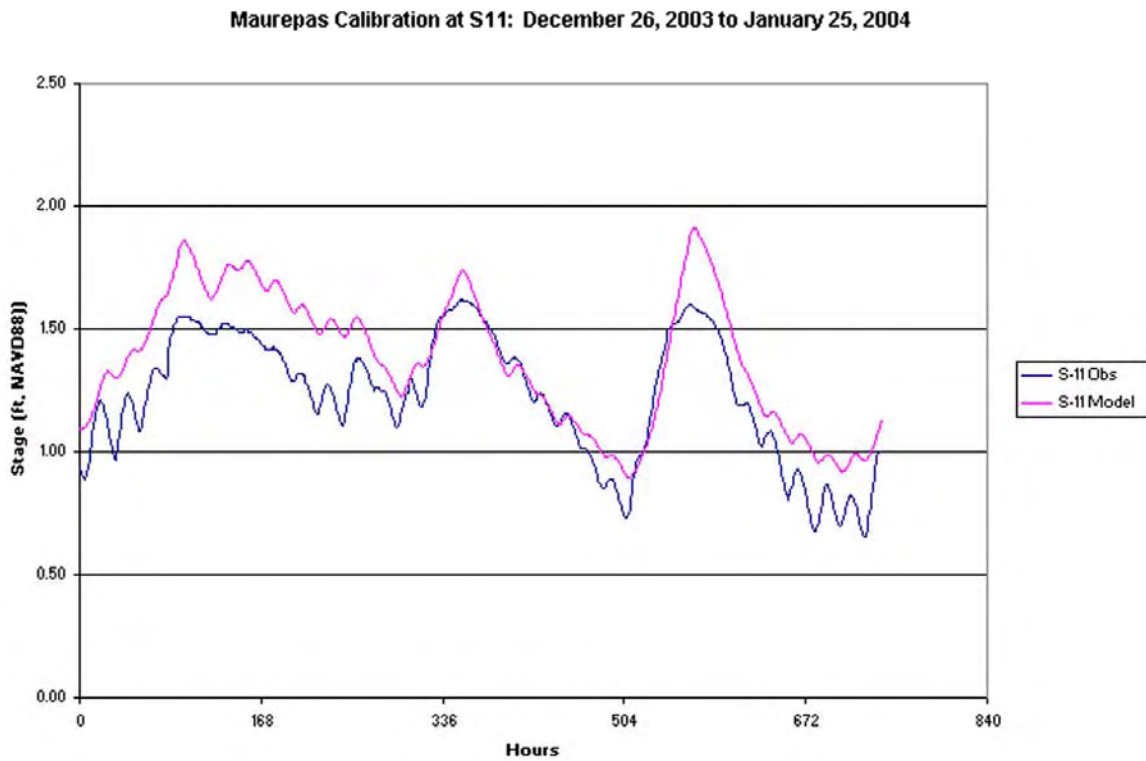


Figure 3.5(e) Calibration series: predicted and observed water level at S11 for December 26, 2003 to January 25, 2004

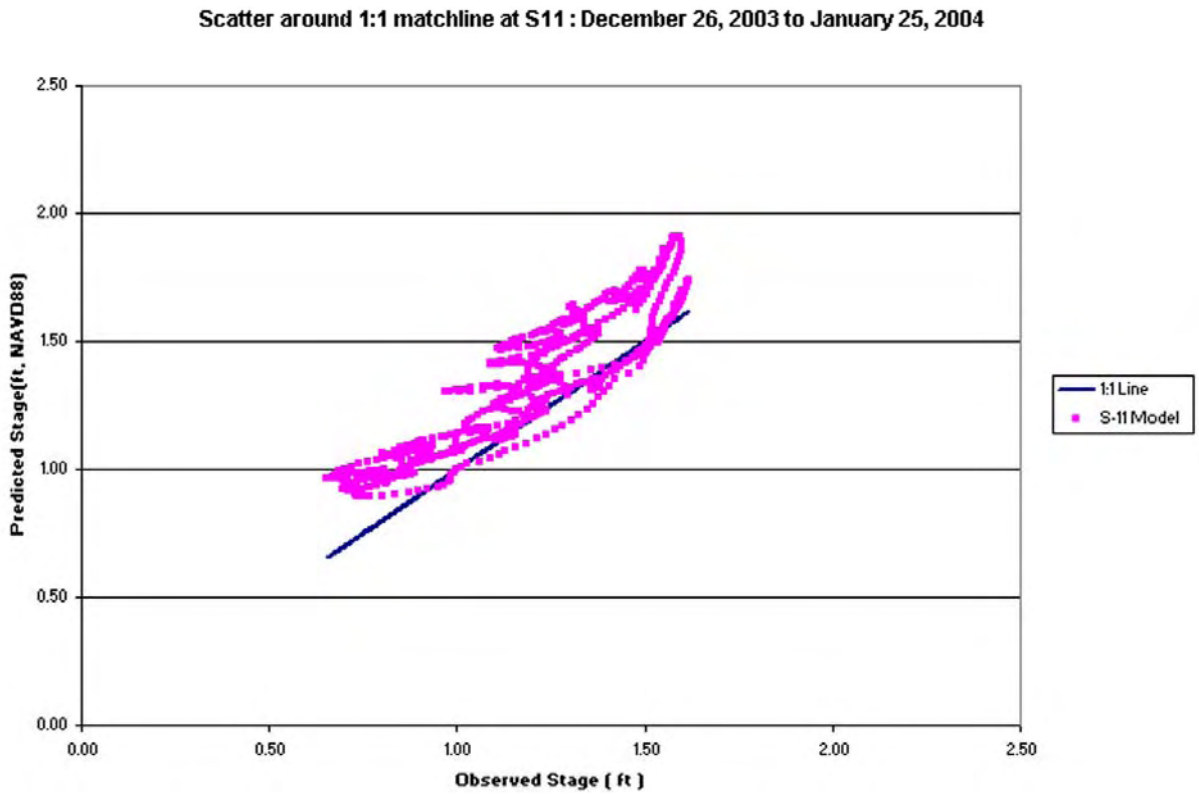


Figure 3.5(e) Calibration series: Scatter around 1:1 match line between predicted and observed water level at S11 for December 26, 2003 to January 25, 2004

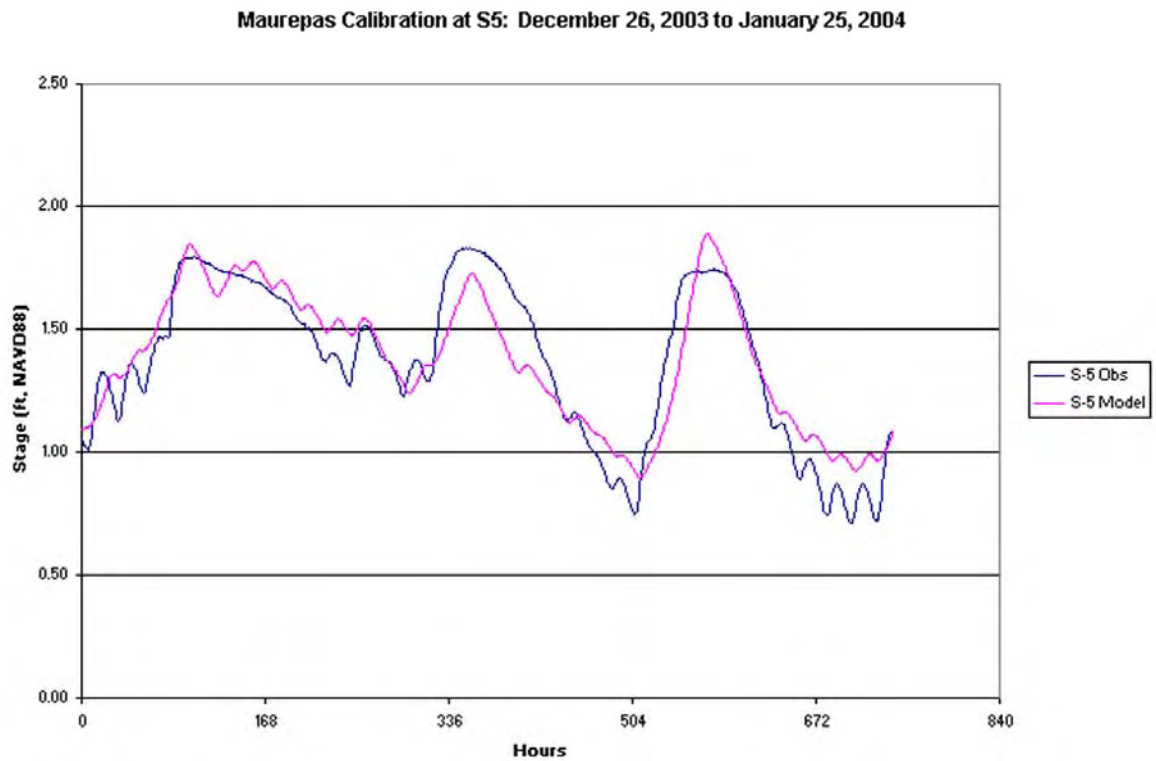


Figure 3.5(f) Calibration series: predicted and observed water level at S5 for December 26, 2003 to January 25, 2004

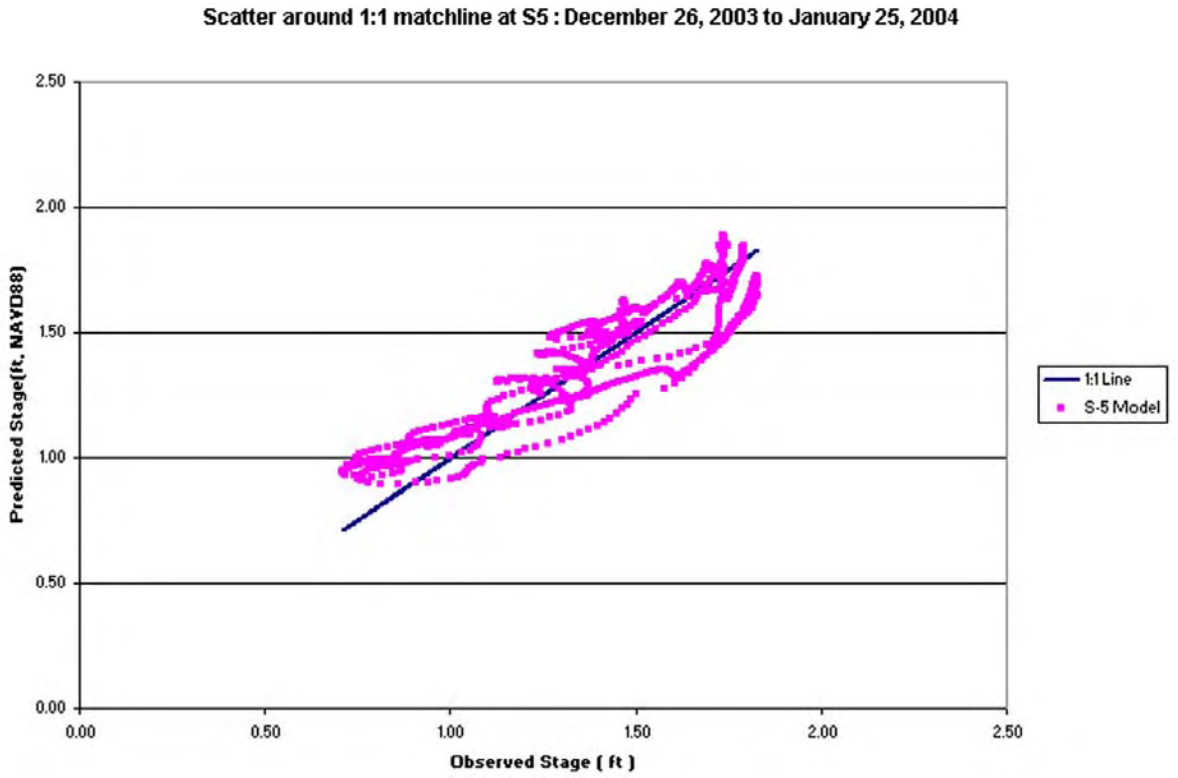


Figure 3.5(f) Calibration series: Scatter around 1:1 match line between predicted and observed water level at S5 for December 26, 2003 to January 25, 2004

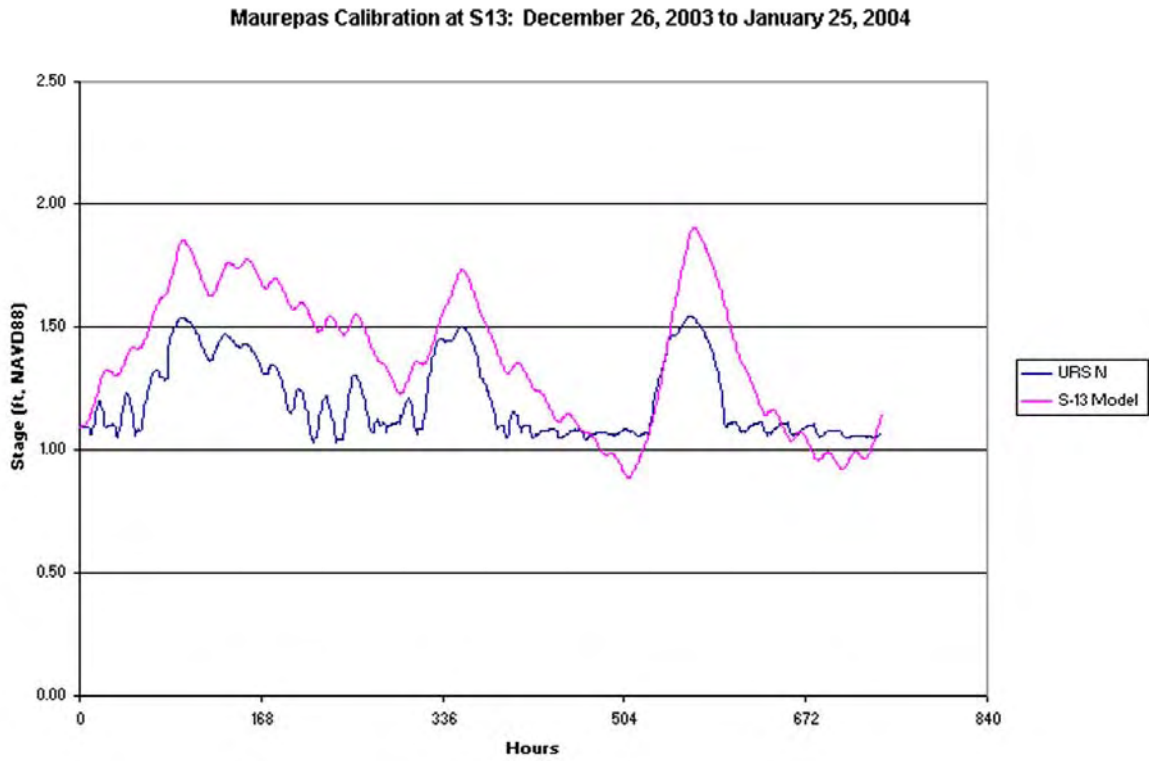


Figure 3.5(g) Calibration series: predicted and observed water level at URS N for December 26, 2003 to January 25, 2004

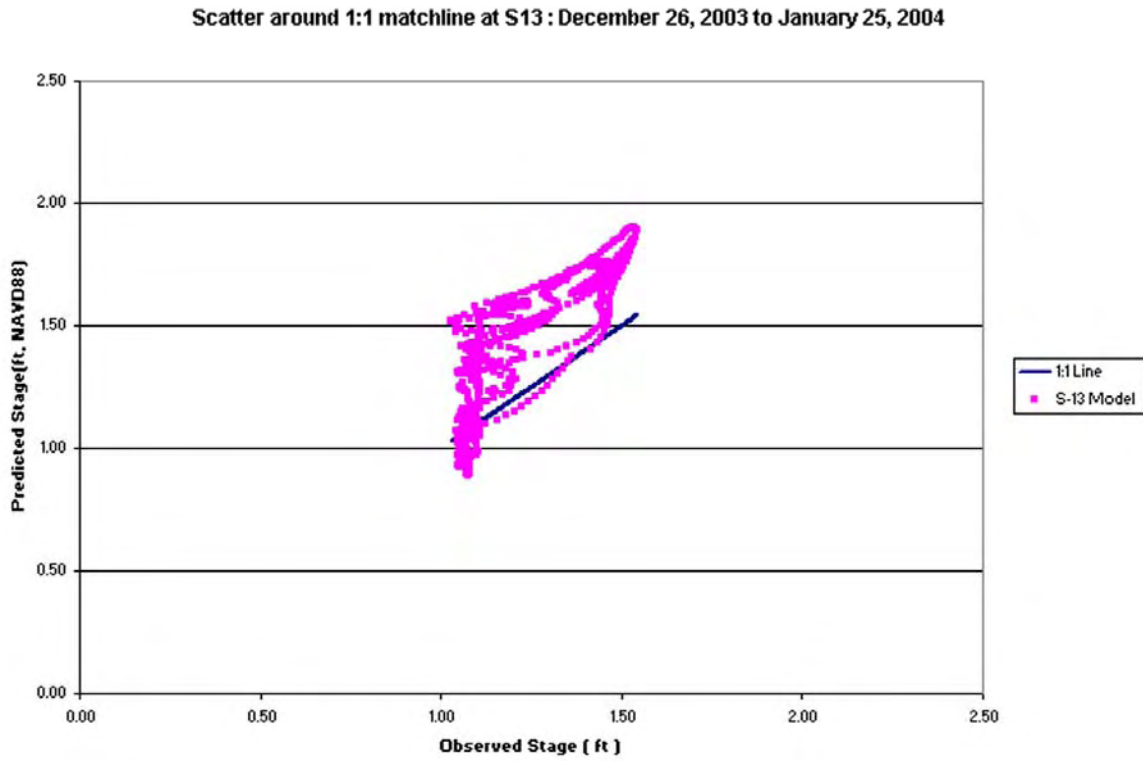


Figure 3.5(g) Calibration series: Scatter around 1:1 match line between predicted and observed water level at URS N for December 26, 2003 to January 25, 2004

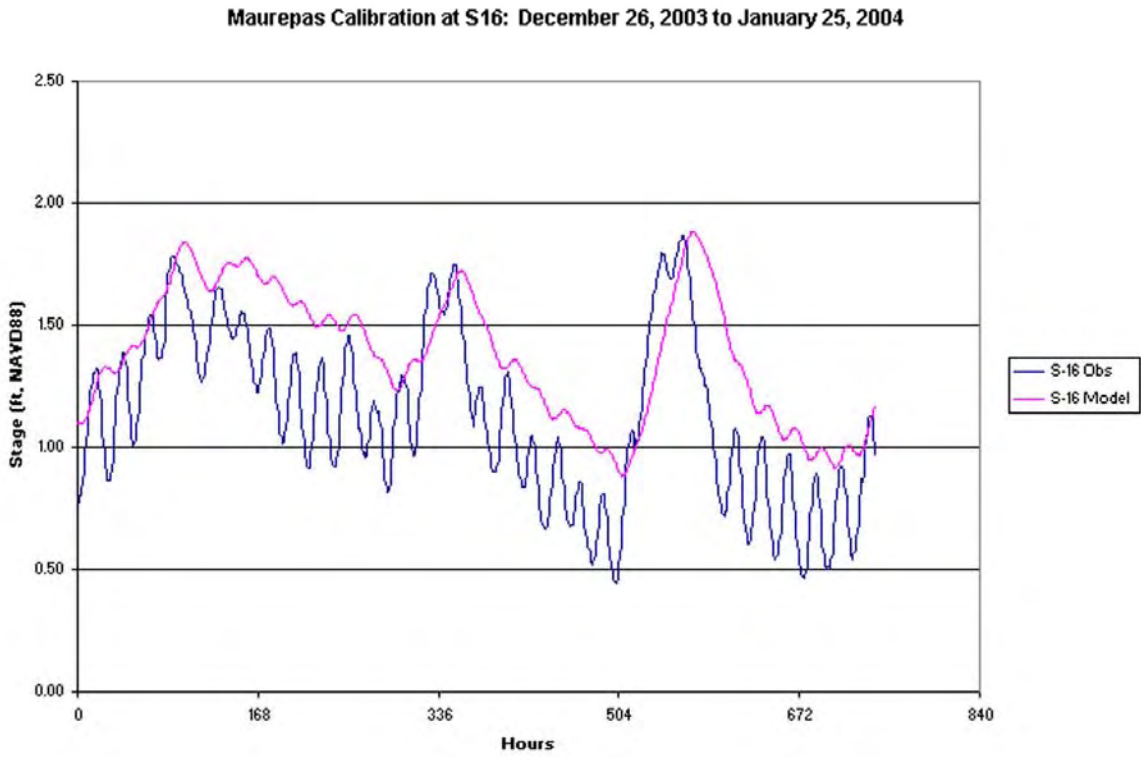


Figure 3.5(h) Calibration series: predicted and observed water level at S16 for December 26, 2003 to January 25, 2004

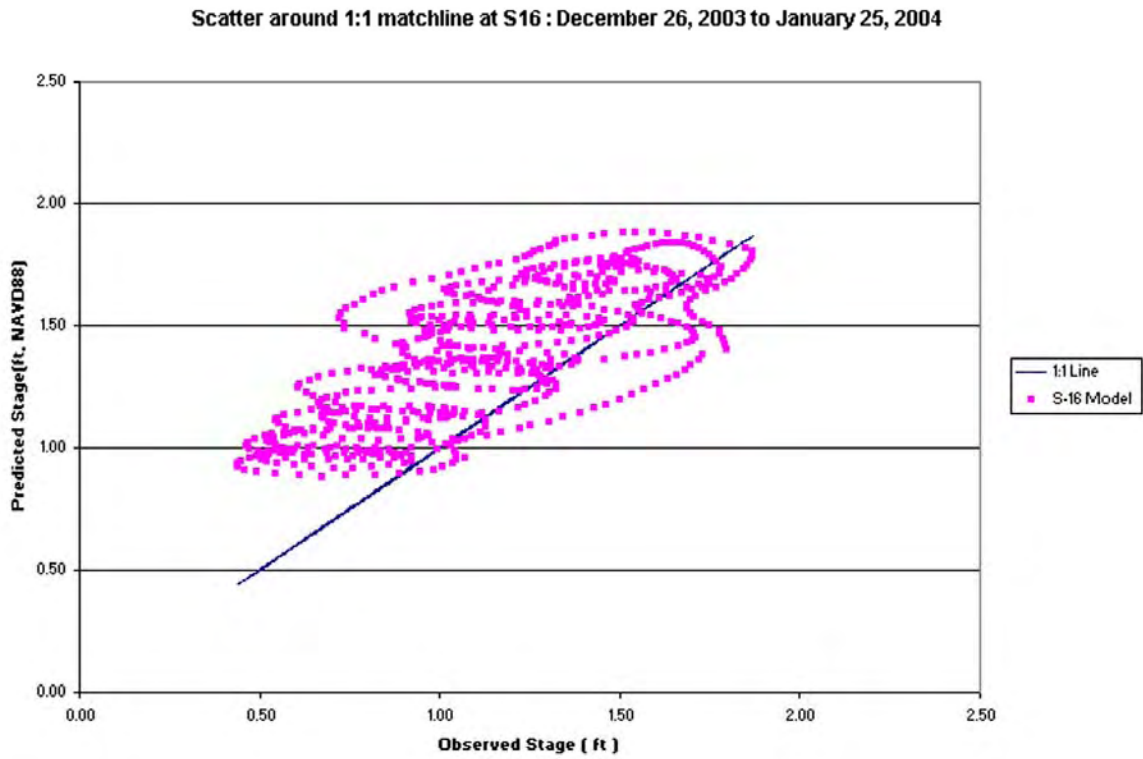


Figure 3.5(h) Calibration series: Scatter around 1:1 match line between predicted and observed water level at S16 for December 26, 2003 to January 25, 2004

Several researchers have determined the goodness of fit of hydrodynamic models by computing the absolute difference mean (ADM) and root mean square differences (RMSD) between observed and simulated stage (Liu et al., 2002; Hsu et al., 1999). The Root Mean Square Difference (RMSD) between observed and modeled data is calculated by summing the square of the difference between the two, then taking the square root of the total and dividing it by the number of records.

$$RMSD = \sqrt{\frac{1}{n} \sum_{i=1}^n (simulated - observed)^2}$$

RMSD provides a measure of variance between observed and simulated stages. Performance of the calibrated Maurepas model was evaluated using the RMSD method (Table 3.2). RMS error for the channel stations varied from 0.11 to 0.34 ft, averaging 14 percent of the observed range. RMS error in the swamp could not easily be determined because an artifact of the model is that it produces predictions for water level below the ground surface (Table 3.2). In Maurepas, stage fluctuation is a complex function of river flow, tide, and wind-driven set-up. Some discrepancies between the model and the observed data should be expected, given that all forcing functions (e.g., wind) were not included in the calibration.

3.2.1.3 Validation. When the model was acceptably calibrated to water level, model output was checked against velocity measurements in Dutch Bayou and the salinity gradient observed during the drought of 2000 (Lane et al. 2003).

Velocities recorded by the ADCP at S9 in Dutch Bayou during the calibration period (Figures 3.6) were compared with those predicted by the model for the same interval. Average simulated velocity was compared to measured velocity (Table 3.2). Predicted and observed mean velocities were similar for the calibration period, indicating a net downstream flow of 5 and 4 $\text{cm}\cdot\text{s}^{-1}$, respectively. Phase agreement was good, but the model predicted significantly higher peak velocities than were observed (Figure 3.7) and this resulted in considerable scatter around the 1:1 match line (Figure 3.8). Because the X and Y components of the model velocity vectors are not precisely oriented in the along-channel direction, it is possible that this is contributing to some of the apparent error. The ADCP reports an average velocity across the entire channel cross-section while the model reports at only three nodes, thus it is possible that the ADCP is including relatively low velocity areas outside the main channel. In any event, further field analysis of exactly what the ADCP is measuring is required to quantitatively relate average velocities to discharges predicted by the model.

Salinities between April 2002 and May 2004 did not exceed 0.5 ppt anywhere in the study area, except near Pass Manchac. Three YSI instruments have been collecting continuous data since January, 2004, within the study area near the lake, but have yet to report more than 0.5 ppt. Synoptic data reported by Lane et al. (2003) from 2000 was useful, however, in establishing the salinity gradient that can develop under extreme conditions. The water quality model (RMA4) was run for 2 months after being started with 7 ppt everywhere, and 10 ppt at the Pass Manchac boundary.

Normal boundary inflows gradually reduced salinity within the model domain (Figure 3.7). After 300 hours, the predicted salinity was compared with observations for September 2000 (Figure 3.8). The model reproduced observed spatial patterns of salinity in the study area, with a small area of zero salinity in the southwest corner of the study area maintained by minimal discharges from the Amite/Blind system.

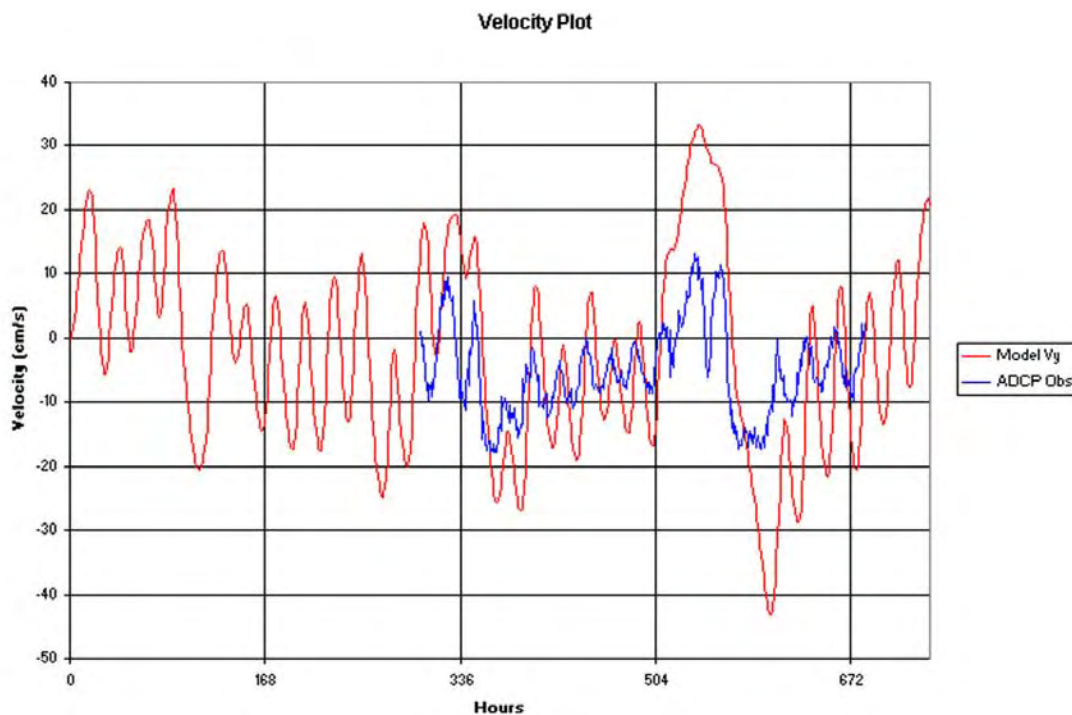


Figure 3.6(a) Validation: predicted and observed (ADCP) velocity at S9 for January 9, 2004 to January 23, 2004

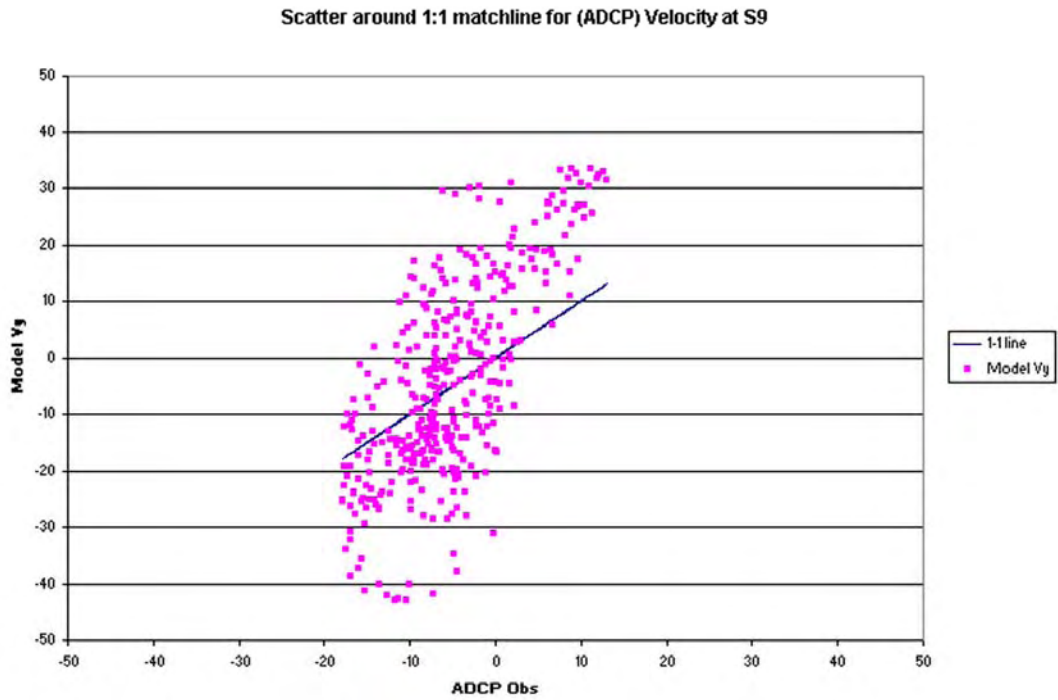
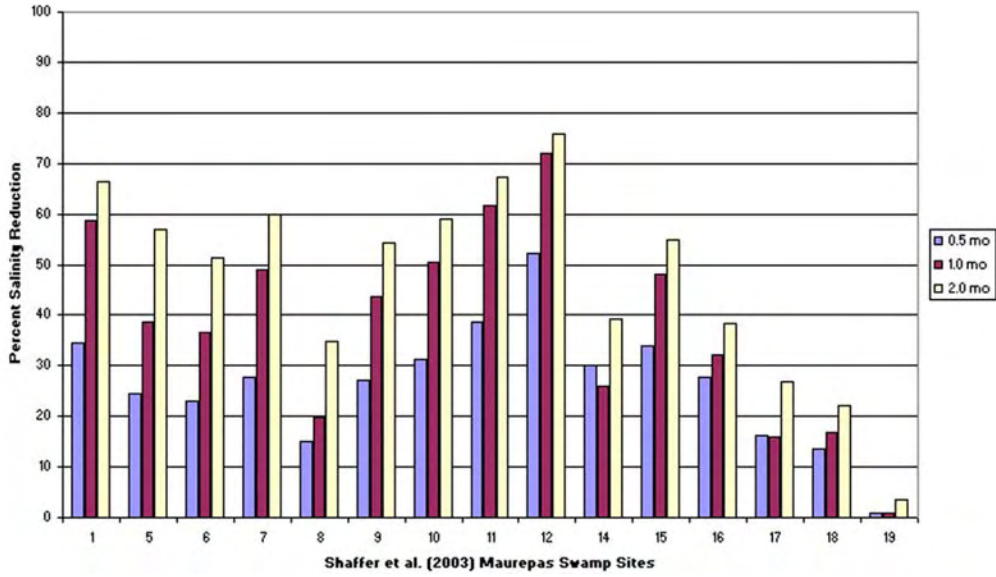


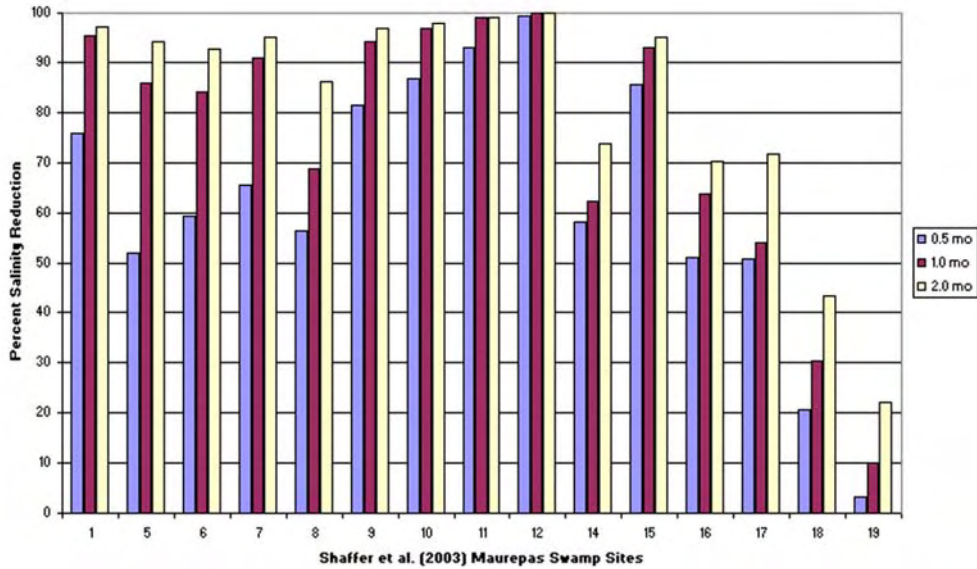
Figure 3.6(b) Validation: Scatter around 1:1 match line between predicted and observed (ADCP) velocity at S9 for January 9, 2004 to January 23, 2004

Salinity Reduction at Maurepas Swamp Sites for Existing Hope Canal Discharge (5 cfs) After 0.5, 1.0 and 2.0 Months

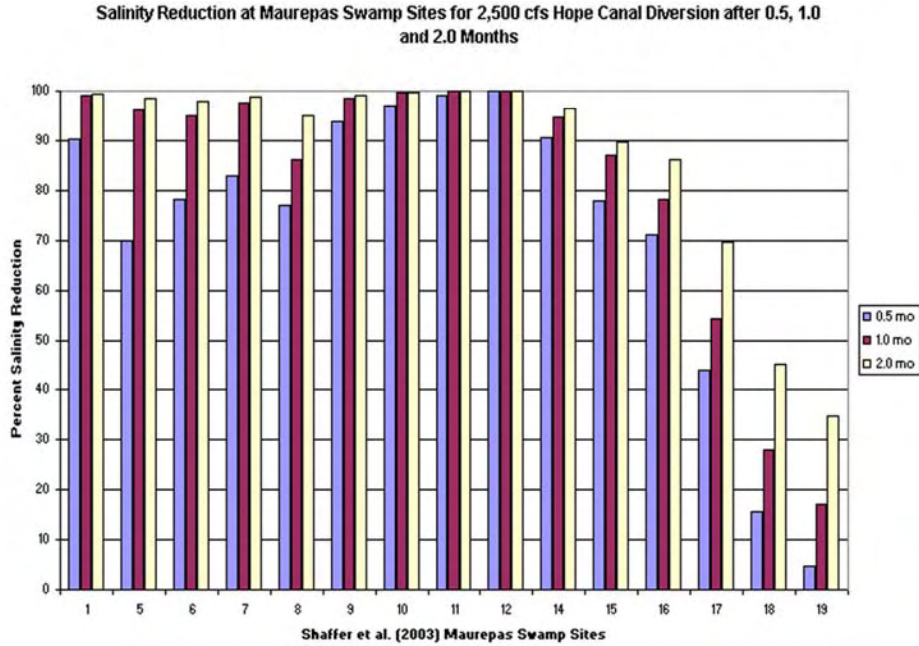


(a)

Salinity Reduction at Maurepas Swamp Sites for 1,500 cfs Hope Canal Discharge After 0.5, 1.0 and 2.0 Months



(b)



(c)

Figure 3.7 Validation: Model predictions of salinity for two months at swamp stations from Shaffer et al (2003) beginning with a uniform 7 ppt distribution and 10 ppt at the Pass Manchac boundary

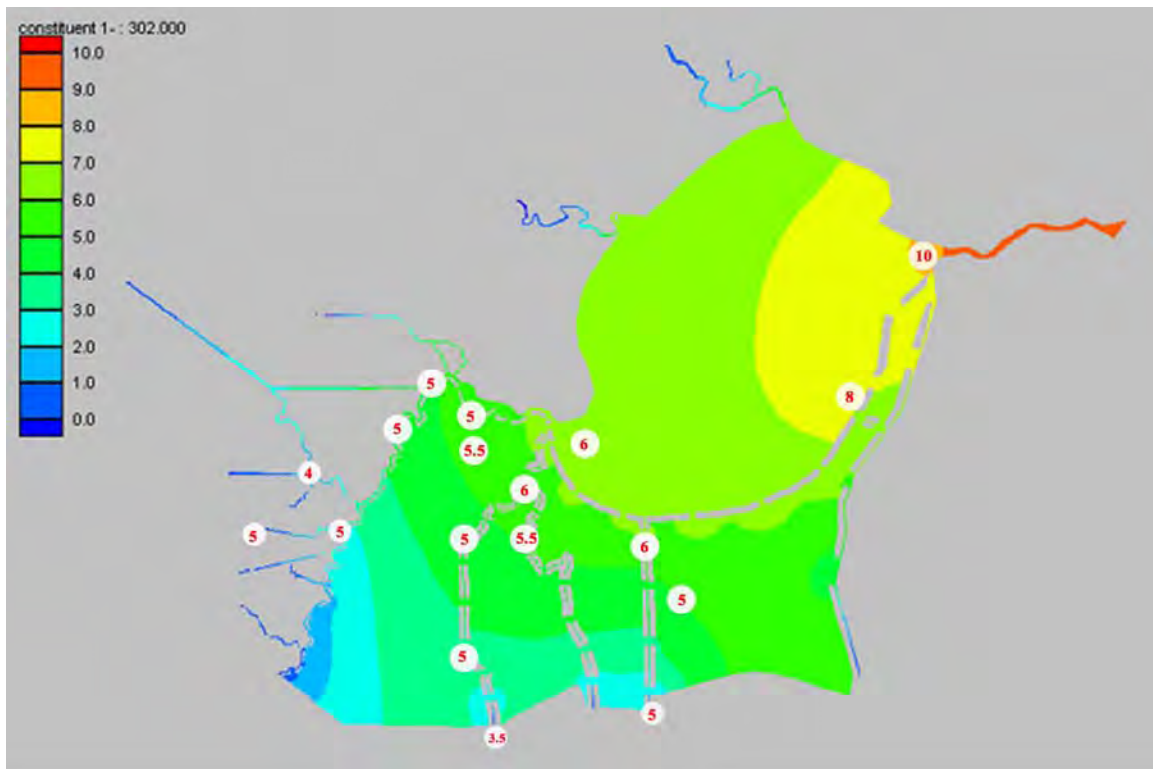


Figure 3.8 Validation: Model prediction for salinity after 302 hours, compared with values observed by Lane et al. (2003) for September 2000

3.2.2 Ecological Forecasting. One objective of this work was to develop a model, or a modeling approach to predict the trajectory of swamp productivity and sustainability, and more importantly, the likely forest response to diverted river water, sediments and nutrients. A successful parameterization requires integration of site-specific information on forest ecology (Shaffer et al. 2003), water quality (Lane et al. 2003) and hydrology. The key is to understand the interplay of hydrologic and biological factors that will together govern the germination, competition and mortality of swamp trees over time.

3.2.2.1 Forest Patchiness. Forest plot data is available from Shaffer et al. (2003), but it would be useful from a modeling perspective to also have a set of ecologically meaningful measurements that provide a more uniform spatial coverage. Accordingly, LIDAR data was extracted in manageable panels and analyzed to develop spatial measures of tree density, size and patchiness. The LIDAR data includes returns from the top of the tree canopy, from the ground, and from layers in between. LIDAR data from a representative panel was “sliced” to extract return counts from various levels above the ground surface. As is expected, the largest number of returns is from the 0 to 1 m slice in all panels as this includes the ground surface. The returns count for 1 to 3 m, 3 to 6 m, 6 to 12 m, and for greater than 12 m were plotted (Figure 3.9). It was found that the returns count showed little difference in slices between 3 and 12 m, but was markedly higher or lower for the 12+ m slice. Because the landscape is not uniformly “painted” by the

LIDAR laser, a way to normalize return counts was necessary if different parts of the forest were to be compared.

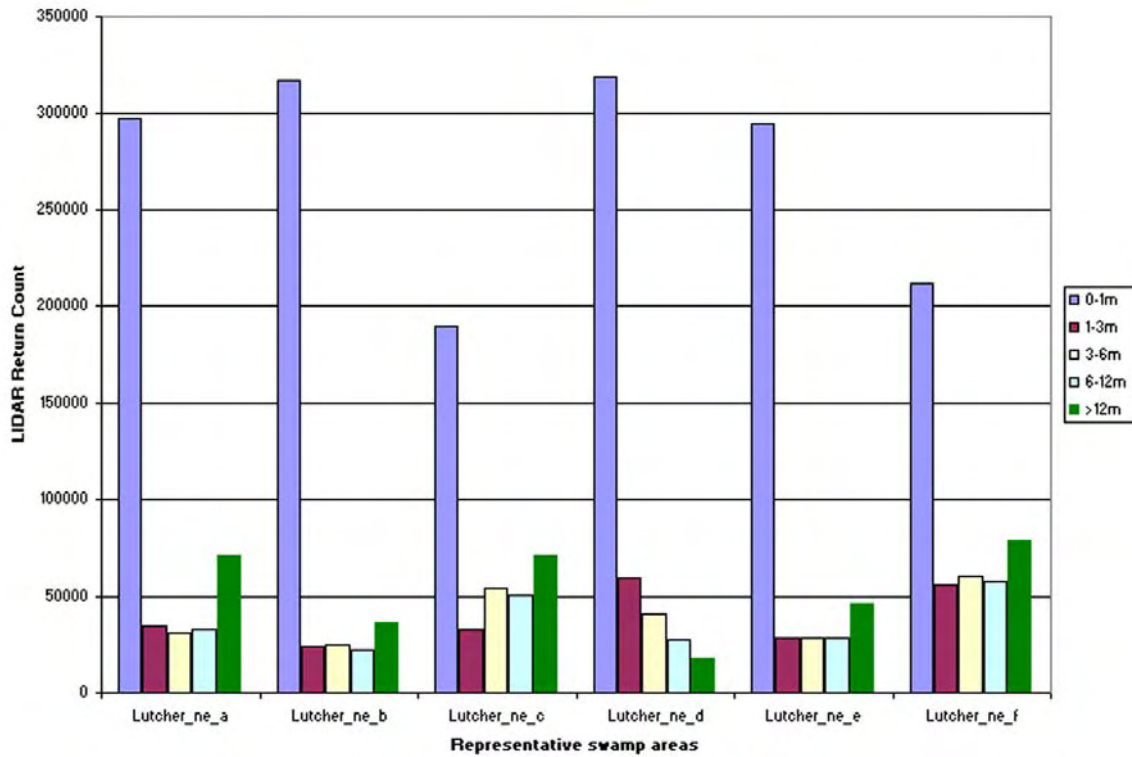


Figure 3.9 LIDAR return count from different elevation slices at representative stations in the Maurepas swamp forest

A simple Canopy Index was developed that would tend to emphasize differences in forest structure, but also facilitate comparison across the study area.

$$CI = 0 - 1 \text{ m Return Count} / 12+ \text{ m Return Count}$$

Thicker forest canopies will result in a lower CI both by generating a larger number of 12+ m returns, and by reducing the number of 0 – 1 m returns. Conversely, more open scrub, shrub areas that are in transition to marsh, or areas dominated by deciduous tupelo trees without leaves will generate a higher CI. These values were derived for the study area, interpolated and mapped (Figure 3.10). If different CI values are found to correspond to some indication of forest health or, conversely, cumulative stress, then it will be possible to generalize the information developed by Shaffer et al. (2003) and from the hydrodynamic model to the landscape as a whole.

3.2.2.2 Nutrient Model. Nitrate nitrogen is the nutrient form that occurs in Mississippi River water at high concentrations relative to background in the swamp or Lake Maurepas. Processing of nitrate by the swamp must be effective if nutrient, and specifically nitrate, loading to the lake is to be reduced to acceptable levels.

When the diversion is initiated, water first flows into storage in the swamp and little reaches Blind River or the lake. Residence time for water entering the swamp at this time is long, allowing for more effective nutrient assimilation. After the diversion is shut down, the head driving transport is removed and, again, residence time rises.

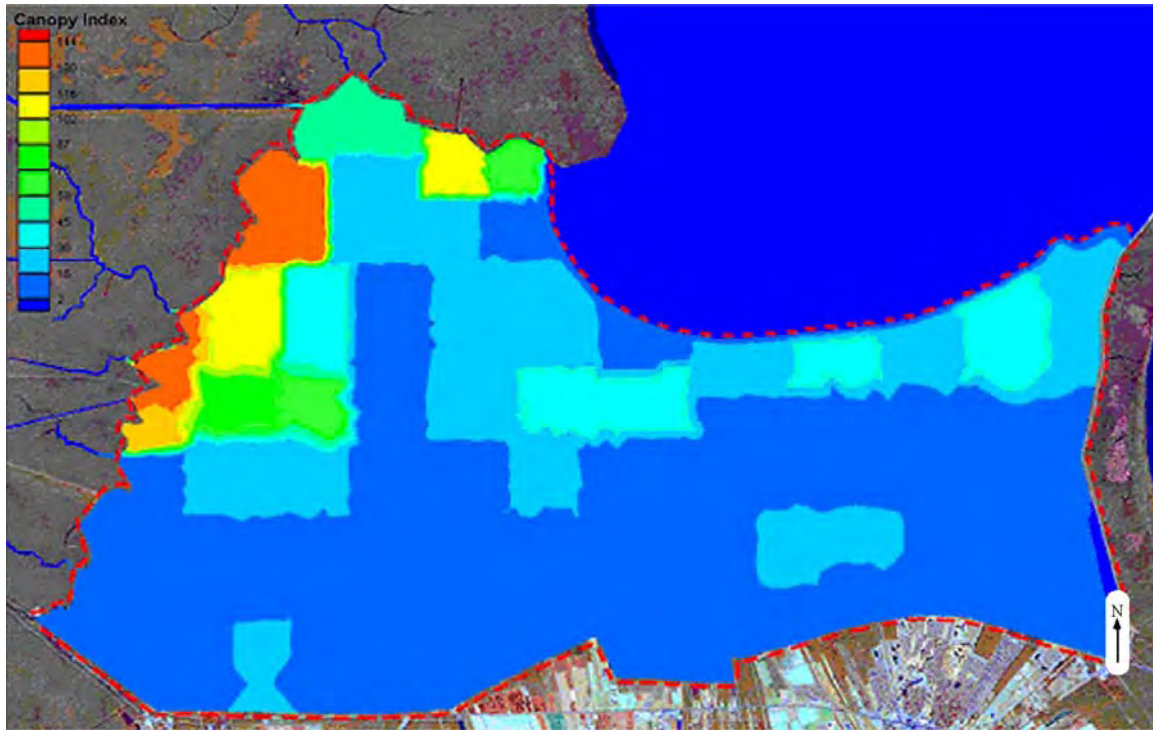


Figure 3.10 Mapping the Maurepas Canopy Index (CI) from LIDAR in the winter. Higher values (warmer colors) indicate fewer tall trees, more deciduous trees and less canopy cover. Lower values (blues) suggest taller trees, less deciduous trees and more canopy cover.

The critical design condition with respect to nitrate uptake is most closely approached when the swamp has reached its full storage capacity. Tides alternately increase and decrease velocities, and cause circulation, mixing and dilution, but Mississippi River water is flowing continuously across the swamp in something of a steady state. One objective of the modeling program was to determine when the diversion discharge would reach a fully developed state. Comparison of conditions developed for up to three months of continuous simulation suggests that this appears to take place within the first month.

Mississippi River water will be conveyed by a large levee-lined channel to the I-10 bridge before it is released into the Hope Canal channel. This channel was determined to have a capacity to convey about 100 cfs at bank-full (Mashriqui et al. 2002). The water that is lost from the channel is discharged into the adjacent swamp through natural and artificial breaks in the banks. In the earlier model the swamp study area was divided into storage cells represented as labeled polygons (Figure 2.1) of known area. A cascade routing scheme was developed to transfer water down gradient between cells after nutrients were processed in the up-gradient cell (Lane et al. 2003).

The most conservative approach to estimating nitrate assimilation and throughput assumes that all water in the swamp is derived from the Mississippi River. This was the approach that was taken in the earlier 1D-modeling program. In reality, water in the swamp comes from a variety of sources that are likely to contribute little nitrate.

The 2D model allows this dilution to be taken into account. The approach used here is to introduce a fictitious artificial tracer at the diversion and capture its concentration within the study area at a single time after fully developed flow is achieved. The cascade of cells employed in the 1D model was modified slightly by dividing two of the larger second (Cell 27) and third tier (Cell 28) cells east of Hope Canal into two cells each (Cells 27a and 27b, Cells 28a and 28b). Mean tracer concentrations in the cells adjacent to Hope Canal, and examination of flow lines, are used to apportion river flow among the first tier of cells. A similar process is followed for the next concentric ring of cells (second tier), and so on. Water leaving the channel cascades from one swamp cell into the next adjacent down-gradient cell until it reaches a boundary, whether Blind River, Lake Maurepas or the Reserve Relief Canal. The Bourgeois Canal and the Mississippi Bayou system have the potential to intercept flow. The 2D hydrodynamic model provides an ability to estimate residence time and throughput from velocity.

Water leaves the Mississippi River and Hope Canal with an assumed nitrate concentration of 1.5 g N m^{-3} (ppm), but the entering concentration for cells receiving water indirectly must be determined based on loading and processing by the up gradient swamp cell. Loading ($\text{g N m}^{-3} \text{d}^{-1}$) is an area function of the input concentration, the rate of water introduction, and size of the receiving swamp cell. Because denitrification occurs so rapidly, and this is the most significant transformation process in the swamp, all loading calculations are made on a daily basis ($\text{g m}^{-2} \text{d}^{-1}$).

The capacity of the surface area of wetlands for removal and assimilation of nitrate is variable but has been plotted for a range of daily loadings (Figure 2.12). Removal efficiency (% removal) decreases in a non-linear fashion as loading increases, as

$$\% \text{Removal} = -14.13 \ln(x) + 25$$

where x is the NO_3 loading ($\text{g m}^{-2} \text{d}^{-1}$). A suite of diversion scenarios using different combinations of monthly discharges of 500, 1,500 and 2,500 cfs was developed for testing nitrogen loading and assimilation under a range of possible operating schedules (Table 3.3).

Discharge (cfs)	Scenario A	Scenario B	Scenario C	Scenario D	Scenario E	Scenario F	Scenario G
500	0	0	3	3	6	9	12
1,500	0	6	7	9	6	3	0
2,500	12	6	2	0	0	0	0
Mean Annual Discharge	2,500	2,000	1,417	1,250	1,000	750	500

3.2.2.3 *Stress Dynamics*. Shaffer et al. (2003) have shown that the application of stress in the form of excessive flooding, nutrient-deprivation and salinity is spatially heterogeneous, while the relict stands of surviving trees on which the stresses operate are also patchy. As the levels of stress are alleviated or changed as a result of the proposed diversion, recovery will not be uniform. We have been working with Drs. K. A. Rose, E. Reyes, and G. Shaffer, along with Susanne Hoepfner, a Ph.D. student, to develop an “individual-oriented model” (IOM) approach to predicting tree growth and competition under various levels of stress. This approach was presented in concept at the Estuarine Research Federation meeting that took place in September, 2003, in Seattle (Hoepfner et al. 2003). The model follows the growth, competition, recruitment, and death of individual trees of the dominant species (bald cypress, water tupelo, red maple, green ash) in 1-ha plots. The plots were arranged to allow for spatial gradients of the main stressors in the model, which consist of salinity, flooding, and nutrient-deprivation.

An IOM will be ready soon, but it is possible now to demonstrate a simpler ecological model (SWAMPSUSTAIN) for the design and management of the diversion. SWAMPSUSTAIN uses the same cell hierarchy as the nutrient model. The Maurepas swamp within the hydrodynamic model domain is not of uniform elevation but includes low-relief ridges and pools (Figure 3.3). The distribution of these features affects not only flow patterns, but also flood duration and depth, the likelihood of salinity intrusion and the potential for sedimentation.

This variability is predicted by the hydrodynamic and water quality models, and will influence the distribution of ecological benefits associated with the proposed diversion.

The SWAMPSUSTAIN model was deployed to predict wetland sustainability under a range of potential diversion scenarios. It relies upon parameterization developed by Rybczyk et al. (1998) for a Louisiana coastal forest in the Barataria Basin. SWAMPSUSTAIN does not predict changes in species composition or forest productivity, but simulates spatial variation in rate of convergence or divergence on a sustainable condition. Such an end state is theoretically one in which mortality is balanced by recruitment. Rybczyk et al. (1998) found that coastal forest sustainability was primarily a function of forest floor elevation if prolonged intrusions of salinity did not occur. Further, Rybczyk et al. (1998) determined that long-term elevation change for a permanently flooded forested wetland receiving adequate nitrogen inputs should be more sensitive to (1) mineral sediment input and (2) long-term subsidence rate than to other factors. Trees may die off at species-specific rates, and thereby change forest composition, but it is unlikely that new trees will become established until after a critical elevation has been achieved. While it is difficult to assess precisely what critical elevation must be reached to initiate forest recovery, a consensus view is that a sustainable coastal swamp forest is one that experiences seasonal rather than continual flooding.

Our hydrologic records, coupled with the LIDAR derived elevation data, allowed us to estimate that level as being approximately 1.9 ft (NAVD88), 0.4 ft above the mean sea level observed during 2003. This critical elevation compares with current swamp cell elevations ranging from 1.00 to 1.36 ft (NAVD88).

It is believed that the relict second-growth forest now found in the Maurepas dates from a 1924-25 germination event (W. Conner, pers. comm.). This tells us that land elevation and other conditions as recently as 80 years ago were suitable for re-establishment of the swamp. This allows estimation of a lower limit on local RSLR. If conditions suitable for swamp colonization existed more recently than 80 years ago, then a higher local RSLR might be appropriate. This is tested in the sensitivity analysis. A spatially varying effective subsidence rate is calculated from the difference between 1.9 ft NAVD88 and the observed current land elevation. SWAMPSUSTAIN then predicts the years necessary for the swamp at various locations to reach the critical elevation under a range of diversion management and RSLR scenarios. The same suite of diversion scenarios developed for testing nitrogen loading and assimilation also served as an input to SWAMPSUSTAIN (Table 3.3).

It was observed during the hydrology field effort that suspended clays originating in Amite River floodwaters were distributed deep into the swamp on rising tides. It is anticipated that this will also occur for river-derived clay sediments under diversion flows.

Absent a fully dynamic sediment model, the approach taken here is to treat sediment distribution as a function of the flow field, and to change that field on a monthly basis for different diversion rates. If primarily fine-grained sediments are introduced by the diversion at a known concentration, then the mass deposited in the most proximal swamp areas becomes unavailable for deposition in more distant areas. SWAMPSUSTAIN was initialized to deposit 53 percent of suspended sediment in the first tier of swamp cells, 26 percent in the second, 13 percent in the third and 8 percent in the fourth. Assumptions about deposition, throughput, accretion and subsidence affect the rate at which long-term aggradation or degradation of the swamp floor will occur and the number of years required to achieve the critical elevation in each cell. Rybczyk et al. (1998) predict that once a critical elevation is reached, nutrient inputs become more effective in sustaining elevation.

Shaffer et al. (2003) have provided bulk density and percent organic matter values for forest soils of the Maurepas study area. The specific densities of mineral and organic matter components of wetland soils (2.61 and 1.14 g cm⁻³, respectively) are known (DeLaune et al. 1983), and provide a means of estimating the uncompacted volume of sediments deposited with a given bulk density. Rybczyk et al. (1998) validated a cohort-based method for estimating consolidation to extract long-term accretion from such short-term estimates. Rybczyk et al. (1998) estimated that addition of 1 kg m⁻² y⁻¹ of mineral sediment can result in between 0.2 and 0.3 cm y⁻¹ of long-term aggradation. Sensitivity to different values in this range was assessed.

4.0 RESULTS AND DISCUSSION

4.1 Water Quality.

The water quality data collected during the 2002 to 2003 period are considered below together with the earlier dataset acquired during the drought of 2000. The influence of more normal runoff from the Amite/Blind River systems must also be taken into account (Figure 2.3).

4.1.1 Nitrogen. Nitrate concentrations at sampling stations (Figure 3.1) ranged from below level of detection (0.01 mg-N L^{-1}) to 0.32 mg-N L^{-1} (ppm), with a mean of 0.09 mg-N L^{-1} (Figure 4.1). The highest concentrations occurred from November, 2002, to May, 2003, in regions L and A. These were generally higher than observed during the 2000 drought, but even the highest was low compared to mean concentrations in the Mississippi River that range from 0.75 to 2.0 mg-N L^{-1} (Lane et al., 1999). More dissolved inorganic nitrogen was in the form of ammonium, $\text{NH}_4\text{-N}$, than $\text{NO}_3\text{-N}$ in 2002-2003. Ammonium concentrations ranged from below detection (0.02 mg-N L^{-1}) to 1.2 mg-N L^{-1} , with an average concentration of 0.40 mg-N L^{-1} . Ammonium concentrations averaged an order of magnitude higher than during the 2000 drought. The highest ammonium concentrations were measured in the Blind River, Reserve Relief Canal, and at the I-55 canal, probably because of inputs from developed areas. Mean values in the Maurepas are higher than ammonium levels in the Mississippi River that are

generally below 0.1 mg-N L^{-1} (Lane et al., 1999). TN concentrations ranged from 0.18 to 1.75 mg-N L^{-1} , with an average of 0.71 mg-N L^{-1} .

About half of all nitrogen in the Maurepas is in an organic or otherwise refractory form. River concentrations of TN are generally higher, between 1.0 and 2.0 mg-N L^{-1} , but the majority is contributed by nitrate (Lane et al., 1999).

An important difference was observed between nitrogen levels measured during the 2000 drought period and the more typical 2002-2003 period. Ammonium was introduced with runoff from populated areas, suggesting a connection to sewage or septic sources. During the drought, most nitrogen found in the Maurepas was in complex organic forms, such as humic substances, tannins, and phytoplankton. During the year with more normal rainfall, only half of the nitrogen found in water samples was in the organic form, while ammonium was the predominant dissolved inorganic form. In the swamp interior, nitrogen concentrations are similar to those found in other wetlands along the Louisiana coastal zone that are not receiving river water (Lane et al., 1999; 2002).

4.1.2 Phosphorus. Phosphate concentrations ranged from below level of detection to 411 ug-P L^{-1} with an average of 82 ug-P L^{-1} (Figure 4.1). The highest concentrations were consistently found at the Airline Highway on Hope Canal, as was Total Phosphorus (TP). TP concentrations ranged from 12 to 1077 ug-P L^{-1} , averaging 203 ug-P L^{-1} . These

concentrations for phosphate and TP are similar to concentrations in the river (Lane et al., 1999), and were three times higher than observed during 2000.

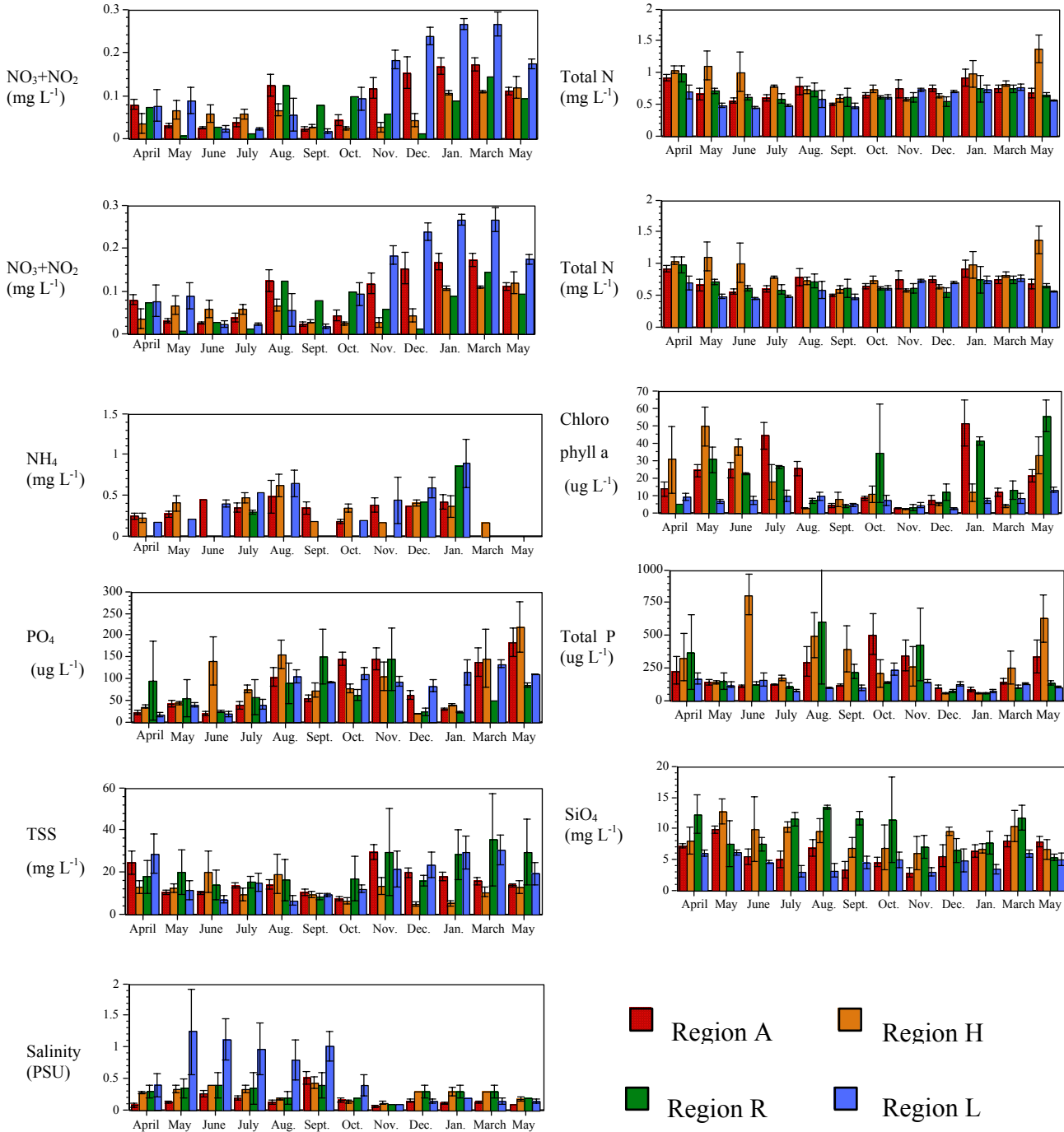


Figure 4.1 Water quality data for each region in the Maurepas swamp from April 2002 to May 2003. (Site Locations in Figure 3.1).

4.1.3 Silicate. Silicate (Si) concentrations ranged from 0.18 to 20.77 mg-Si L⁻¹ with an average of 82 mg-Si L⁻¹ (Figure 4.1). The highest concentrations were consistently found in the Hope and Reserve canals.

4.1.4 Si:N:P Ratios. If all are available, dissolved inorganic silicate, nitrogen and phosphorus will be selected by the photosynthetic process in the proportions of 16:16:1 (Si:N:P; Redfield, 1958). While N:P ratios of 16:1 and greater were found in individual samples, they were generally confined to the vicinity of the Amite and Blind Rivers that receive direct inputs from developed areas to the west. Si:N ratios never fell below 1:1. These low N:P and high Si:N ratios indicate that the Maurepas basin is almost always nitrogen limited. Introduction of inorganic nitrogen to a nitrogen limited ecosystem supports increased algal production, even if the concentrations of other nutrients remain unchanged.

4.1.5 Salinity. Salinity ranged from 0 to 3.3 PSU (ppt), with an average of 0.3 PSU for the entire study (Figure 4.1). These values were an order of magnitude lower than during the drought of 2000. The highest levels were at the two stations located on the eastern side of Lake Maurepas, but the swamp was fresh for the entire year. Region A had the lowest salinities in the study area during spring and summer, coinciding with high flow in the Amite River.

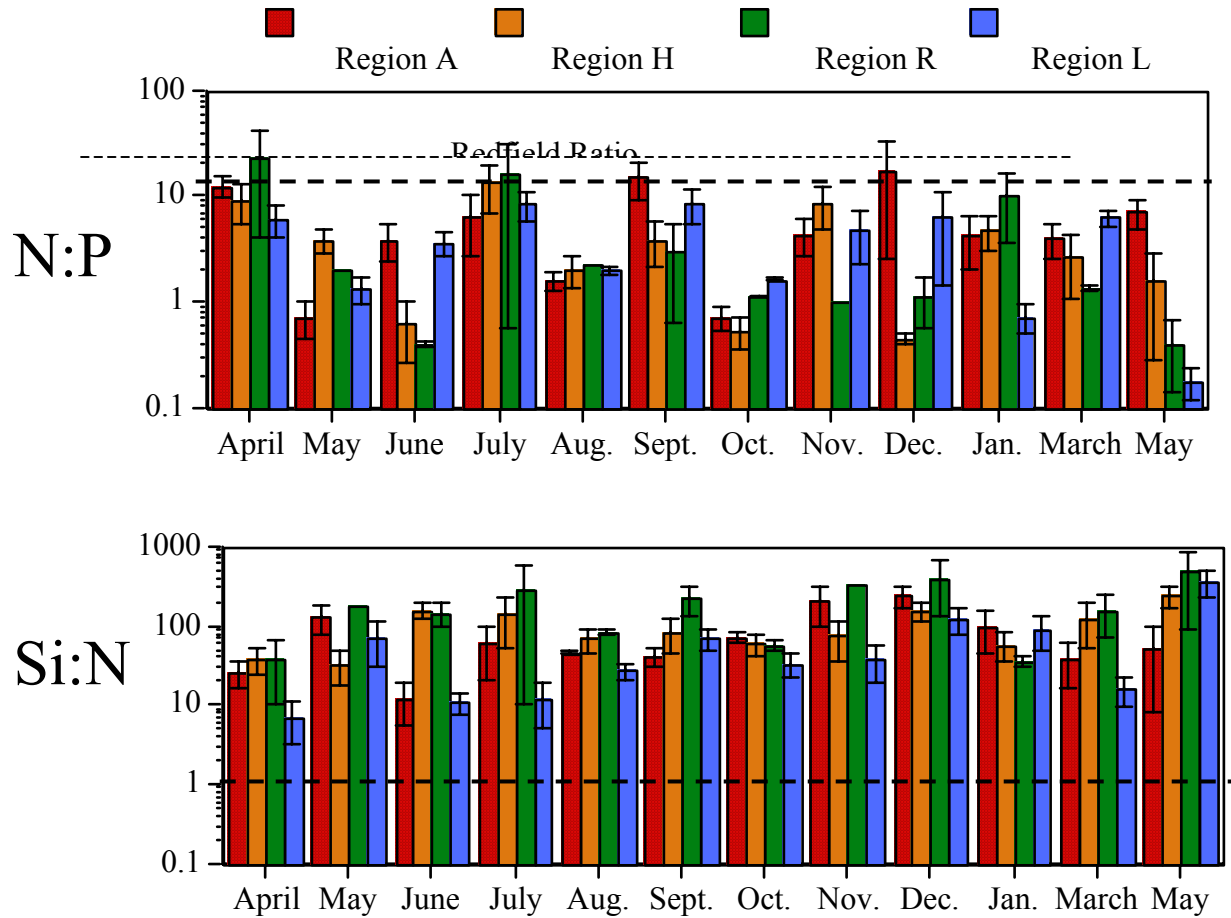


Figure 4.2 Si:N:P Ratios for four Maurepas regions from April 2002 to may 2003

4.1.6 Suspended Sediment and Chlorophyll *a*. Total suspended sediment concentrations ranged from 1 to 58 mg L⁻¹ (ppm), averaging 15 mg L⁻¹, and were similar to those observed during 2000. Stations in Lake Maurepas region had the highest TSS concentrations, probably due to high wave energy and resuspension of bottom sediments.

These TSS concentrations, however, are considerably less than those in the Mississippi River, which range between 100 and 300 mg L⁻¹. Chlorophyll *a* ranged from 1 to 81 ppb, averaging 16 ppb, with the highest concentrations occurring during Spring and Summer (Figure 4.1). Lake Maurepas had consistently lower chlorophyll *a* concentrations than the other regions, perhaps due to the increased turbidity in the region that attenuated light penetration (Cloern, 1987).

4.2 Swamp Geometry and Hydrology

This study produced the first comprehensive picture of Maurepas swamp geometry and hydrology. The geometry is critical to understanding flow paths that diverted river water will take when introduced, and the stress patterns that intruding salt water will produce during droughts.

4.2.1 Swamp Geometry. LIDAR derived topography (Figure 3.3) shows that all of the swamp study area exclusive of anthropogenic features occurs in a narrow elevation band ranging from 1.0 to 1.8 ft (NAVD88). Features of a regional scale still are visible, however, within the overall planar aspect. The highest lands define the edges of the Mississippi River natural levee that rises farther to the south. Most of these lands higher than 1.5 ft lie south of the I-10 and the swamp area targeted for diversion benefits. Two peninsulas with an average elevation of about 1.2 ft, each 3 to 4 km wide, extend south to north toward the lake as a continuation of features originating on the natural levee. These may be surface expressions of buried crevasse splays.

The first, a more prominent feature on the western margin of the study area, follows the east bank of the Blind River. The second occurs east of the Reserve Relief Canal. The Tent/Mississippi/Dutch Bayou watershed occupies the swale beneath these two higher areas. This swale includes some of the lowest lying swamp in the study area ranging from 1.0 to 1.2 ft (NAVD88). Areas as low as these also occur along the eastern boundary of the study and south of the Blind River between the junction with the Amite River Diversion Canal and the lake (Figure 3.3)

Table 4.1. Maurepas Water Level Statistics: November 2002 to November 2003

Station	Manchac	S10	S4	S9	SLUA	S8	S6
# Obs.	9081	4044	3919	4698	3639	4206	780
Maximum	4.15	3.35	3.64	2.85	2.93	2.82	2.16
Minimum	-0.24	0.13	-0.71	-0.68	0.56	-0.15	-0.13
Mean	1.39	1.56	1.54	1.46	1.70	1.53	1.31
Std. Dev	0.62	0.66	0.63	0.63	0.43	0.60	0.68

4.2.2 Swamp Hydrology. Water level elevations over the 19-month period monitored are presented in groups for the first year (November 2002-November 2003) and for a portion of the second year used for model calibration (December 2003-January 2004). Six gages in addition to the USACE Manchac gage operated during the first year, but only two months of record are available for S6 (Table 4.1). Mean water level at all channel gages but S6 during the first year ranged from 1.46 ft at S9 to 1.56 ft at S10, averaging 1.53 ft NAVD88. The Manchac gage, which is listed as being on the NGVD27 datum, produced a mean of 1.39 ft, 0.13 ft lower.

During the winter calibration period, the Manchac gage was 0.19 ft lower than those in the swamp channels. Based on this analysis, a datum adjustment value of +0.2 ft was added to hourly USACE Manchac gage records to create the dynamic tidal boundary in the model.

4.2.2.1 Lake Group. This group includes from east to west the USACE (Pass Manchac), USGS1 ([Reserve@Lake](#)), S4 ([Dutch@Lake](#)), and S10 ([Blind@AmiteD](#)). Lake gages exhibit the most range of all groups. Three gages were active in the first year (Figure 4.3a). The USACE Manchac gage reached 4.15 ft on May 30, 2003 as a result of Tropical Storm Bill. On the other side of the lake, S4 ([Dutch@Lake](#)) reached 3.64 ft, while S10 ([Blind@AmiteD](#)) reached only 3.35 ft for the same event. Minimum values were recorded by all Lake gages after a cold front passage on April 1, 2003, with S4 reaching - 0.71 ft, USACE Manchac at - 0.24 ft, and S10 at 0.13 ft. S10 rarely dropped as low as S4 or the Manchac gage. S10 exceeded all other Lake gages only on February 26, 2003, and on April 9, 2003, following large runoff events in the Amite basin (Figure 2.3). This pattern continued into the second year when an additional gage was installed at USGS1 ([Reserve@Lake](#)) (Figure 4.3b). All lake gages were coherent in phase and amplitude with the USACE gage at Pass Manchac. URS, Inc., is conducting a new survey in the study area and will provide guidance on datum adjustments.

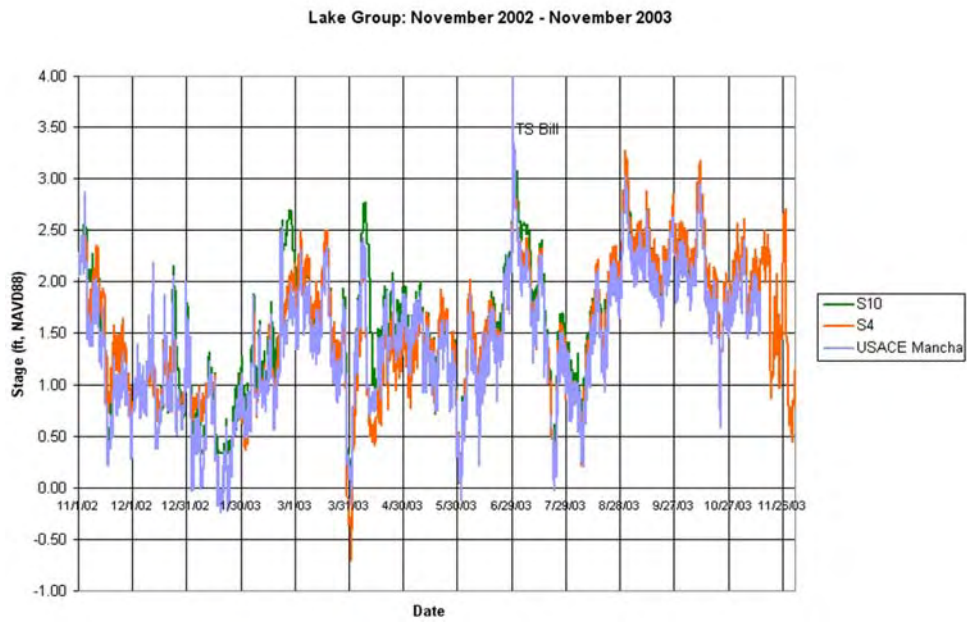


Figure 4.3(a) Lake Group water level time-series in first year: November 2002 to November 2003

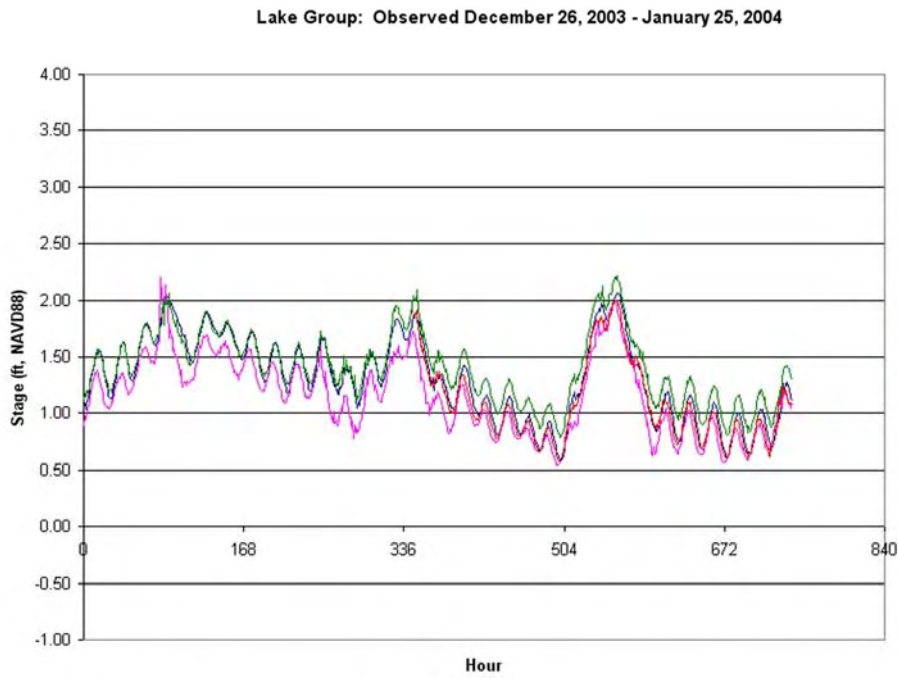


Figure 4.3(b) Lake Group water level time-series in second year: December 2003 to January 2004

4.2.2.2 *River Group*. From upstream to downstream, this group includes S16 ([Blind@I-10](#)) and S10 ([Blind@AmiteD](#)). Only S10 ([Blind@AmiteD](#)) was active during the first year. This gage generally tracked with those of the Lake group except during runoff events when it could rise by as much as 0.5 ft (Figure 4.3a). Another gage upstream on the Blind River was added in the second year at S16 ([Blind@I-10](#)) (Figure 4.4). Runoff events exert relatively minor and short-lived effects on stage within the lower reaches of the Blind and Amite Rivers. A large flood occurred on the Amite in May, 2004, and will permit additional analysis of runoff effects.

4.2.2.3 *Diversion Group*. This group includes S5 ([Hope@Hy61](#)), S7 ([Hope@I-10](#)), S6 ([Hope@Pipeline](#)) and S9 (Dutch@MissB) from south to north. Only three Diversion gages, S6 ([Hope@Pipeline](#)) and S8 ([Hope@Tent](#)), were active in the first year, and the equipment at S6 disappeared after recording only 2 months of data in the spring (Figure 4.5a). During those two months, it tracked S8 nearly perfectly. The surge due to Tropical Storm Bill, which raised the USACE gage at Manchac to 4.15 ft, and to 3.64 ft downstream at the mouth of Dutch Bayou (S4) resulted in a peak at S8 of 2.82 ft. The gage at S8 malfunctioned in December 2004, but two new gages were added to the diversion group at S5 and S7 at about the same time (Figure 4.5b). The Hope Canal gages behave quite differently than S9 downstream in Dutch Bayou. At higher stages, no tidal signal is observed. While the swamp channel rises quickly, it drains more slowly

upstream of Dutch Bayou. Gage records in Hope Canal appear decoupled from those in Dutch Bay on falling tides.

While servicing gages, it was noted qualitatively that the discharge of Mississippi Bayou on falling tides far exceeds that of the Hope Canal/Tent Bayou system where they meet to form Dutch Bayou. It seems likely that the Mississippi Bayou system drains more rapidly and temporarily blocks discharge from the Hope Canal tributary.

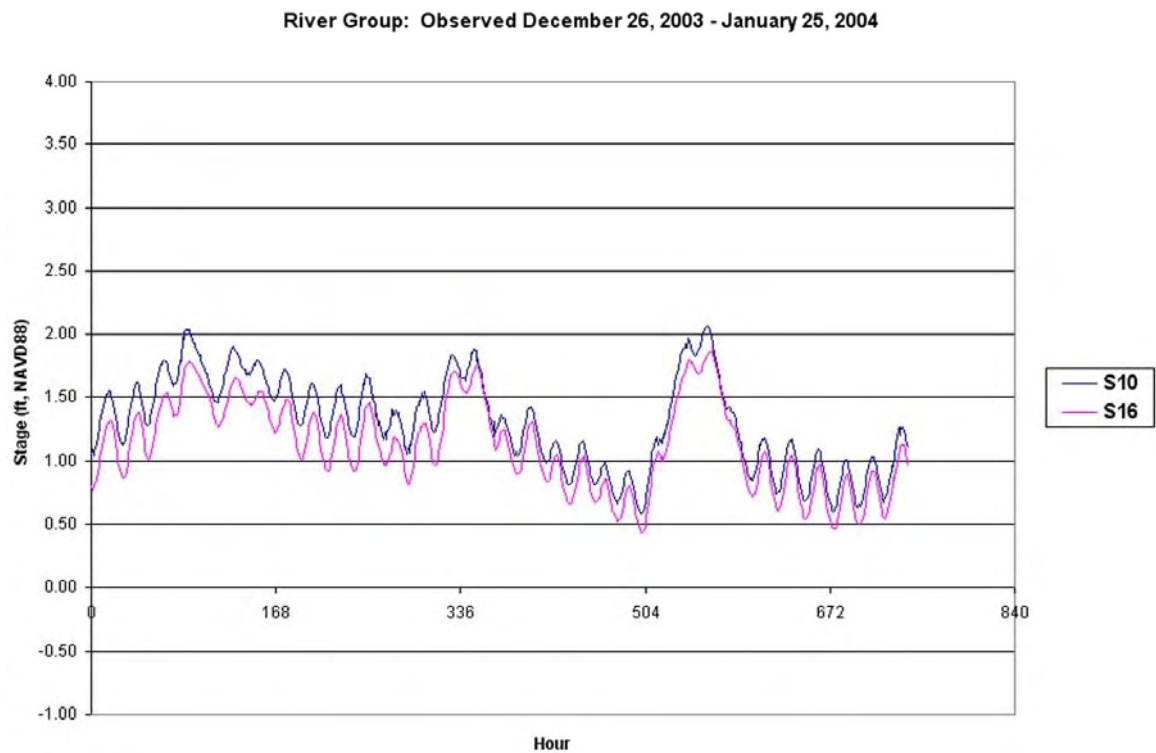


Figure 4.4 River Group water level time-series in second year: December 2003 to January 2004

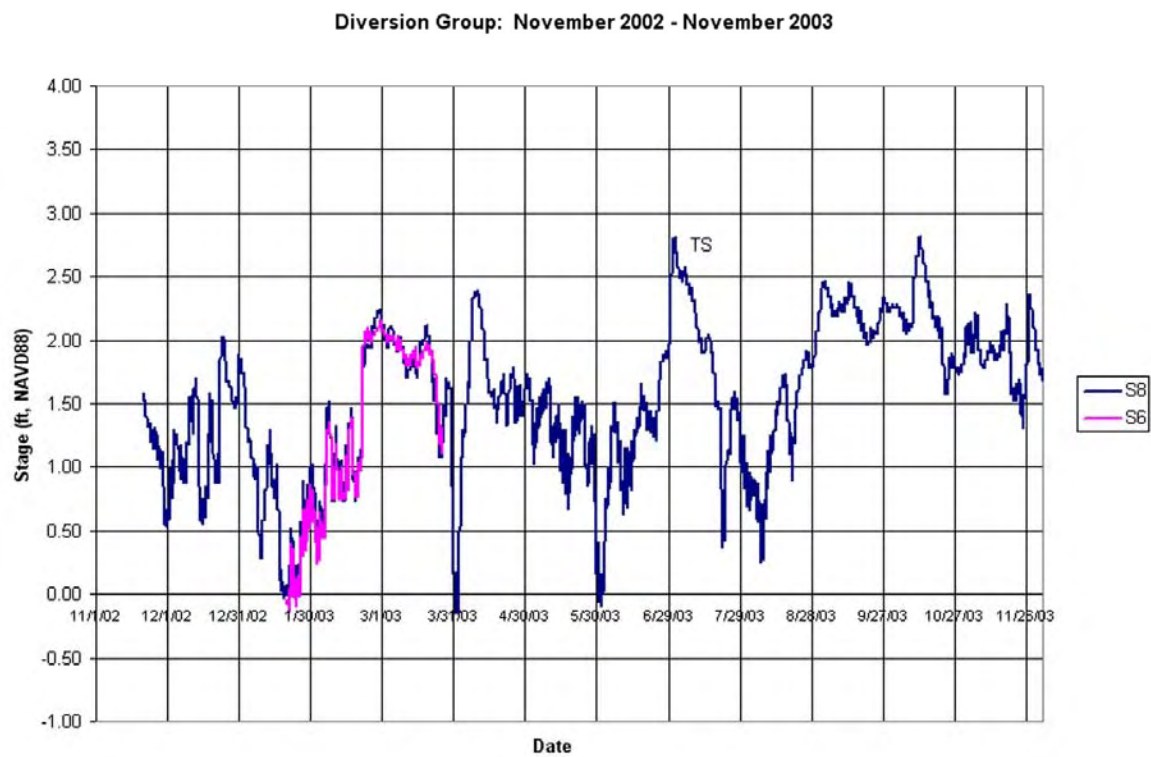


Figure 4.5(a) Diversion Group water level time-series in first year: November 2002 to November 2003

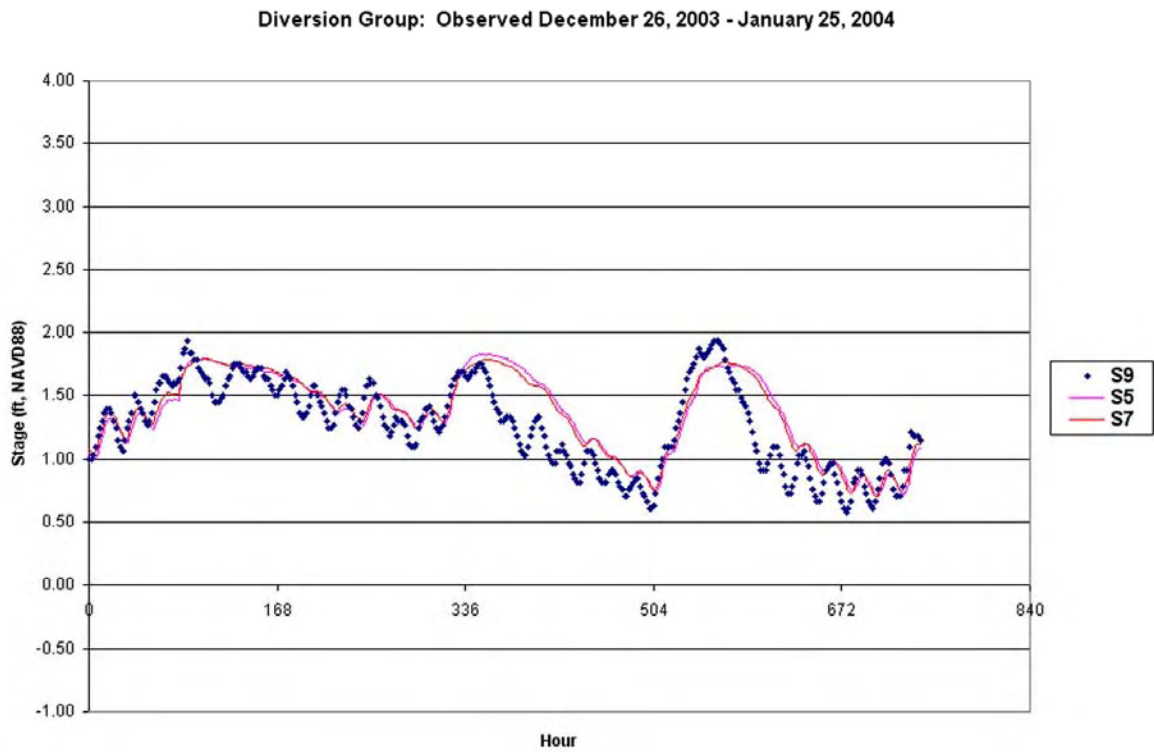


Figure 4.5(b) Diversion Group water level time-series in second year: December 2003 to January 2004

4.2.2.4 *Swamp Group*. From south to north, this group includes S11 ([MissB@I-10](#)), URS N ([Swamp@S13](#)) and S9 ([Dutch@MissB](#)), SLUA ([Swamp@S9](#)), S4 ([Dutch@Lake](#)) from south to north. A single swamp gage was active in the first year at SLUA (actually site 8a in Shaffer et al. 2003) and it is shown with S9 ([Dutch@MissB](#)), the closest channel gage (Figure 4.6a). The swamp elevation at the site was determined from LIDAR to be at 1.1 ft (NAVD88), but the gage was in a well casing inserted into the soil so that it reported water levels below this value on two occasions during the summer, June 1, 2003 (0.61 ft) and August 11, 2003 (0.59 ft). The water table dipped below the surface at these times, probably as a result of evapotranspiration. When S9, the channel gage a km away, went above 1.5 ft, water elevation at the SLUA swamp gage read the same. Both, for example, reached the same elevation of 2.9 ft during Tropical Storm Bill, indicating an attenuation of the surge of about 0.7 ft in 3 kms from S4 at the mouth of Dutch Bayou. The swamp gage deviated from S9 again only when S9 went below 1.5 ft, suggesting that small connections through swamp channels were broken at this point, and the swamp floor was in puddles rather than submerged. Because the excursion below 1.5 ft was truncated, mean water level recorded at the SLU A swamp gage was 1.62 ft, 0.35 ft higher than at the nearby S9 channel gage (Table 3.3). A new swamp channel gage at S11 ([MissB@I-10](#)) and a second swamp gage nearby at URS N ([Swamp@S13](#)) were added for 2004 (Figure 4.6b). Fluctuations at the frequency of the diurnal tide are filtered out of the water level signal at gages on small swamp channels like the upper reaches of the Mississippi Bayou, and in the swamp itself.

During the winter, the swamp floods every two weeks on spring tides. In the more inland setting at URS N, the swamp drains more rapidly than closer to the lake, suggesting a less impounded condition.

4.2.2.5 *Canal Group*. This group includes USGS2 ([Reserve@Hy61](#)), USGS1 ([Reserve@Lake](#)) from south to north, both added in the second year. The damping of the tidal signal observed at Hope Canal or Mississippi Bayou does not occur in the larger Reserve Relief Canal (Figure 4.7). Some datum issues remain at these stations to be resolved by the new URS survey. The tide, and presumably salinity, propagates the full length of the channel without attenuation. Reserve Relief Canal acts as an extension or arm of the lake.

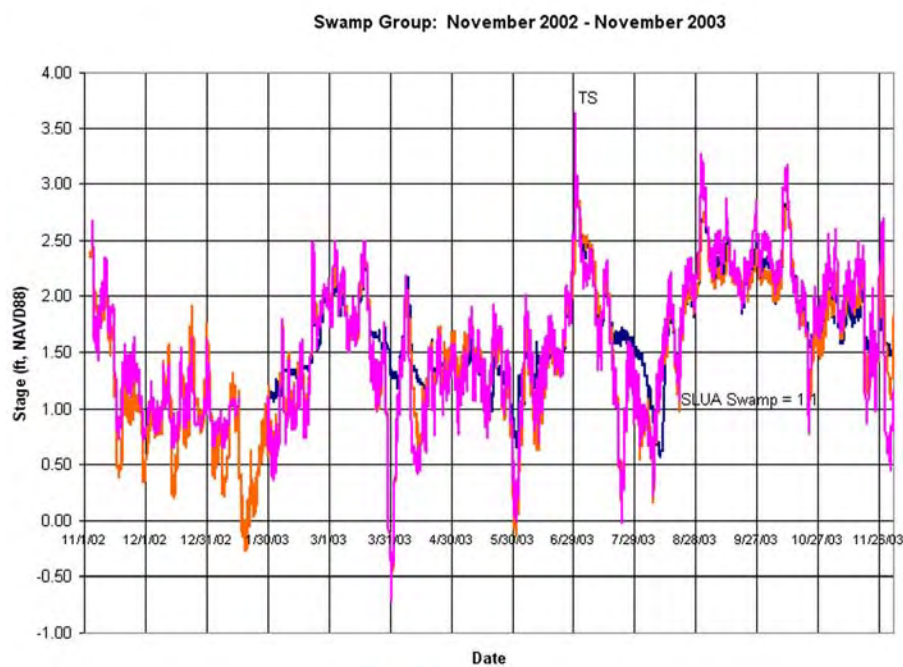


Figure 4.6(a) Swamp Group water level time-series in first year: November 2002 to November 2003

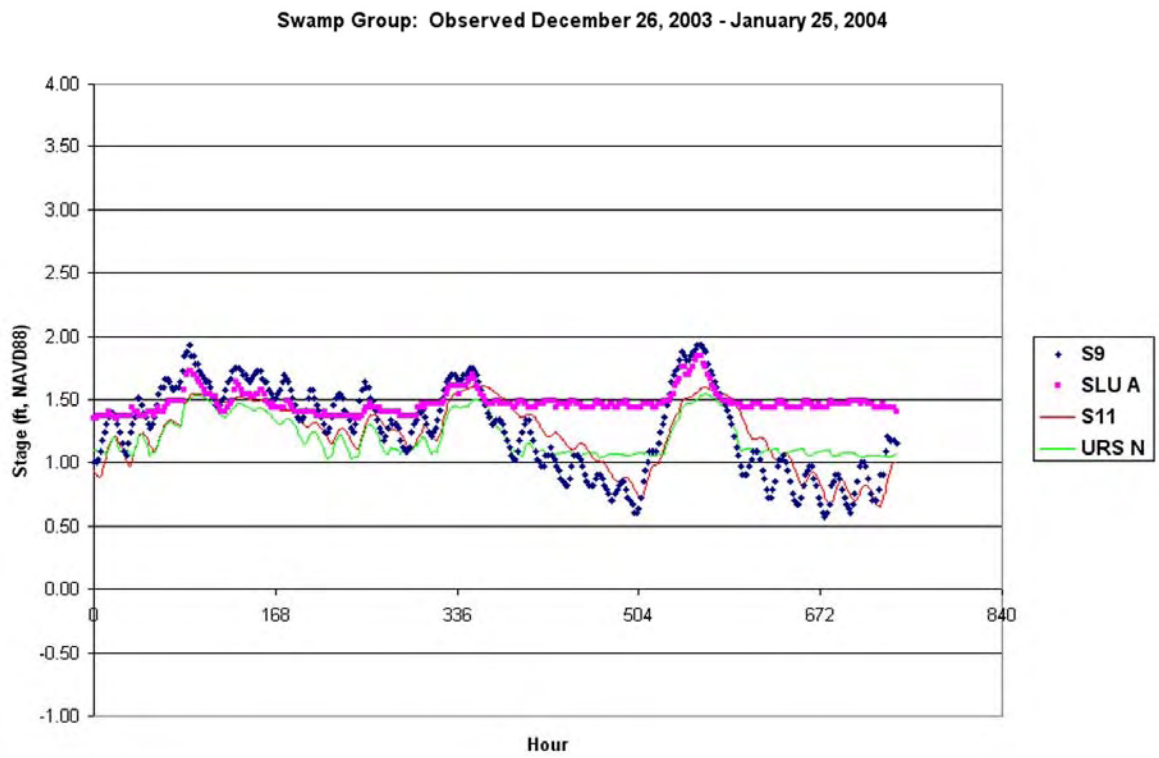


Figure 4.6(b) Swamp Group water level time-series in second year: December 2003 to January 2004

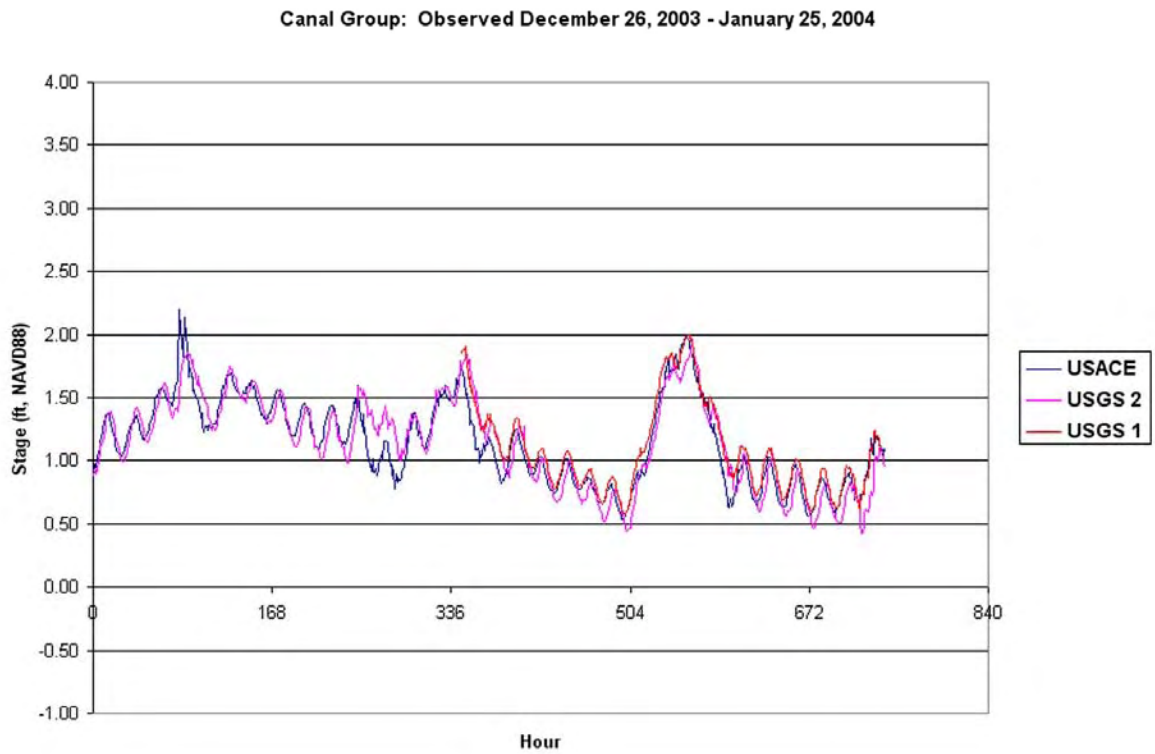


Figure 4.7 Canal Group water level time-series in second year: December 2003 to January 2004

4.3 Hydrodynamic and Water Quality Modeling

The calibrated hydrodynamic (RMA2) and water quality (RMA4) models were used to simulate 1 to 2 months in the Maurepas prototype. Base case runs were made to establish the current regional situation, particularly the flooding regime and response to salinity. Results were reported at nodes near the swamp forest sites investigated by Shaffer et al. (2003). Model runs were made for diversions through Hope Canal that reached maximum discharges of 500, 1500 and 2500 cfs. Water level and the concentration of a fictitious conservative tracer introduced with river water (at 10 ppt) are reported. The tracer can be considered an analog for sediment or nutrients, though these real constituents of river water do not behave conservatively. Because the tracer is introduced with freshwater, the time-series produced by the model indicate mixing and dilution. They are the inverse of those developed earlier to validate salinity response for the base case (Figure 3.7). Model results are presented in two ways, either in tables summarizing conditions at each of the swamp sites established by Shaffer et al. (2003), or in plan view maps produced by the SMS software.

4.3.1 Base Case Analysis. The standard model set-up was modified to examine water quality effects of normal and increased discharges from the Amite River and the Amite River Diversion Canal. Most runoff events on the Amite system are of short duration, persisting for a maximum of two weeks (Figure 2.3).

4.3.1.1 Runoff from the Amite River. A tracer was introduced sequentially into the Amite and Amite River Diversion Canal at a concentration of 100 ppt. The tracer plumes for the two river input points remain distinct and separate, no matter how much water is introduced (Figure 4.9). The tracer plume from the Amite River Diversion Canal for a normal base flow encompasses a relatively small triangle on the western margin of the study area near the junction of the Blind River and the Amite River Diversion Canal. This is the zone that includes most of the interior forest stations (Figure 2.9) studied by Shaffer et al. (2003). It is also a low area (Figure 3.3). It is important to note that this zone experienced salinities of 5 and 6 ppt in September and October 2000, respectively (Figure 3.10). This suggests that the lower Blind River is an efficient conduit for higher salinity water when base flow is low and estuarine salinities are high. Because discharge is flashy, swamp sites near the rivers still experience salt stress even if they enjoy other benefits of river inputs.

4.3.1.2 Swamp inundation. The Maurepas swamps are flooded more than half the time, given a mean annual water level of 1.5 ft (NAVD88) (Table 4.1), and swamp elevations that average less than 1.3 ft (Table 4.2). No pattern is apparent in either elevation or duration of flooding among the classes of stations studied by Shaffer et al. (2003), except that the intermediate stations appear to be most frequently flooded, and to a greater average depth than the others (Table 4.2). Ground elevation estimated from LIDAR ranged from 1.05 to 1.29 ft (NAVD88).

Flood duration during the winter calibration period (low water) varied from 38 to 68 percent, which corresponds to a range of 50 to 78 percent for the full year (Table 4.2).

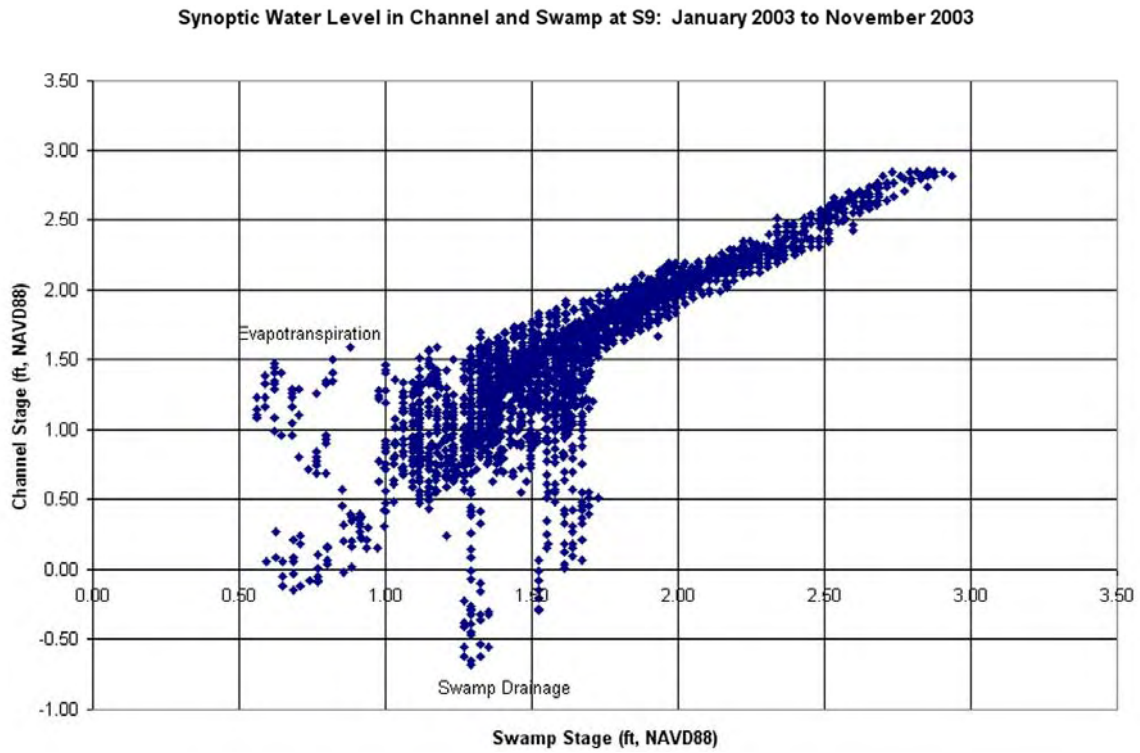


Figure 4.8. Synoptic Water Level in Channel and Swamp at S9: January 2003 to November 2003

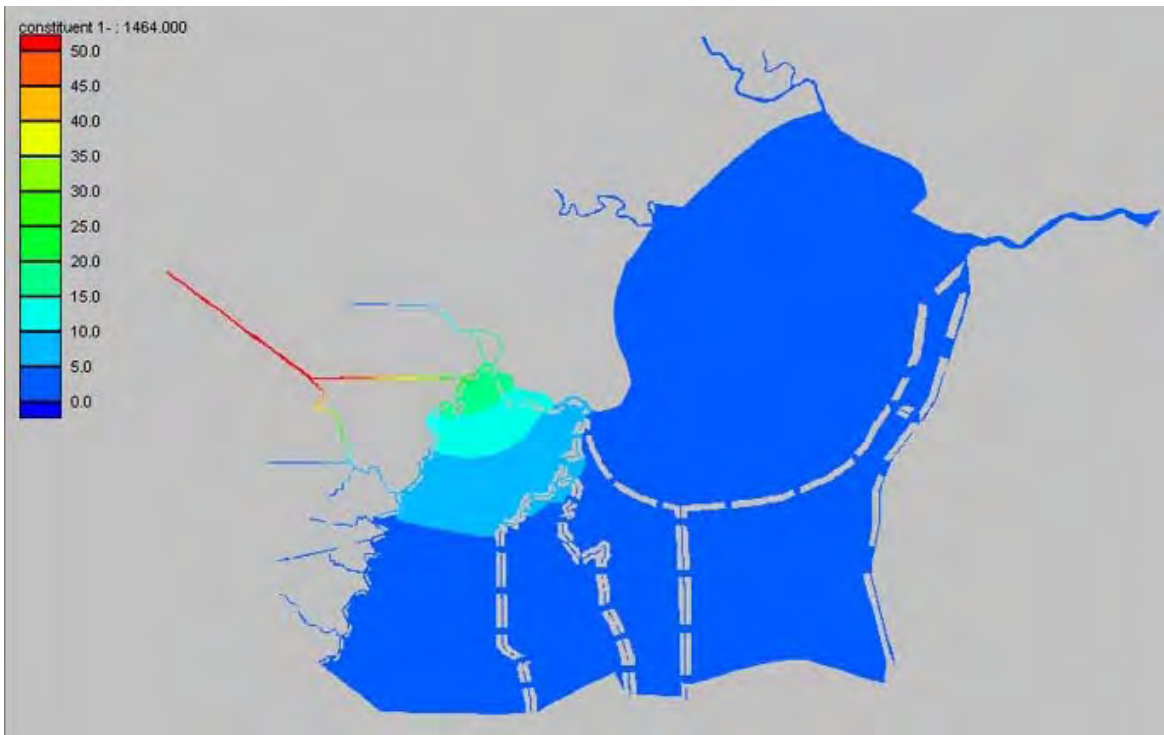


Figure 4.9(a) Predicted Influence of Amite River Discharge

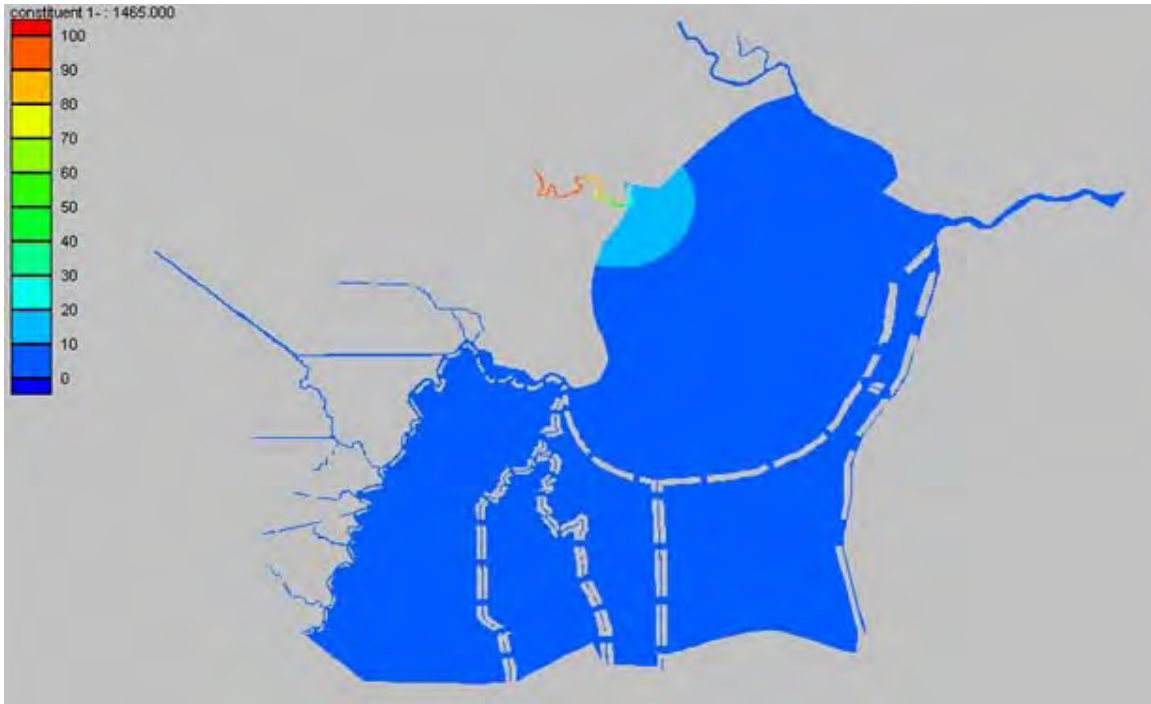


Figure 4.9(b) Predicted Influence of Amite River Discharge

Table 4.2. Stressor Conditions at Shaffer et al. (2003) Maurepas Swamp Stations With and Without Diversion (1 month)

Site	Class	Elevation		% Time Flood	Base Depth (ft)	Add Depth 500cfs (ft)	Add Depth 1500cfs (ft)	Add Depth 2500cfs (ft)	% Salinity Reduce	% Salinity Reduce	% Salinity Reduce
		(ft)	CI						Base	1500cfs	2500cfs
1	Interior	1.28	77	51	0.31	0.04	0.13	0.19	59	95	99
5	Through	1.09	57	70	0.42	0.02	0.05	0.08	39	86	96
6	Interior	1.14	22	65	0.38	0.02	0.07	0.11	37	83	95
7	Interior	1.28	83	51	0.31	0.03	0.09	0.14	50	91	97
8	Intermediate	1.04	13	75	0.44	0.02	0.06	0.10	20	69	86
9	Interior	1.24	16	55	0.32	0.06	0.17	0.28	44	94	99
10	Through	1.14	13	65	0.37	0.08	0.21	0.34	51	97	100
11	Through	1.15	10	64	0.37	0.09	0.28	0.49	61	99	100
12	Through	1.29	3	50	0.29	0.06	0.16	0.26	73	100	100
14	Intermediate	1.25	4	54	0.33	0.03	0.10	0.15	26	62	94
15	Intermediate	1.01	19	78	0.44	0.05	0.13	0.20	49	92	87
16	Intermediate	1.22	14	57	0.34	0.01	0.03	0.04	33	63	78
17	Lake	1.13	115	66	0.33	0.02	0.08	0.13	16	53	54
18	Lake	1.25	26	54	0.33	0.00	0.01	0.02	17	31	28
19	Lake	1.05		74	0.45	0.00	0.01	0.02	2	10	17
MEAN											
(stdev)											
		1.14	71	65	0.37	0.01	0.03	0.06	12	31	33
	Lake	(0.10)	(63)	(10)	(0.07)	(0.01)	(0.04)	(0.06)	(8)	(22)	(19)
		1.13	13	65	0.51	0.03	0.08	0.12	32	72	86
	Intermediate	(0.12)	(6)	(13)	(0.06)	(0.02)	(0.04)	(0.07)	(12)	(14)	(7)
		1.24	50	56	0.33	0.04	0.12	0.18	48	91	98
	Interior	(0.07)	(35)	(7)	(0.03)	(0.02)	(0.04)	(0.07)	(9)	(5)	(2)
		1.17	21	62	0.36	0.06	0.18	0.29	56	96	99
	Through	(0.09)	(25)	(8)	(0.05)	(0.03)	(0.10)	(0.17)	(15)	(6)	(2)

4.3.1.3 Salinity. During most drought conditions, it is anticipated that local runoff will be sufficient to establish a salinity gradient similar to that observed by Lane et al (2003). This is predicted by the model (Figure 3.8). Salinities stabilized at all forest sites after the first month when salinities were initially set to 7 ppt, and the Pass Manchac boundary was maintained at 10 ppt (Figure 3.7). In plan view, the low salinity zone (<2 ppt) was confined to the south-western corner of the study area while the lake reached between 6 and 8 ppt (Figure 3.8)

4.3.2 Diversion Analysis. Three diversion runs of two months duration were made to examine the inundation duration regime, salinity reduction and constituent transport (tracer) compared to the base case. The tracer information was used as part of the nitrate removal model.

4.3.2.1 Inundation Duration. Shaffer et al. (2003) have reported that the Maurepas swamp forest is populated by relict tree stands that are under stress from submergence. It may well be that the dry conditions necessary for germination and success of new trees do not generally occur except when combined with salinity stress. The proposed diversions will raise water levels in the receiving swamp (Figure 4.11). These sites are flooded continuously for much of the year under current conditions (Table 4.2). Predicted increases range up to almost 0.5 ft for the 2,500 cfs diversion in the vicinity of the I-10 bridge over Hope Canal, the inflow point, but diminish significantly within a short radius of the discharge point (Figure 4.11).

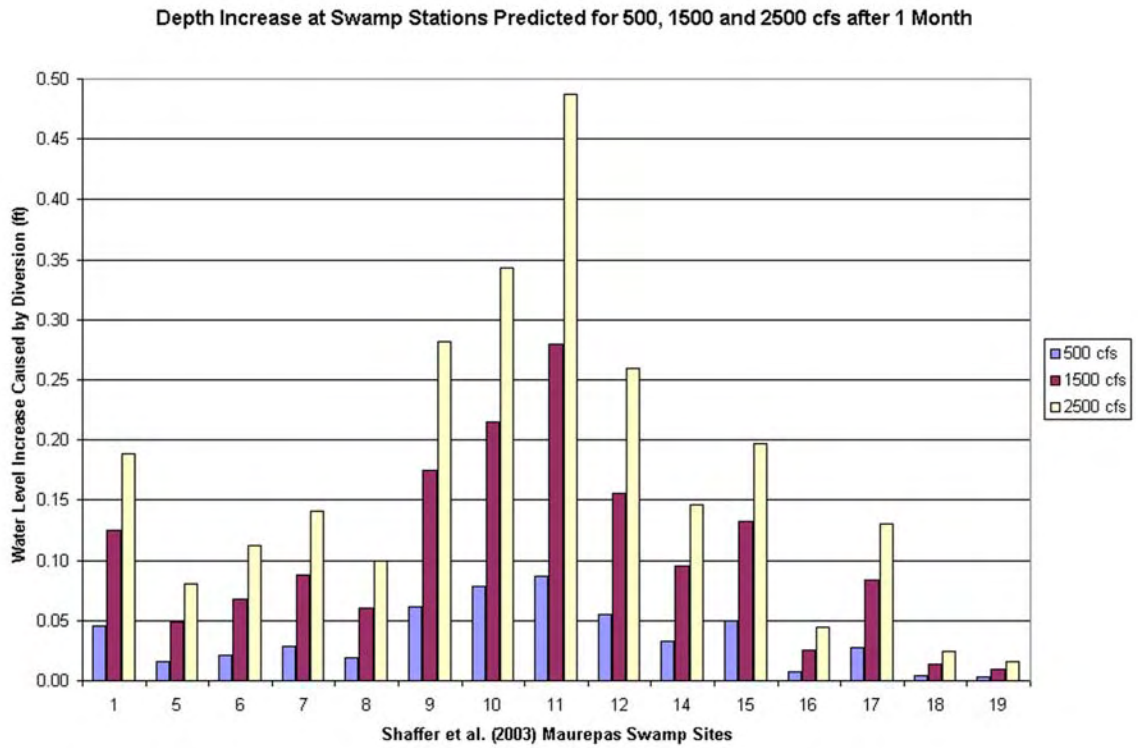
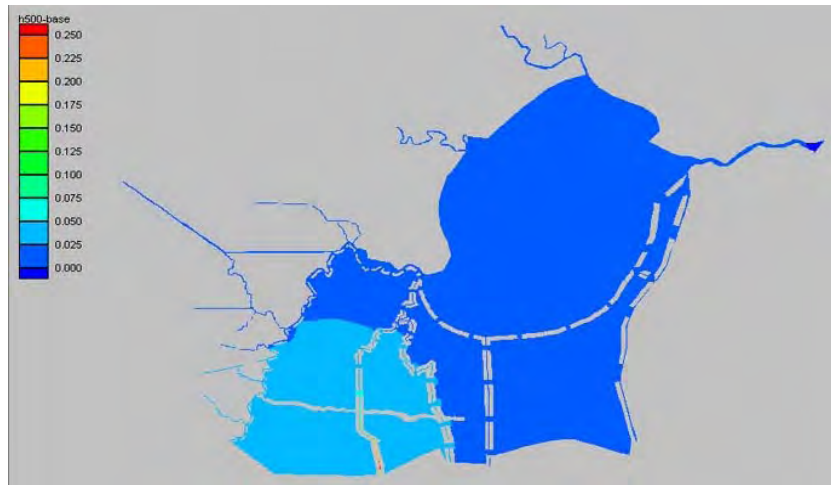
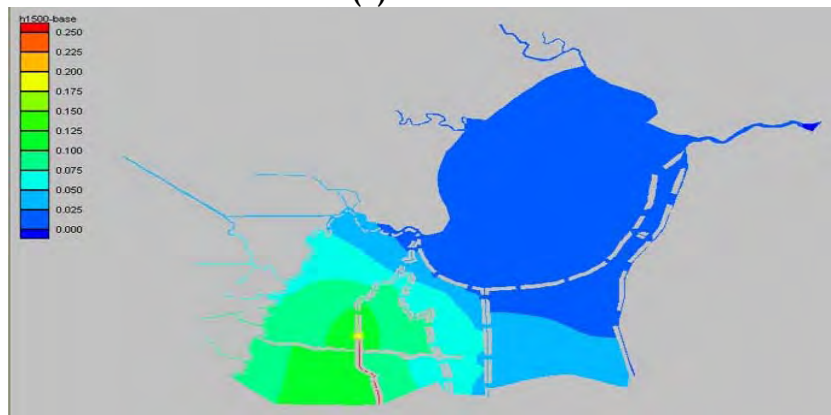


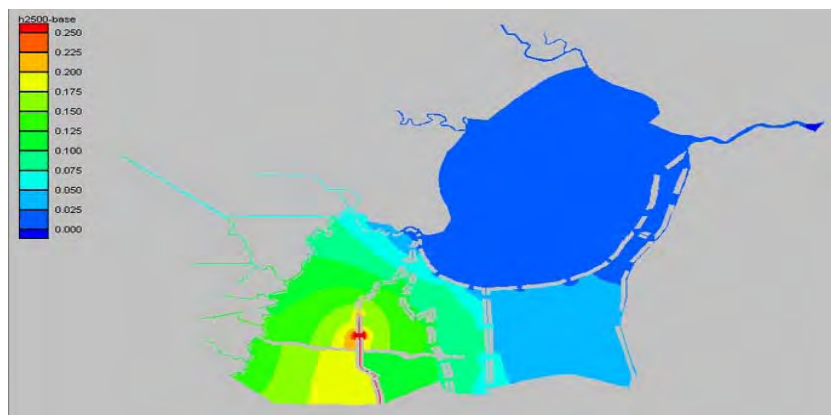
Figure 4.10 Predicted water level response at Shaffer et al. (2003) swamp sites to 500, 1500 and 2500 cfs diversion discharges



(a) 500 cfs



(b) 1500 cfs



(c) 2500 cfs

Figure 4.11 Predicted influence of diversions on water level (ft) after 0.5 months.

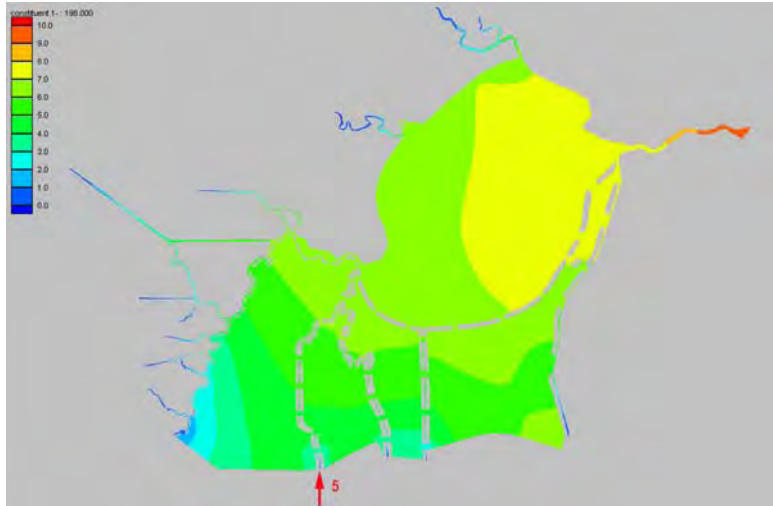
The 500 cfs diversion produces less than 0.05 ft of rise over about a third of the study area. The 1500 cfs diversion raises water level in most of the study area except the lake by 0.05 ft or more, with highest values approaching 0.2 ft. For a 2500 cfs diversion, most of the swamp west of Reserve Relief Canal is raised more than 0.1 ft, and the largest increases approach 0.25 ft. Shaffer et al. (2003) lake sites would see less than 0.06 ft increase for the largest diversion. Intermediate and interior sites are predicted to see maximum rises of 0.12 and 0.18 ft, respectively, while the throughput sites clustered along Hope Canal would see the greatest effect, 0.29 ft (Table 4.2). Given that the swamp generally lies below the mean annual water level today, these increases will exacerbate the tendencies toward submergence, but will drop quickly once the diversion is reduced or shut down. This analysis generally supports predictions from the earlier 1D model for the channel, but the 2D model is predicting much lower stage increases for the swamp.

4.3.2.2 Salinity Reduction. All diversion scenarios have a dramatic effect on salinity, if any salinity is present in the initial condition (Figure 4.12). The diversion effect increases over the duration of the discharge (Figure 3.7). One way to portray this is as the percent reduction from a uniform initial condition (Table 4.2). Shaffer et al. (2003) lake sites were least affected, but it is important to note that Lake Maurepas salinity drops by a third after only one month at 1,500 cfs.

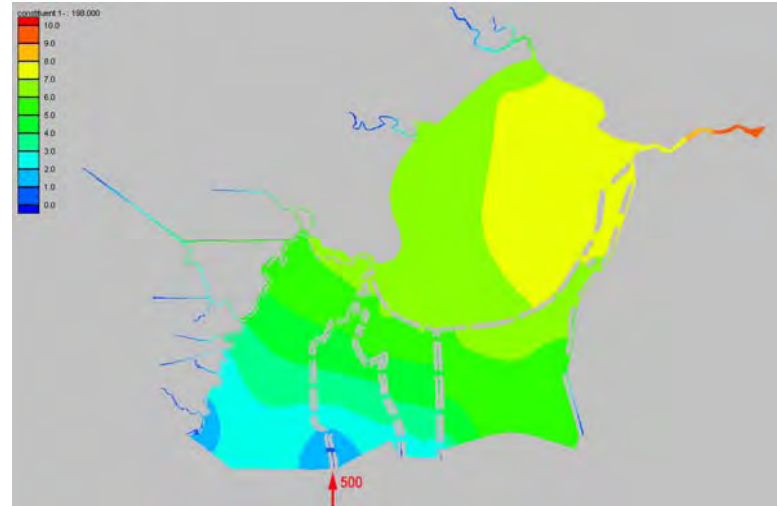
A 2,500 cfs diversion has little additional effect on the lake as long as salinities are kept high (10 ppt) at the Pass Manchac boundary. The intermediate swamp sites experience 72 and 86 percent reductions with 1,500 and 2,500 cfs diversions, respectively. The interior and throughput sites experience nearly complete reduction of salinity to zero for all modeled diversions (Table 4.2).

4.3.2.3 Constituent Transport. The tracer utility in the SMS software provides an excellent way to map the pattern followed by diverted river water (Figure 4.13). The vectors show relatively uniform flow in the swamp radiating away from Hope Canal at less than 0.3 fps for the diversion discharges. Water discharging from the Blind River hugs the south shore of the lake but these patterns are very tide-dependent. The tracer moves into the swamp evenly from both sides of Hope Canal (Figure 4.14). After one month of simulation the centroid of the expanding plume moves slightly to the east and toward the lake generally following the Mississippi Bayou drainage. Tracer information compiled for the Shaffer et al. (2003) swamp sites indicates that this picture changes little over another month (Table 4.3). The zone of diversion influence includes most of the swamp in the study area, but little of the lake after a single month of a 500 cfs discharge (Figure 4.3). This zone is expanded for a 1,500 cfs discharge to include all of the swamp in the study area and half of the lake. Finally, a 2,500 cfs diversion reduces lake salinity by 30 percent after one month (Table 4.3).

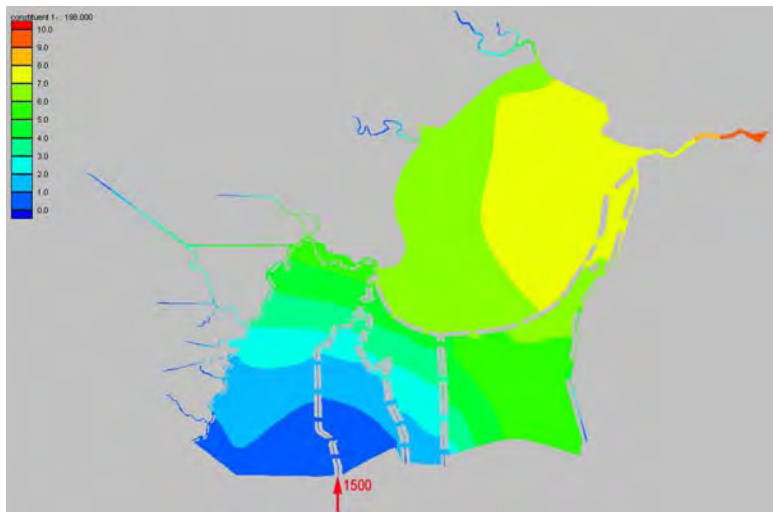
The throughput and interior swamp sites are affected more by diverted river water than the intermediate sites located in the vicinity of Reserve Relief Canal. Even when the diversion channel to the I-10 is enclosed by levees, the model predicts that river water will get into the forest to the south around the ends of the I-10 roadbed, particularly between Hope and Reserve Relief Canals where the land is lower (Figure 3.3).



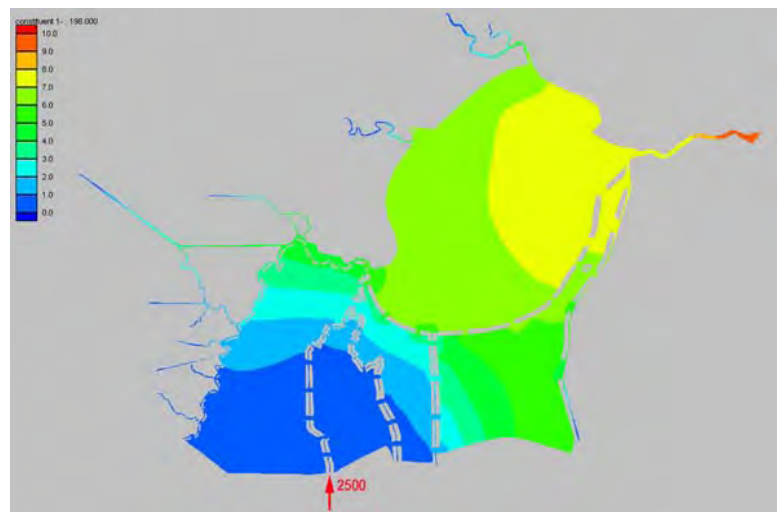
(a) Base



(b) 500 cfs

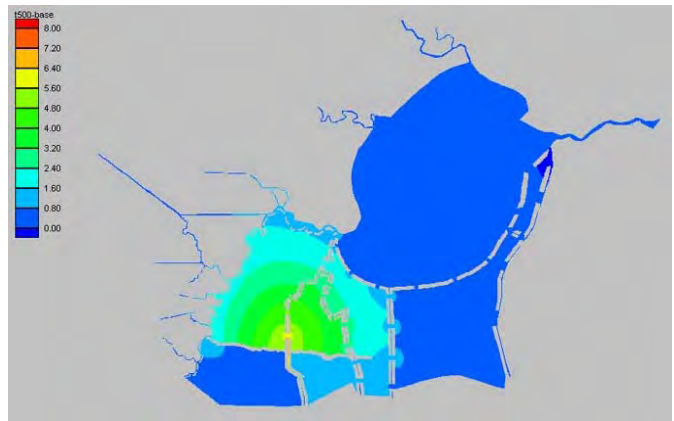


(c) 1500 cfs

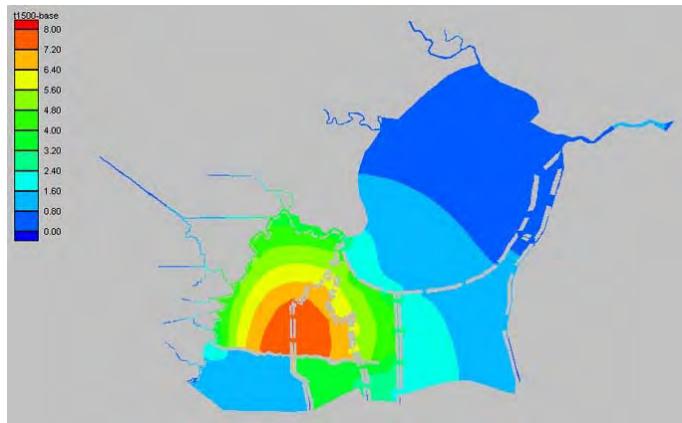


(d) 2500 cfs

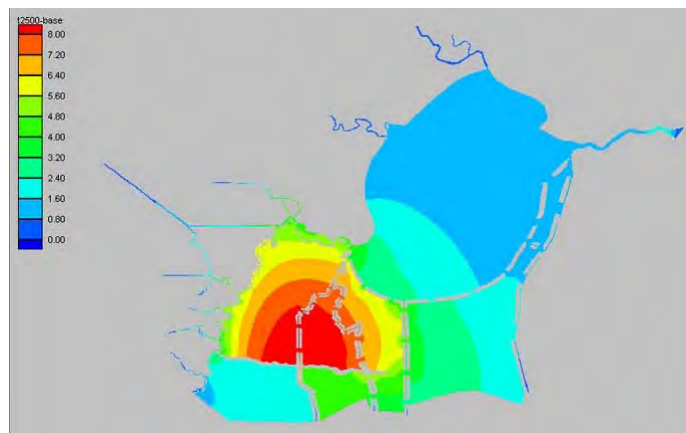
Figure 4.12 Predicted influence of diversions on salinity after 2months



(a) 500 cfs

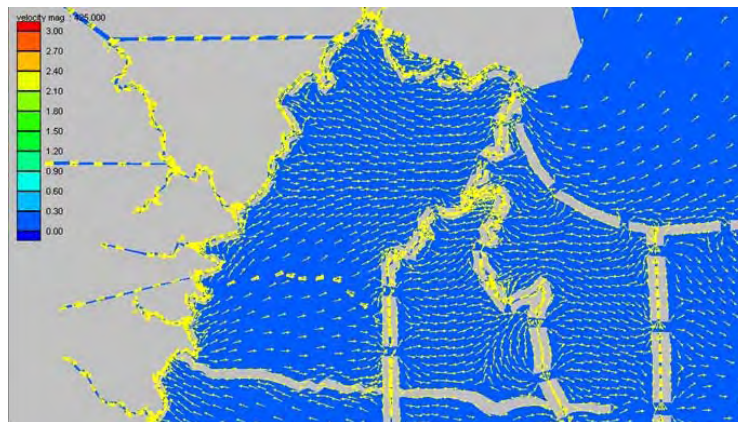


(b) 1500 cfs

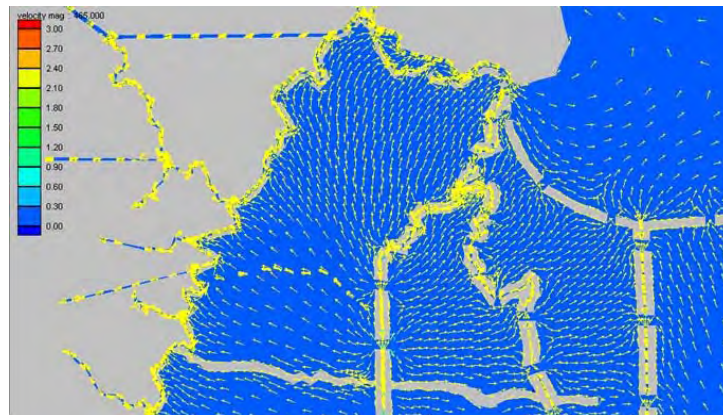


(c) 2500 cfs

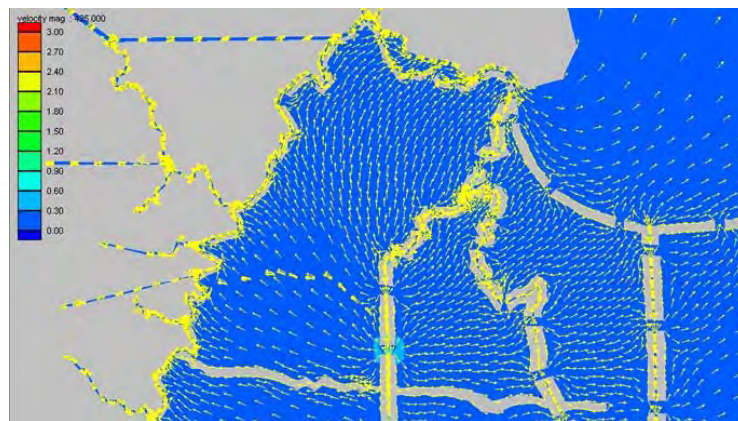
Figure 4.13 Predicted influence of diversions on conservative tracer transport after 1 month



(a) 500 cfs



(b) 1500 cfs



(c) 2500 cfs

Figure 4.14 Predicted flow direction and velocity at in the swamp.

Table 4.3. River influence after 2 months at Shaffer et al. (2003) stations from tracer (10 ppt) introduced with river water for 500, 1500 and 2500 cfs discharges.

Site	Class	Elevation (ft)	CI	% Flood	Base Depth (ft)	%	%	%
						Tracer 500	River Tracer 1500	River Tracer 2500
1	Interior	1.28	77	51	0.31	26	57	69
5	Through	1.09	57	70	0.42	13	35	47
6	Interior	1.14	22	65	0.38	17	44	58
7	Interior	1.28	83	51	0.31	19	47	60
8	Intermediate	1.04	13	75	0.44	18	47	62
9	Interior	1.24	16	55	0.32	36	70	80
10	Through	1.14	13	65	0.37	40	73	82
11	Through	1.15	10	64	0.37	57	81	84
12	Through	1.29	3	50	0.29	14	36	49
14	Intermediate	1.25	4	54	0.33	14	37	52
15	Intermediate	1.01	19	78	0.44	25	57	71
16	Intermediate	1.22	14	57	0.34	7	21	32
17	Lake	1.13	115	66	0.33	14	38	53
18	Lake	1.25	26	54	0.33	4	13	22
19	Lake	1.05		74	0.45	2	9	16
MEAN		(stdev)						
	Lake	1.14(0.10)	71(63)	65(10)	0.37(0.07)	7(6)	20(16)	30(20)
	Intermediate	1.13(0.12)	13(6)	65(13)	0.51(0.06)	16(8)	41(15)	54(17)
	Interior	1.24(0.07)	50(35)	56 (7)	0.33(0.03)	25(9)	55(12)	67(10)
	Through	1.17(0.09)	21(25)	62(8)	0.36(0.05)	31(21)	56(24)	66(20)

4.4 Ecological Forecasting

The hydrodynamic and water quality models that have been developed are too computationally intensive to continuously simulate more than a few months in the prototype. This is adequate to understand the immediate hydrodynamic effects of diversion on water, sediment and nutrient distribution. Such models cannot directly drive an ecological model for a period of 50 to 200 years, the appropriate time-frame over which forest evolution should be evaluated. We have dealt with this problem in two ways. First, we are working on a long-range approach, in which the hydrodynamic and water quality information produced by the models is used to produce probability functions. Second, we have produced a short-term solution based on predicted elevation response to introduced sediment. Both approaches benefit from the land elevation and canopy characteristics that are derived from the LIDAR dataset.

4.4.1 Forest Characteristics from LIDAR. The Canopy Index, a ratio of LIDAR returns from the swamp floor (0 – 1 m) to those from the canopy (greater than 12 m), was mapped for the same sections of the study area that were used to generate the topography (Figure 3.10). The appropriate CI was also assigned to each of the swamp sites (Table 4.2) studied by Shaffer et al. (2003). CI ranged from 2 to more than 140, with the highest values north of the Bourgeois Canal between Hope Canal and the Blind River. The southern more inland half of the study area is characterized by CI values less than 16.

A low CI may indicate relatively healthy conditions for a cypress swamp in winter, in that the canopy greater than 12 m is largely intact. Not enough information is yet available to determine whether a CI threshold can be determined that will distinguish between healthy and stressed forest. The higher CI found along the lake rim probably is indicative of stressed conditions. Along the Blind River, however, where all of the values greater than 80 occur, CI is probably more of an indicator of tupelo dominance. Shaffer et al. (2003) note that tupelo and other deciduous trees contributed 75 percent of the basal area found at the interior sites, with cypress adding only 25 percent for trees greater than 30 cm in diameter. Cypress, which retains leaves year-round, was either dominant or co-dominant with tupelo at all other sites.

4.4.2 Nutrient Assimilation. Information from the models on flow distribution, nutrient concentrations and loading in swamp cells was input to a spreadsheet to predict the rate at which river-derived nitrate leaves the swamp. The 2D hydrodynamic and water quality models provided much better information about dilution, flow rates and paths than was available before. The throughput or escape rate developed can be used to generate a diversion-induced loading for the Lake. The spreadsheet is separated into sections grouping primary cells that receive water directly from Hope Canal, secondary cells outside this radius that receive water leaving the primary cells, and so on through the cascade following Lane et al. (2003). Diversions with discharges of 500, 1500 and 2500 cfs were modeled, and a river nitrate concentration of 1.5 mg L^{-1} was used for all scenarios (Table 4.4).

Table 4.4. Predicted nitrate removal for 500, 1500 and 2500 cfs discharges

Input Characteristics			
Diversion Discharge (cfs)	500	1,500	2,500
Diversion Discharge ($\text{m}^3\text{-s}^{-1}$)	14	42	71
[NO ₃ -N] in River (mg-L^{-1})	1.5	1.5	1.5
Output Routing			
Flow to Blind (cfs)	285	795	1,225
Flow to Lake (cfs)	85	240	375
Flow to Reserve (cfs)	130	465	900
<i>% Total Flow to Blind</i>	<i>57</i>	<i>53</i>	<i>49</i>
<i>% Total Flow to Lake</i>	<i>15</i>	<i>16</i>	<i>14</i>
<i>% Total Flow to Reserve</i>	<i>26</i>	<i>31</i>	<i>36</i>
[NO ₃ -N] entering Blind River (mg-L^{-1})	0.07	0.22	0.31
[NO ₃ -N] entering Lake (mg-L^{-1})	0.05	0.20	0.28
[NO ₃ -N] entering Reserve Canal (mg-L^{-1})	0.00	0.00	0.00
<i>% Removal on Blind River Route</i>	<i>95</i>	<i>85</i>	<i>79</i>
<i>% Removal on Lake Route</i>	<i>97</i>	<i>87</i>	<i>81</i>
<i>% Removal on Reserve Canal Route</i>	<i>100</i>	<i>100</i>	<i>100</i>
<i>Overall Removal Efficiency (%)</i>	<i>99</i>	<i>90</i>	<i>86</i>
Nitrate Throughput to Blind River (kg-d^{-1})	33	423	1,097
Nitrate Throughput to Lake (kg-d^{-1})	0	115	257
Nitrate Throughput to Reserve Canal (kg-d^{-1})	0	0	218
Nitrate Summary			
Total Nitrate to Swamp (kg-d^{-1})	1,835	5,504	9,173
Active Area of Swamp (ha)	10,534	10,534	10,534
Total Nitrate Throughput to Waterbody (kg-d^{-1})	18	550	1,284
Nitrate Retained or Removed in Swamp (kg-d^{-1})	1,817	4,954	7,889
[NO ₃ -N] entering adjacent Waterbody (mg-L^{-1})	0.05	0.15	0.19

Three primary routes were identified with different receiving boundary waters. The shortest route is to the Blind River and is predicted to receive between 57 and 49 percent of diverted water, decreasing as discharge increases. The path directly to the Lake is somewhat longer but is predicted to receive only 15 to 18 percent of discharge. The longest path is to the Reserve Relief Canal, and received between 26 and 36 percent of flow, with the percentage increasing with discharge.

Nitrate loadings in the swamp cells adjacent to Hope Canal range from 0.1 to 0.5 $\text{g m}^{-2} \text{d}^{-1}$ (37–183 $\text{g m}^{-2} \text{y}^{-1}$), relatively high values that will ensure significant swamp benefits (Table 4.5). Removal efficiencies for these cells range from 38 percent for the 2,500 cfs discharge to 68 percent for the 500 cfs input. Concentrations of nitrate entering the next tier of downgradient swamp cells were from 0.5 to 1.0 ppm depending on the path, cell size and the diversion discharge. Loadings in the second tier of cells in the swamp cascade range from 0.01 to 0.2 $\text{g m}^{-2} \text{d}^{-1}$ (37–183 $\text{g m}^{-2} \text{y}^{-1}$), and would experience further reductions of 90 to 50 percent, respectively, for the 500 and 2500 cfs diversions. Nitrate concentrations in water exiting this tier ranged from 0.05 to 0.5 ppm. The minimal reduction in nitrate from Mississippi River concentrations, 79 to 95 percent, occurred along the Blind River route, for the 2500 and 500 cfs diversions, respectively. An 85 percent reduction was predicted for a 1500 cfs diversion, with an exiting concentration of 0.22 ppm. This concentration is higher than that measured in 93 percent of all pre-diversion samples collected, and is more than one standard deviation above the mean (Figure 4.1).

Reductions for the longer paths that the other half of the water follows are greater, from 81 to 97 percent on the Lake route for the 2,500 and 500 cfs discharges, and 100 percent reduction for all discharges along the Reserve Canal path.

The predicted overall removal efficiency for all diversions ranged from 86 percent for the 2500 cfs diversion to 99 percent for a 500 cfs flow. The predicted mean nitrate concentration of all diverted river water leaving the swamp is 0.15 mg-L^{-1} for a 1,500 cfs diversion. This is higher than concentrations measured in 78 percent of samples acquired during the baseline period, but is within one standard deviation of the mean observed in 2002-2003. The 2,500 cfs diversion produced a mean exit concentration of 0.19 mg-L^{-1} . This is greater than values measured in 96 percent of all samples collected, and is slightly more than one standard deviation above the mean (Table 4.4). This analysis supports the earlier finding that a 1,500 cfs diversion will provide a significant nutrient infusion to more than 10,000 ha of nutrient deprived swamp forest, about half of the swamp south of the Lake, while reducing nitrate concentration by 90 percent in transit to essentially background levels.

Seven diversion operation scenarios (A – G) were simulated that produced annual mean discharges ranging from 500 to 2,500 cfs (Table 3.3). Annual loadings were determined for each swamp cell (Table 4.5). Even under the least ambitious scenario (G, 500 cfs), first tier cells experience loadings of $0.05 \text{ g m}^{-2} \text{ d}^{-1}$ ($18 \text{ g m}^{-2} \text{ y}^{-1}$), Second tier cells see loadings in this range in Scenarios A through D (Appendix C).

4.4.3 Long-Term Ecological Simulation. SWAMPSUSTAIN is designed to bridge the gap toward a fully functional IOM ecological model. Progress on the IOM is described in the first section, while SWAMPSUSTAIN results are given in the next. SWAMPSUSTAIN permits assessment today of long-term forest benefits while incorporating realistic spatial and temporal heterogeneity in geometry and hydrology.

4.4.3.1. The Individual Oriented Model Approach. Given that Lake level drives observed flooding and draining of the swamp at tidal and lower frequencies, the hydrograph at any point in the study area is a modified version of the hydrograph observed at the long-term USACE Manchac gage, with the signal damped or lagged by location-specific factors that can be determined from the hydrodynamic model. The input time-series from the Manchac gage can be compared in the frequency domain with the output time-series predicted by the model at any point to develop a covariance function that includes the modification effected by the model. This function can then be used to generate a synthetic water-level time-series at any point from any long-term Pass Manchac input series, no matter how long.

The effect of a diversion on water level at any point is an additional location-specific function of the hydrology that can also be determined as a residual from the model, and superimposed for any operating schedule that might be selected. A synthetic water level time-series might then be constructed with two inputs, the boundary time-series at Pass Manchac, and the schedule of diversion discharge.

Water level at any point can be used to derive the frequency and depth of flooding if the swamp surface elevation is known. These are the easiest of the swamp stressors to predict. Salinity and nutrient-deprivation are more difficult to address rigorously, but some approaches offer promise. First, data presented by Lane et al. (2003) and Shaffer et al. (2003) suggest that the penetration of salinity into the swamp (and into swamp soils) is a low-frequency function of salinity at Pass Manchac modulated by the discharge of the Amite/Blind River system. If Lake Maurepas salinity is today determined by these factors, it would also be modified by diversion discharges. The RMA4 model has been used to test this assumption about Lake salinities (Figure 3.8), but can also provide an indication of how fast the salinity front will advance from Lake Maurepas into the swamp and what spatial gradients are typical. If the forest stress model includes salinity then the Amite/Blind discharge time-series is required, in addition to the two already specified (Manchac water level, Diversion discharge), along with the spatial distribution of salinity for a given salinity at Manchac, or preferably at a station in the Lake.

The abiotic stressors presumably limit tree productivity, and favor some species over others. The IOM could be configured to generate CI index values (eg. Figure 3.10), along with other habitat information, that would allow generalizations from field plot data (eg. Shaffer et al. 2003) to the forest landscape at various times in the future. This analysis suggests a means to develop a long-term ecological forecasting model that preserves the detailed spatial heterogeneity of the landscape, and the influences of that heterogeneity on the hydrology.

Fifty-year time-series of sedimentation and nutrient enrichment, as well as flooding frequency, depth and duration, and salinity for a network of swamp locations, could be derived from hourly observations of water level and salinity at the Manchac gage, the discharge on the Amite/Blind River system and any diversion schedule that might be proposed. This record can then be recycled to provide a synthetic time-series of whatever length is appropriate. Important long-term trends, like that of sea level rise, can be superimposed.

4.4.3.2 SWAMPSUSTAIN – a Sediment-Driven Approach. Rybczyk et al. (1998) found that mineral sediment inputs and effective subsidence rates largely govern coastal forest sustainability when the forest floor is semi-permanently submerged, as in the Maurepas study area. Nutrient inputs became significant in maintaining elevation only when a critical elevation with respect to mean sea level had been attained. The spatial distribution of river-derived sediments above the baselines identified in the water quality study can be derived to a first approximation from the tracer model output. The flow field is used to drive sedimentation and elevation change.

The seven annual diversion discharge scenarios introduced for the nutrient analysis are also applied here (Table 3.3). These scenarios cover the range of possibilities for proposed diversion structure and conveyance channel designs. In the base case, clay-sized river sediment is introduced to Hope Canal north of the I-10 at a concentration of 190 ppm such that 100 ppm is deposited in the first tier of cells (Cells 17, 18, 25, 26 and 33), 50 ppm is deposited in the second tier cells (Cells 16, 27a, 24, 27b, 43, 32, and 41).

25 ppm is deposited in the third tier (Cells 28a, 28b, and 34) and 15 ppm is deposited in the fourth tier (Cells 35, 29 and 21). Mean current forest floor elevations for each cell are calculated from LIDAR data incorporated in the hydrodynamic model. An elevation deficit is calculated for each cell by assuming that the existing forest was established 80 years ago at an elevation of 0.4 ft above local mean sea level, which would now be 1.9 ft NAVD88. Maurepas swamps would be seasonally, rather than semi-permanently flooded, if the forest floor were at this elevation. Calculated deficits ranged from 0.20 to 0.35 cm y⁻¹, averaging 0.29 cm y⁻¹ for the cells considered. These values appear reasonably consistent with a regional RSLR on the order of 0.5 cm y⁻¹, to allow for some organic matter accumulation and for limited mineral sediment inputs from the Lake. These are assumptions tested under the sensitivity program.

SWAMPSUSTAIN distributes mineral sediment inputs through the cells on a monthly basis based on the flow field associated with each level of diversion discharge specified. A sediment deposition loading is calculated for each cell for each month. This deposition is then accumulated over 12 months. A relationship derived from Rybczyk et al. (1998) is used to convert short-term sedimentation to long-term accretion, assuming a logarithmic compaction curve. The base conversion used is 0.24 cm y⁻¹ for every kg m⁻² y⁻¹ deposited, though values from 0.20 to 0.30 were tested. The long-term elevation deficit is subtracted from the long-term accretion to yield a net annual change in elevation for each cell.

Scenarios	Area (ha)	A	B	C	D	E	F	G
<i>Tier 1 Cell 18 (years to target elevation)</i>	664	13	17	26	31	44	74	233
<i>Tier 1 Cell 25 (years to target elevation)</i>	434	17	22	34	41	58	99	339
<i>Tier 1 Cell 26 (years to target elevation)</i>	355	21	28	47	57	85	171	No
<i>Tier 1 Cell 33 (years to target elevation)</i>	485	21	28	44	53	76	132	513
<i>Tier 2 Cell 16 (years to target elevation)</i>	1,026	101	161	502	1277	No*	No	No
<i>Tier 2 Cell 27a (years to target elevation)</i>	469	50	74	166	256	1434	No	No
<i>Tier 2 Cell 24 (years to target elevation)</i>	621	87	128	333	556	No	No	No
<i>Tier 2 Cell 27b (years to target elevation)</i>	364	43	63	129	185	533	No	No
<i>Tier 2 Cell 43 (years to target elevation)</i>	1,186	No	No	No	No	No	No	No
<i>Tier 2 Cell 32 (years to target elevation)</i>	600	No	No	No	No	No	No	No
<i>Tier 2 Cell 41 (years to target elevation)</i>	816	No	No	No	No	No	No	No
<i>Tier 3 Cell 28b (years to target elevation)</i>	894	No	No	No	No	No	No	No
<i>Tier 3 Cell 28a (years to target elevation)</i>	387	No	No	No	No	No	No	No
<i>Tier 3 Cell 34 (years to target elevation)</i>	574	No	No	No	No	No	No	No
<i>Tier 4 Cell 35 (years to target elevation)</i>	298	No	No	No	No	No	No	<i>No</i>
<i>Tier 4 Cell 29 (years to target elevation)</i>	268	No	No	No	No	No	No	No
<i>Tier 4 Cell 21 (years to target elevation)</i>	238	No	No	No	No	No	No	No

* 'No' means cell will never reach sustainability

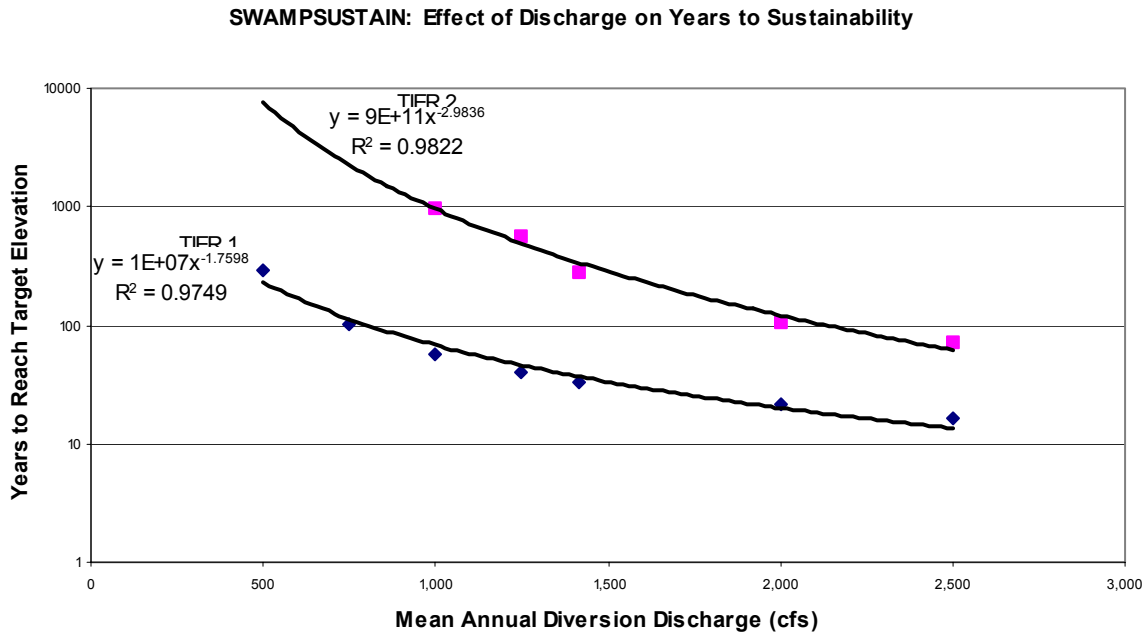


Figure 4.15 Sensitivity of Tier 1 and Tier 2 Swamp Cells to Discharge

Tier 2 cells receive sediment at half the concentration of those in tier 1, but take, on average, ten times longer to reach sustainability. The effect of discharge is apparent on cells in both tiers (Figure 4.15). Were the difference in input sediment concentration between Tier 1 and Tier 2 to increase, so that more sediment is deposited in Tier 1 and less in Tier 2, the two curves would move farther apart. Conversely, if more sediment transited Tier 1 to reach Tier 2, the two curves would move closer together (Figure 4.15). SWAMPSUSTAIN predicts that A, the area restored in hectares for mean annual discharges between 1,000 and 2,500 cfs can be determined as:

$$A = 5.8481e^{0.4745xy - 0.8596}$$

where X is the number of years of diversion operation and Y is the mean annual discharge in cfs.

Scenario D, with a mean discharge of 1,417 cfs, was selected for further sensitivity analysis (Table 4.7). This is a relatively aggressive diversion schedule that would require a structure capable of diverting 2,500 cfs during high river stages. A 50 percent increase in the concentration of sediment entering the system resulted in a 34 percent reduction in the number of years to reach sustainability in Tier 1 cells, but a 62 percent reduction in Tier 2 cells (Figure 4.16). The effect of a 50 percent reduction in the concentration of sediment entering the system was more dramatic, resulting in a 202 percent increase in the number of years to reach sustainability in Tier 1 cells. No Tier 2 cells reached sustainability when input sediment concentration was halved.

Table 4.7 Effect on Years to Sustainability in Tier 1 Cells of Changing SWAMPSUSTAIN Parameters

Parameter	% Change	% Response	Result	Ratio: Response/Change
Increase Sediment Concentration	50	34	Reduce Years	0.68
Reduce Sediment Concentration	50	202	Increase Years	4.04
Reduce Consolidation	50	31	Reduce Years	0.62
Increase Consolidation	50	202	Increase Years	4.04
Reduce Elevation Deficit	50	12	Reduce Years	0.24
Increase Elevation Deficit	50	17	Increase Years	0.34
Reduce Target Elevation	50	35	Reduce Years	0.70
Increase Target Elevation	50	44	Increase Years	0.88

Changing the Rybczyk et al. (1998) consolidation factor had the same effect on years to sustainability as adding or subtracting a comparable percentage of input sediment (Table 4.7). Increasing the consolidation coefficient reduces the consolidation rate and results in greater long-term accretion for each $\text{kg m}^{-2} \text{y}^{-1}$ introduced to the cell (Figure 4.17). The effect of changing sediment input concentration or the effectiveness of deposited sediment to contribute to long-term accretion depends strongly on the direction of the change. A reduction in sediment input or effectiveness (lower consolidation coefficient) results in a far greater effect on years to sustainability than a comparable increase in sediment input (Table 4.7). Any significant decrease in sediment input or increase in consolidation rate generally condemns all Tier 2 cells to never reach sustainability.

Long-term accretion must be greater than the historic elevation deficit for the swamp floor to build up toward the sustainable target elevation. The elevation deficit for each swamp cell is a number derived from a number of assumptions about RSLR, time since sustainability and historic accretion rate. Rybczyk et al. (1998) found that his swamp model was very sensitive to assumptions about RSLR. In SWAMPSUSTAIN, a 50 percent reduction in the elevation deficit resulted in a 12 percent reduction in the number of years to reach sustainability in Tier 1 cells, but a 50 percent reduction in Tier 2 cells (Table 4.7). A 50 percent increase in the elevation deficit caused a 17 percent increase in the number of years to reach sustainability in Tier 1 cells, and a 170 percent increase in Tier 2 cells.

While there is some asymmetry, particularly for Tier 2, the effect of increasing or decreasing the historic elevation deficit on years to sustainability is more uniform and less significant than sedimentation factors.

The effect of increasing or decreasing the distance between current sea level and the target swamp floor elevation is also relatively uniform. A 50 percent decrease in the difference between the target elevation and mean sea level (lowering of target elevation by 0.2 ft) resulted in a 35 percent reduction in the number of years to reach sustainability in Tier 1 cells, and a 50 percent reduction in Tier 2 cells. Increasing the target elevation from 1.9 to 2.1 ft NAVD88 caused a 44 percent increase in the number of years to reach sustainability in Tier 1 cells, and a 111 percent increase in Tier 2 cells.

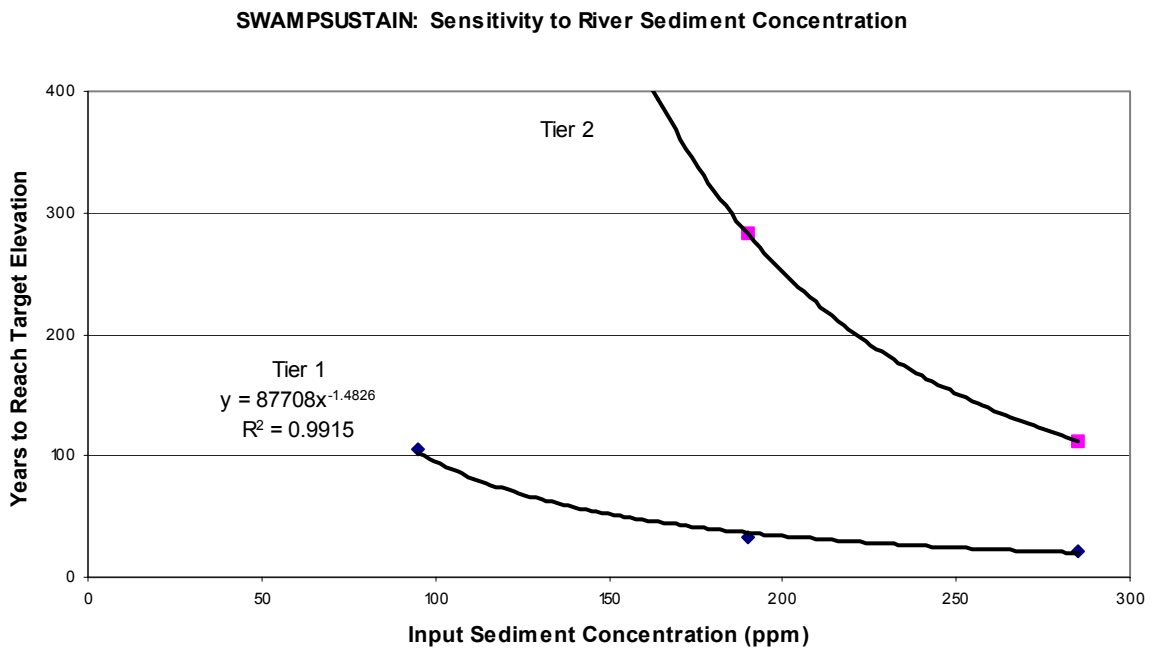


Figure 4.16 Sensitivity of Tier 1 and Tier 2 Swamp Cells to Sediment Concentration

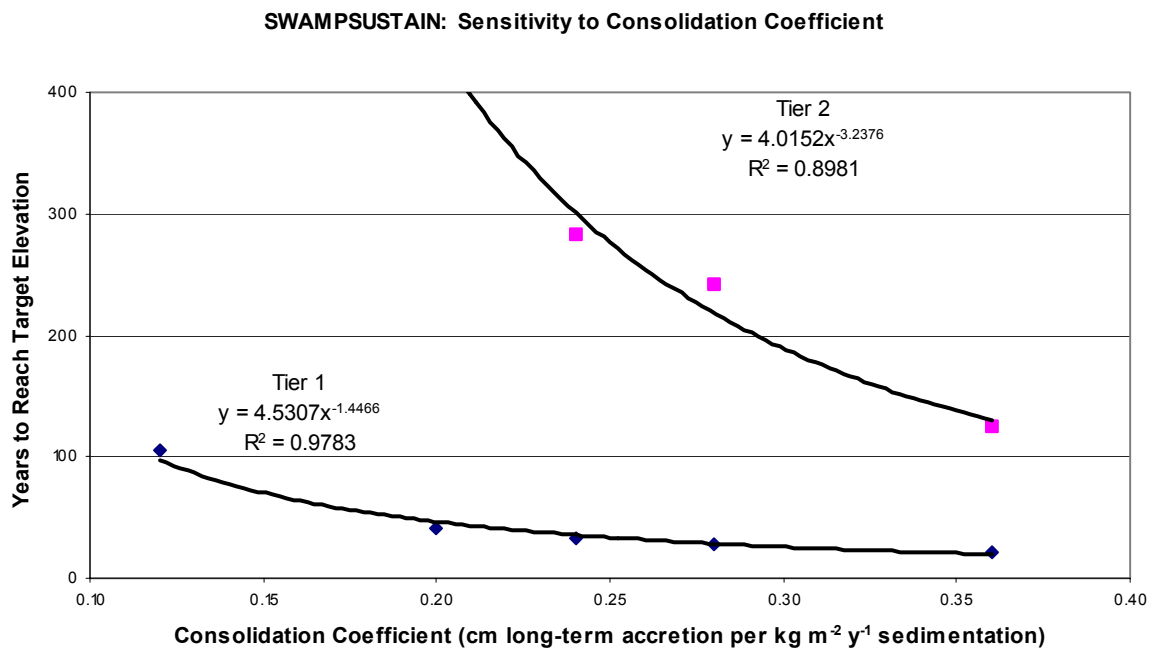


Figure 4.17 Sensitivity of Swamp Cells to Consolidation Coefficient

The period forecast by SWAMPSUSTAIN to be needed for restoration is an exponential function of the area to be restored and the mean annual discharge (Figure 4.18).

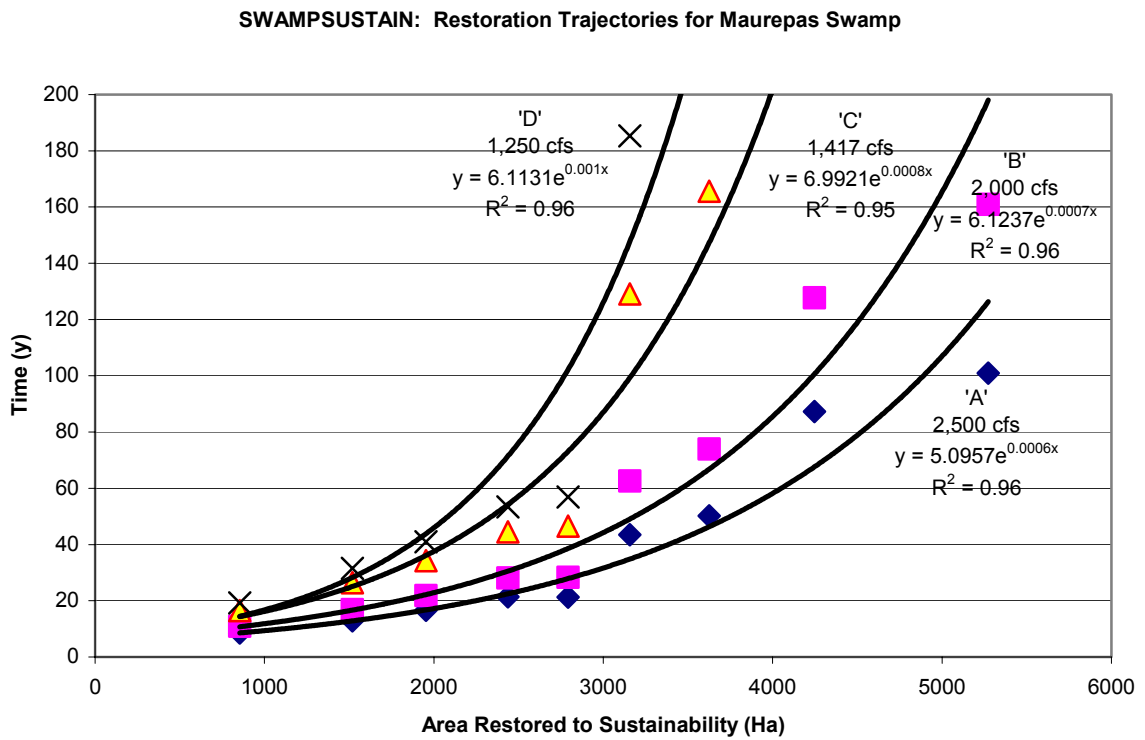


Figure 4.18 Forecast Swamp Restoration Trajectories for Discharge Scenarios A (diamonds), B (squares), C (triangles) and D (X's)

SWAMPSUSTAIN forecasts that a 50-year restoration program has the potential to restore 2,000 to 4,000 ha of the Maurepas swamp.

5.0 CONCLUSIONS

Will it be effective to divert up to 2,500 cfs of Mississippi river water into an estuarine cypress-tupelo (*Taxodium distichum* – *Nyssa aquatica*) swamp with the purpose of saving the trees? The answer to this question involves a complex mix of history, hydrology, chemistry and ecology. EPA funded work to answer this question has been in progress in the Maurepas swamp since 2000.

Critical baseline hydrologic and water quality information was acquired during this study through a field program that lasted nearly two years. Extensive use was also made of information acquired during the drought of 2000. These results were used to calibrate and validate linked hydrodynamic and water quality models. The calibrated models were set up to answer questions about nutrient uptake and the likely response of the forest community to diversions operated at maximum discharges of 500, 1,500 and 2,500 cfs (14, 42 and 71 cms). To improve the linkage to the ecology, all results were reported for specific forest plot locations that have been studied for three years (Shaffer et al. 2003).

Monthly water samples were acquired from April, 2002, to May, 2003 throughout the study area in a pattern established to support the forest ecology work. Samples were analyzed for the constituents of most importance to diversion design, namely suspended sediment, nitrogen, phosphorus, silicate, chlorophyll *a*, and salinity. These provided a baseline for a year of normal rainfall.

Nitrate concentrations at sampling stations ranged up to 0.32 mg-N L^{-1} (ppm), with a mean of 0.09 mg-N L^{-1} . Highest concentrations occurred from November, 2002, to May, 2003, in Lake Maurepas and the Amite River. These were generally higher than observed during the 2000 drought, but even the highest was low relative to concentrations in the Mississippi River (0.75 to 2.0 mg-N L^{-1}). More dissolved inorganic nitrogen in waters of the Maurepas was in the form of ammonium, $\text{NH}_4\text{-N}$, rather than as nitrate in 2002-2003. Ammonium concentrations ranged up to 1.2 mg-N L^{-1} , and averaged 0.40 mg-N L^{-1} . This is an order of magnitude higher than measured during the 2000 drought. The highest ammonium concentrations were measured in the Blind River, Reserve Relief Canal, and at the I-55 canal, probably because of runoff from developed areas. Mean values in the Maurepas are higher than ammonium levels in the Mississippi River that are generally below 0.1 mg-N L^{-1} (Lane et al., 1999). TN concentrations ranged from 0.18 to 1.75 mg-N L^{-1} , with an average of 0.71 mg-N L^{-1} . During the drought, most nitrogen found in the Maurepas was in complex organic forms, such as humic substances, tannins, and phytoplankton. During 2002-2003, however, only half of the nitrogen found in water samples was in the organic form, while ammonium was the predominant dissolved inorganic form. In the swamp interior, nitrogen concentrations are similar to those found in other wetlands along the Louisiana coastal zone that are not receiving river water (Lane et al., 1999; 2002).

Phosphate concentrations ranged up to 411 ug-P L^{-1} and averaged 82 ug-P L^{-1} . Highest concentrations were consistently found at the Airline Highway on Hope Canal.

TP concentrations ranged up to 1077 ug-P L⁻¹, averaging 203 ug-P L⁻¹. These concentrations for phosphate and TP are similar to concentrations in the river (Lane et al., 1999), and are three times higher than observed during 2000.

N:P ratios of 16:1 and greater, higher than the Redfield threshold, were found in individual samples from the Maurepas but were generally confined to the Amite and Blind Rivers. These streams receive runoff from developed areas to the west. Si:N ratios never fell below 1:1. Low N:P and high Si:N ratios are evidence that the Maurepas basin is nearly always nitrogen limited. Introduction of inorganic nitrogen to such a nitrogen-limited ecosystem will support increased plant production, particularly for algae and floating vegetation, even if other nutrients are not increased.

Light Imaging Detection And Ranging (LIDAR) data acquired in 1999 was used to construct the geometry of a receiving swamp that ranges in elevation between 1.0 and 1.8 ft (NAVD88), and averages 1.15 ft. The mean tide elevation, in contrast, is 1.5 ft, meaning that the swamp is inundated more than half of the year. A Canopy Index (CI) created from LIDAR returns from different elevation slices was used to create a map of forest canopy integrity. Results showed the promise of this approach for generalizing from forest plot data to the landscape scale.

TABS finite-element hydrodynamic and water quality models produced predictions of the immediate effects of river water diversion on the swamp and adjacent

water bodies. Water levels were raised generally by less than 0.25 ft under discharge scenarios ranging from 500 to 2,500 cfs and were fully developed in less than one month.

This stage increase was less than estimated earlier. Flow velocities in the swamp for all diversion discharges were predicted to be less than 0.3 fps. A 2,500 cfs diversion reduced Lake Maurepas salinity by 30 percent after only one month, showing one important benefit to a swamp forest that experienced salinities greater than 5 ppt in fall 2000.

The simulated diversion plume, studied using a tracer approach, expanded radially and showed little distortion by topography or channels. This supported earlier expectations about spreading from the relatively inefficient Hope Canal inlet channel. The hydrodynamic model predicted that a little more than half of the diversion discharge flowed west and north through the swamp to the Blind River, with most of the remainder following longer paths to reach Lake Maurepas. Nitrate nitrogen was modeled using a cascade model modified from that of Lane et al. (2003). The model predicted that 99 percent of all nitrate introduced in a 500 cfs diversion with an initial Mississippi River concentration of 1.5 ppm would be retained or removed before it reached the nearest open water boundary. Reduction decreased to 90 percent for a 1,500 cfs diversion, and to 86 percent for a 2,500 cfs discharge. Predicted Nitrate loadings in the swamp cells adjacent to Hope Canal range from 0.1 to 0.5 g m⁻² d⁻¹ (37 to 183 g m⁻² y⁻¹), comparable to rates measured in the Atchafalaya River estuarine complex (Lane et al. 2002) and in experimental wetlands along the Olentangy River, Ohio (Spieles and Mitsch 2000).

Mean nitrate concentration for river water reaching Blind River or the Lake is predicted to range from 0.05 to 0.15 to 0.19 ppm, respectively, for 500, 1,500 and 2,500 cfs diversions. The value for a 1,500 cfs diversion is higher than concentrations measured in 78 percent of samples acquired during the baseline period, but is within one standard deviation of the mean observed in 2002-2003. The mean exit concentration predicted for a 2,500 cfs diversion is greater than values measured in 96 percent of all samples collected, and is slightly more than one standard deviation above the mean. This analysis supports the earlier finding that a 1,500 cfs diversion will provide a significant nutrient infusion to more than 10,000 ha of nutrient deprived swamp forest, about half of the swamp south of the Lake, while reducing transiting nitrate by 90 percent to background levels.

Seven diversion operation scenarios were simulated that resulted in mean annual discharges ranging from 500 to 2,500 cfs. These scenarios cover the range of possibilities for proposed diversion structure and conveyance channel designs. Even under the least ambitious scenario (500 cfs), cells adjacent to Hope Canal experience loadings of $0.1 \text{ g m}^{-2} \text{ d}^{-1}$ ($37 \text{ g m}^{-2} \text{ y}^{-1}$), Second tier cells see loadings of 0.05 to $0.15 \text{ g m}^{-2} \text{ d}^{-1}$ (18 to $55 \text{ g m}^{-2} \text{ y}^{-1}$), in all scenarios with mean annual discharges greater than 1,000 cfs.

The hydrodynamic and water quality models are too computationally intensive to continuously simulate more than a few months in the prototype. Such models cannot directly drive an ecological model for a period of 50 to 200 years, the appropriate time-frame over which forest evolution should be evaluated.

SWAMPSUSTAIN was developed to bridge the gap between the hydrodynamic model and a fully functional Individual Oriented Model (IOM).

Rybczyk et al. (1998) found that mineral sediment inputs and effective subsidence rates largely govern coastal forest sustainability when the forest floor is semi-permanently submerged, as in the Maurepas study area. Nutrient inputs became significant in maintaining elevation only when a critical elevation with respect to mean sea level had been attained. The spatial distribution of river-derived sediments above the baselines identified in the water quality study was derived from the tracer model output. The flow field drives sedimentation and elevation change for the seven annual diversion discharge scenarios introduced for the nutrient analysis.

SWAMPSUSTAIN calculates the years necessary at a given discharge schedule (scenario) for the swamp in each cell to reach 1.9 ft NAVD88, the target elevation for sustainability. The model predicts that first tier cells reach sustainability in 50 years or less for scenarios A through D, with mean annual diversion discharges greater than 1,250 cfs, and in less than 100 years for scenario E (1,000 cfs). Two second tier cells east of Hope Canal are predicted to reach sustainability in less than 100 years for scenarios A

and B with mean discharges greater than 2,000 cfs. Additional cells in the first and second tiers experience long-term aggradation, but cannot be expected to reach sustainability before the existing forest is gone (<100 y). All other second, third and fourth tier cells are predicted to continue to lose elevation under even the most aggressive diversion scenario.

Two to three month pulses of 2,500 cfs flows will be useful for salinity control and sediment introduction, but should not be maintained year-round. Diverting 1,500 cfs will more than double the volume of freshwater reaching Lake Maurepas during average or low flow periods. It will also introduce 5,000 kg a day of nitrogen, along with more than 500,000 kg of sediment, to more than 10,000 ha of low-productivity, nitrogen-depleted swamp forest. On the other hand, another 10,000 ha east of the Reserve Relief Canal will receive only salinity reduction benefits, even for a 2,500 cfs diversion.

SWAMPSUSTAIN predicts that between 2,000 and 4,000 ha of the Maurepas swamp can be restored to sustainability within 50 years if mean diversion discharges greater than 1,000 cfs are initiated. This leaves a substantial portion of the project area that will benefit from salinity control and nutrient addition, but will not be restored to sustainability without additional restoration efforts. The research documented here provides the first rigorous documentation of what the proposed diversion project can be reported to achieve. This understanding permits restoration program planners to consider (1) adding additional Mississippi River diversions up or downstream, and (2) developing other restoration efforts in the project area. Dredging sediments from Lake Maurepas and

pumping them into the swamp, for example, could quickly create additional islands of sustainable wetlands outside the tier of swamp cells adjacent to the proposed Hope Canal diversion.

6.0 ACKNOWLEDGEMENTS

This research was sponsored by the Environmental Protection Agency and funded by the Coastal Wetlands Planning, Protection, and Restoration Act (CWPPRA). We thank Lee Wilson & Associates for involving LSU in this project. We especially thank Anna Hamilton and Lee Wilson for getting things going during the first year of the study in 2000, and Beverly Ethridge, Jeanene Peckham, Wes McQuiddy, Ken Teague, Patricia Taylor, Sondra McDonald, and Troy Hill of EPA for their understanding and excellent review comments. We would like to thank Glen Martin for his generosity in allowing us access to his land and to the Louisiana Department of Wildlife and Fisheries for the help they have provided in the new Manchac Wildlife Management Area. We want to acknowledge the important assistance that Chris Williams of the Louisiana Department of Natural Resources provided in funding additional gaging equipment, and our collaboration with Bob Jacobsen and others at URS, Inc. We would like to thank Emily Hyfield and Chris Bush for their help in the field and laboratory, and Rekha Katragadda, Subhadra Devi Ganti, and Michelle Borne for all their efforts to get the figures right.

7.0 REFERENCES

- Blahnik, T., and Day, J. W. 2000. The effects of varied hydraulic and nutrient loading rates on water quality and hydrologic distributions in a natural forested treatment wetland. Wetlands. 20: 48-61
- Boesch, D. F., M. N. Josselyn, A. J. Mehta, J. T. Morris, W. K. Nuttle. 1994. Scientific assessment of coastal wetland loss, restoration and management. Journal of Coastal Research. Special Issue No. 20
- Boustany, R. G., Croizer, C. R., Rybczyk, J. M., and Twilley, R. R. 1997. Denitrification in a south Louisiana wetland forest receiving treated sewage effluent. Wetlands Ecology and Management. 4: 273-283
- Breaux, A. M. and J. W. Day. 1994. Policy considerations for wetland wastewater treatment in the coastal zone: a case for Louisiana. Coastal Management. 22: 285-307.
- Burnison, B. K. 1980. Modified Dimethyl Sulfoxide (DMSO) Extraction for Chlorophyll Analysis of Phytoplankton. Canadian Journal of Fisheries and Aquatic Sciences. 37:729-733.
- Caffey, R.H., and Schexnayder, M. 2002. Floods, fisheries and river diversions in coastal Louisiana. Proc. Coastal Water Resources Spring Specialty Conf., May 13-15, 2002, Am. Water Res. Assoc., New Orleans, LA.. 301-306.

- Capps, S.A., and Willson, C.S. 2002. Modeling of a Mississippi River diversion into Maurepas swamp. Proc. Coastal Water Resources Spring Specialty Conf., May 13-15, 2002, Am. Water Res. Assoc., New Orleans, LA.. 189-194.
- Cedarwall, H., and Elmgren, R. 1990. Biological effects of eutrophication in the Baltic Sea, particularly the coastal zone. Ambio. 19: 109-112
- Chatry, M., and Chew, D. 1985. Freshwater diversion in coastal Louisiana: recommendations for development of management criteria. 4th Coastal Marsh and Estuary Mgt. Symposium. : 71-84
- Chew, D. L., and Cali, F. J. "Biological considerations related to freshwater introduction in coastal Louisiana." Proceedings of the National Symposium on Freshwater Inflow to Estuaries, Slidel, LA, 367-386.
- Cloern, J. E. 1987. Turbidity as a control on phytoplankton biomass and productivity in estuaries. Continental Shelf Research. 7: 1367-1381.
- Cloern, J. E. 2001. Our evolving conceptual model of the coastal eutrophication problem. Marine Ecology Progress Series. 210: 223-253.
- Conner, W. H. 1993. Artificial regeneration of baldcypress in three South Carolina forested wetland areas after hurricane Hugo. *In* Proceedings of the seventh Biennial Southern Silviculture Research Conference, Mobile, Alabama. USDA Southern Forest Experiment Station, New Orleans, General Technical Report SO-93.

- Conner, W. H., and Day, J. W., Jr. 1988. Rising water levels in coastal Louisiana: implications for two coastal forested wetland areas in Louisiana. *J. Coastal Research* 4: 589-596.
- Day, F. P., and Megonigal, J. P. 1993. The relationship between variable hydroperiod, production allocation and below-ground organic turnover in forested wetlands. *Wetlands* 13: 115-121
- Day, J. W., Britsch, L. D., Hawes, S., Shaffer, G., Reed, D. J., and Cahoon, D. 2000. Pattern and process of land loss in the Mississippi Delta: a spatial and temporal analysis of wetland habitat change. *Estuaries*. 23: 425-438
- Davis, D. W. 2000. Historical perspective on crevasses, levees and the Mississippi River *In* Colten, C. E. (ed.) *Transforming New Orleans and its Environs*. Univ. Pittsburg Press, Pittsburg.
- DeLaune, R. D., Buresh, R. J., and Patrick, W. H. 1979. Relationship of soil properties to standing crop biomass of *Spartina alterniflora* in a Louisiana marsh. *Estuarine and Coastal Marine Science*. 8: 477-487
- DeLaune, R. D., Reddy, C. N., and Patrick, W. H. 1981. Accumulation of plant nutrients and heavy metals through sedimentation processes and accretion in a Louisiana salt marsh. *Estuaries*. 4: 328-334

- DeLaune, R. D., Baumann, R. H., and Gosselink, J. G. 1983. Relationships among vertical accretion, coastal submergence, and erosion in a Louisiana Gulf Coast marsh. Journal of Sedimentary Petrology. 53: 0147-0157
- Dettmann, E. H. 2001. Effect of water residence time on annual export and denitrification of nitrogen in estuaries: a model analysis. Estuaries. 24: 481-490
- Dortch, Q., T. Peterson, and R.E. Turner. 1998. Algal bloom resulting from the opening of the Bonnet Carré Spillway in 1997. In Basics of the Basin Research Symposium, May 12-13, University of New Orleans, Louisiana.
- Faulkner, S. P., and Richardson, C. J. (1989). "Physical and chemical characteristics of freshwater wetland soils." Constructed wetlands for wetland wastewater treatment, D. A. Hammer, ed., Lewis Publishers, 41-72.
- Gleason, M. L., Elmer, D. A., Pien, N. C., and Fisher, J. S. 1979. Effect of stem density upon sediment retention by salt marsh cord grass, *Spartina alterniflora* Loisel. Estuaries. 2: 271-273
- Gornitz, V., Lebedeff, S., and Hansen, J. 1982. Global sea level trend in the past century. Science. 215: 1611-1614
- Greenberg, A. E., R. R. Trussell, L. S. Clesceri, M. A. H. Franson, eds. 1985. Standard Methods for the examination of water and wastewater. American Public Health Association. Washington D.C.

- Gunter, G. 1953. The Relationship of the Bonnet Carre` Spillway to Oyster Beds in Mississippi Sound and the "Louisiana Marsh", with a Report on the 1950 Opening. 70: 22-71
- Hatton, R. S., R. D. Delaune and J. W. H. Patrick. 1983. Sedimentation, accretion, and subsidence in marshes of Barataria Basin, Louisiana. Limnology and Oceanography. 28: 494-502.
- Hoeppner, S. S., K. A. Rose, E. Reyes, and J. W. Day, Jr. 2003. An individual-based modeling approach to predict multiple stressor effects on swamp productivity and forest dynamics in a coastal landscape. Poster, ERF2003, Sept. 14-18, 2003. Seattle.
- Howarth, R. W. 1988. Nutrient limitation of net primary production in marine ecosystems. Ann. Rev. Ecol. 19: 89-110
- Jenkins, M. C., and Kemp, W. M. 1984. The coupling of nitrification and denitrification in two estuarine sediments. Limnology and Oceanography. 29: 609-619
- Justic, D., Rabalais, N. N., and Turner, R. E. 1995. Stoichiometric nutrient balance and origin of coastal eutrophication. Marine Pollution Bulletin. 30: 41-46
- Kesel, R. H. 1988. The decline in the suspended load of the Lower Mississippi River and its influence on adjacent wetlands. Environmental and Geological Water Science. 11: 271-281.

- Kesel, R. H. 1989. The role of the lower Mississippi River in wetland loss in southeastern Louisiana, USA. Environmental and Geological Water Science. 13: 183-193.
- Khalid, R. A. and W. H. Patrick. 1988. Removal of nitrogen and phosphorus by overland flow. Proceedings, National Seminar on Overland Flow Technology for Municipal Wastewater, U. S. Environmental Protection Agency. 219-245.
- Koike, I., and Hattori, A. 1978. Denitrification and ammonia formation in anaerobic coastal sediments. Applied and Environmental Microbiology. 35: 278-282
- Lane, R. R., Day, J. W., and Thibodeaux, B. 1999. Water quality analysis of a freshwater diversion at Caernarvon, Louisiana. Estuaries. 22: 327-336
- Lane, R. R., Day, J. W., Kemp, G. P., and Demcheck, D. M. 2001. The 1994 experimental opening of the Bonnet Carre Spillway to divert Mississippi River water into Lake Pontchartrain, Louisiana. Ecological Engineering. 17: 411-422
- Lane, R. R., Day, J. W., Kemp, G. P., Marx, B., and Reyes, E. 2002. Seasonal and spatial water quality changes in the outfall plume of the Atchafalaya River, Louisiana, USA. Estuaries. 25:30-42
- Lane, R. R., Day, J. W., Jr., Kemp, G. P., Mashriqui, H.S., Day, J.N., and Hamilton, A. 2002b. Potential nitrate removal of the Maurepas swamp Mississippi River diversion. Proc. Coastal Water Resources Spring Specialty Conf., May 13-15, 2002, Am. Water Res. Assoc., New Orleans, LA.. 171-176.

- Lane, R. R., Mashriqui, H. S., Kemp, G. P., Day, J. W., Jr., Day, J. N., and A. Hamilton
2003. Potential nitrate removal from a river diversion into a Mississippi delta
forested wetland. *Ecological Engineering* 20: 237-249.
- Lee Wilson & Associates 2001. Diversion into the Maurepas Swamps, a complex project
under the coastal planning, protection, and restoration act. Final Report to EPA
Region 6, Dallas.
www.epa.gov/earth1r6/6wq/ecopro/em/cwppra/maurepas/a_maur_report2.pdf
- Lindau, C. W., and DeLaune, R. D. 1991. Dinitrogen and nitrous oxide emission and
entrapments in 'Spartina alterniflora' saltmarsh soils following addition of N-15
labeled ammonium and nitrate. *Estuarine, Coastal and Shelf Science*. : 161-172
- LDNR 2003. Caernarvon Freshwater Diversion Project: Annual Report. December,
2003, Louisiana Department of Natural Resources, Baton Rouge.
www.savelawetlands.org/site/Projects/B508/B508_2003AR_1.pdf
- Mashriqui, H.S., Kemp, G.P., Day, J.W., Jr., Lane, R.R. and Cunningham, R. 2002.
Mississippi River diversion into the Maurepas swamp – hydrologic and ecological
modeling. Proc. Coastal Water Resources Spring Specialty Conf., May 13-15,
2002, Am. Water Res. Assoc., New Orleans, LA.. 177-182.
- Mitsch, W. J., J. W. Day, J. W. Gilliam, P. M. Groffman, D. L. Hey, G. W. Randall, N.
Wang, 2001. Reducing nitrogen loading to the Gulf of Mexico from the

- Mississippi River basin: Strategies to counter a persistent ecological problem. BioScience. 51: 373-388.
- Mossa, J. 1996. Sediment dynamics in the lowermost Mississippi River. Engineering Geology. 45: 457-479
- Nixon, S. W., Ammerman, J. W., Atkinson, L. P., Berounsky, V. M., Billen, G., Boicourt, W. C., Boynton, W. R., Church, T. M., Ditoro, D. M., Elmgren, R., Garber, J. H., Giblin, A. E., Jahnke, R. A., Owens, N. J. P., Pilson, M. E. Q., and Seitzinger, S. P. 1996. The fate of nitrogen and phosphorus at the land-sea margin of the North Atlantic Ocean. Biogeochemistry. 35: 141-180
- Nowicki, B. L., Kelly, J. R., Requentina, E., and Keuren, D. V. 1997. Nitrogen losses through sediment denitrification in Boston Harbor and Massachusetts Bay. Estuaries. 20: 626-639
- Pearl, H. W., Pinckney, J. L., Fear, J. M., and Peierls, B. L. 1998. Ecosystem responses to internal and watershed organic matter loading: consequences for hypoxia in the eutrophying Neuse River Estuary, North Carolina, USA. Marine Ecology Progress Series. 166: 17-25
- Pezeshki, S. R. 1990. A comparative study of the response of *Taxodium Distichum* and *Nyssa aquatica* seedlings to soil anaerobiosis and salinity. Forest Ecology and Management. 33/34: 531-541

- Phipps, R. L. 1979. Simulation of wetland forest vegetation dynamics. *Ecological Modeling* 7: 257-288.
- Phipps, R. L., and Crumpton, W. G. 1994. Factors affecting nitrogen loss in experimental wetlands with different hydrologic loads. *Ecological Engineering*. 3: 399-408
- Rabalais, N. N., Wiseman, W. J., and Turner, R. E. 1994. Comparison of continuous records of near-bottom dissolved oxygen from the hypoxia zone along the Louisiana coast. *Estuaries*. 17: 850-861
- Reddy, K. R., and Patrick, W. H. 1984. Nitrogen transformation and loss in flooded soils and sediments. *Critical reviews in environmental control*. 13: 273-309
- Redfield, A. C. 1958. The biological control of chemical factors in the environment. *American Scientist*. 46: 205-22
- Reilly, J. F., Horne, A. J., and Miller, C. D. 2000. Nitrate removal from a drinking water supply with large free-surface constructed wetlands prior to groundwater recharge. *Ecological Engineering*. 14: 33-47
- Richardson, C. J., and Nichols, D. S. (1985). "Ecological analysis of wastewater management criteria in wetland ecosystems." *Ecological considerations In wetlands treatment of municipal wastewaters*, E. R. K. Paul J. Godfrey, Sheila Pelczarski, ed., Van Nostrand Reinhold Company, New York, 351-391.

- Rosenberg, R. 1985. Eutrophication-the future marine coastal nuisance? Marine Pollution Bulletin. 16: 227-231.
- Rybczyk, J. M., Callaway, J.C., and Day, J.W., Jr. 1998. A relative elevation model for a subsiding coastal forested wetland receiving wastewater effluent. Ecological Modeling 112: 23-44.
- Rybczyk, J. M., Day, J.W., Jr., and Conner, W.H. 2002. The impact of wastewater effluent on accretion and decomposition in a subsiding forested wetland. Wetlands 22: 18-32.
- Shaffer, G. P., Thais, E. P., Hoepfner, S., Howell, S., Benard, H., and Parsons, A. C. 2003. Ecosystem Health of the Maurepas Swamp: Feasibility and Projected Benefits of a Freshwater Diversion. Final Report to EPA, Region 6, Dallas. 105pp
- Smith, C. J., DeLaune, R. D., and Patrick, J., W. H. 1983. Nitrous oxide emission from Gulf Coast Wetlands. Geochemica et Cosmochimica Acta. 47: 1805-1814
- Smith, C. J., R. D. DeLaune, and W. H. Patrick. 1985. Fate of riverine nitrate entering an estuary: I. denitrification and nitrogen burial. Estuaries 8: 15-21.
- Speiles, D. J., and Mitsch, W. J. 2000. The effects of season and hydrologic and chemical loading on nitrate retention in constructed wetlands: a comparison of low- and high-nutrient riverine systems. Ecological Engineering. 14: 77-91

- Strickland, J. D. H., and T. R. Parsons. 1972. A Practical Handbook of Seawater Analysis. Bulletin of the Fisheries Research Board of Canada 167
- Suhayda, J. N. 1991. Restoration of wetlands using pipelines transported sediments. GCSSEPM Foundation 12th Annual Research Conference: 257-262.
- 3001, Inc. 2001. Ground Control Survey: LIDAR survey of the Amite River Basin, Louisiana. FEMA Map Modernization Program Phase 1, Task 1 Report to U.S. Army Corps of Engineers, St. Louis District, St. Louis, MO
- Turner, R. E., and Rabalais, N. N. 1991. Changes in Mississippi River water quality this century. BioScience. 41: 140-147
- Valderrama, J. C. 1981. The simultaneous analysis of TN and TP in natural waters. Marine Chemistry. 10: 109-122
- Viosca, P., Jr. 1928. Flood control in the Mississippi Valley and its relation to Louisiana fisheries. Proc. 1927 Convention Am. Fish. Soc., Tech Paper No. 4.
- Wilson, L., Axtman, T., Hamilton, and Hill, T. 2002. Diversion into the Maurepas Swamp – engineering, cost and benefit considerations. Proc. Coastal Water Resources Spring Specialty Conf., May 13-15, 2002, Am. Water Res. Assoc., New Orleans, LA.. 183-188.
- Wilson, L., Hamilton, A., Teague, K., and McQuiddy, W. 2002b. Diversion into the Maurepas Swamp – project history and overview. Proc. Coastal Water Resources

Spring Specialty Conf., May 13-15, 2002, Am. Water Res. Assoc., New Orleans, LA.. 165-169.

Zhang, X., S. Feagley, J. Day, W. Conner, I. Hesse, J. Rybczyk, and W. Hudnall. 2000. A water chemistry assessment of wastewater remediation in a natural swamp. *Journal of Environmental Quality*. 29: 1960-1968

APPENDIX A

WATER QUALITY MEASUREMENTS IN MAUREPAS SWAMP

APRIL 2002 TO MAY 2003

Date	Sample	NH ₄ -N (mg/L)	NO ₃ -N (mg/L)	PO ₄ -P (ug/L)	SiO ₄ -Si (mg/L)	TP (ug/L)	TN (mg/L)	TSS (mg/L)	Sal (PSU)	CHL (ug/L)
5/13/03	1	BDL	0.22		9.81	465.22	0.95	23.30	0.2	26.51
5/13/03	2	BDL	0.09	104.05	11.48	NS	NS	16.10	0.3	74.90
5/13/03	3	BDL	0.10	298.60	4.44	995.49	1.60	9.40	0.1	26.66
5/13/03	4	BDL	0.09		3.62	198.00	1.58	8.30	0.1	26.96
5/13/03	5	BDL	0.10	253.97	3.75	845.78		8.30	0.2	12.47
5/13/03	6	BDL	0.12	310.17	5.48	983.10		10.60	0.2	11.68
5/13/03	7	BDL	0.14	215.44	5.91	771.30	1.00	12.20	0.1	10.16
5/13/03	8	BDL	0.09	280.68	4.96	696.48	0.82	13.30	0.1	30.89
5/13/03	9	BDL	0.10	76.86	10.55	115.77	0.51	12.20	0.1	32.64
5/13/03	10	BDL	0.13	163.29	7.92	191.59	0.61	12.20	0.1	15.47
5/13/03	11	BDL	0.12		9.96	101.74	0.50	16.70	0.1	18.06
5/13/03	12	BDL	0.09	181.50	8.01	145.41	0.62	16.10	0.1	21.32
5/13/03	13	BDL	0.11	184.90	7.55	155.70	0.56	11.10	0.1	23.47
5/13/03	14	BDL	0.10	90.74	4.80	147.47	0.62	45.10	0.2	46.70
5/13/03	15	BDL	0.09	79.57	5.86	115.94	0.69	13.90	0.2	65.08
5/13/03	16	BDL	0.13		8.68	108.45	0.53	34.40	0.1	12.13
5/13/03	17	BDL	0.20		4.78	82.14	0.57	17.20	0.1	14.62
5/13/03	18	BDL	0.18		4.28	100.79	0.58	10.00	0.2	16.73
5/13/03	18				4.39					
5/13/03	19	BDL	0.18	110.73	2.99	98.85	0.56	15.60	0.2	10.55
5/13/03	19	BDL	0.18	109.16		112.51	0.56			

APPENDIX - B

HYDROLOGIC GAGING EQUIPMENT SPECIFICATIONS

Sontek Argonaut -SL

Acoustic Doppler Profiler

The Argonaut-SL (Side-Looking) is designed for horizontal operation, making a remote velocity measurement from an underwater structure (pier, bridge, channel, etc.) while allowing a simple and secure instrument mounting. The Argonaut-SL measures 2D currents in an adjustable measurement volume located at a range up to 120 m. Like the Argonaut-XR, the Argonaut-SL can be used for real-time or autonomous applications.

The Argonauts belong to a class of instruments known as monostatic Doppler current meters. Monostatic refers to the fact that the same transducer is used as transmitter and receiver. A monostatic Doppler uses a set of acoustic transducers with precisely known relative orientations. Each transducer produces a narrow beam of sound perpendicular to the transducer face. The operation of a 3D Argonaut (with three transducers) is shown here.

During operation, each transducer produces a short pulse of sound at a known frequency that propagates along the axis of the acoustic beam. Sound from the outgoing pulse is reflected ("scattered") in all directions by particulate matter in the water. Some portion of the scattered energy travels back along the beam axis to the transducer. This return signal has a frequency shift proportional to the velocity of the scattering material. This frequency change (Doppler shift), as measured by the Argonaut, is proportional to the projection of the water velocity onto the axis of the acoustic beam. By combining data from three beams, and knowing the relative orientation of those beams, the Argonaut measures the 3D velocity. In the same manner, the Argonaut-SL measures 2D velocity in the plane defined by its two acoustic beams.

Doppler technology has several inherent advantages that make it the preferred method for current measurement. Combining this with SonTek's proven ability to develop instruments that are both powerful and easy to use, the Argonaut is the ideal choice for a wide range of applications. Argonaut advantages include:

- Measurements are made in a remote sampling volume free from flow distortion.
- Velocity data are free from drift; the Argonaut never requires calibration.
- Doppler technology has no inherent minimum detectable velocity, giving excellent performance at low flows.
- The Argonaut has no moving parts, is immune to biofouling contamination, and the user can directly apply anti-fouling paint to prevent growth.
- The same robust computational algorithms are used for velocities from 1 cm/s to 10 m/s.

SonTek's user interface allows easy operation with minimal training and experience. First time users can collect test data within minutes of receiving the Argonaut. Deployments require only a few minutes to configure the Argonaut and start collecting data. The basic operating parameters include the following:

averaging time, time between samples, and start time. The Argonaut provides the highest quality Doppler velocity data without requiring the user to become an expert on Doppler technology.

Argonaut velocity data has a specified accuracy of $\pm 1\%$ of measured velocity and ± 0.5 cm/s. These specifications have been verified using laboratory simulations, tow-carriage testing, and field comparisons with other meters. Results from one tow-carriage test are presented here.

An Argonaut was mounted from the bottom of a moving carriage at the Offshore Model Basin (OMB) tow facility in Escondido, California. The meter was towed over a working tank length of 45 m at eight speeds in both directions. Two different mounting orientations were used with no effect on velocity performance. Tow carriage speed at OMB has been independently verified to $\pm 0.5\%$. Results from all runs are shown in the plot below. A least squares linear fit of the velocity data to the carriage speed gives a slope of 0.996 with an offset of 0.1 cm/s.

The Argonaut-SL is designed for current monitoring from underwater structures such as piers, bridges, and channel walls. The two-beam configuration measures the 2D water velocity in a plane defined by its acoustic beams. This is typically the two horizontal components of velocity. Mounted on an underwater structure, the Argonaut-SL measures velocity in a user-programmable sampling volume located up to 120 m from the sensor. Thus it measures the true flow away from any interference generated by the structure, while allowing for easy installation and protecting of the sensor from damage. The Argonaut-SL comes standard with programmable sampling volume size, internal memory, and a temperature sensor. Optional features include an external battery pack, pressure sensor, and integrated CTD.

Standard Features

- User-programmable sampling volume size measured horizontally from the sensor:
 - 3.0-MHz systems - Up to 8 m
 - 1.5-MHz systems - Up to 22 m
 - 500-kHz systems - Up to 120 m
- Supports multiple serial communication protocols:
 - RS232 – Single system operation for short cables (to 100 m)
 - RS422 – Single system operation for long cables (to 1500 m)
 - RS485 – Multiple system operation from a single power and communication cable with total cable lengths to 1500 m
 - SDI-12 communication protocol
- Flexible sampling strategies for reduced duty cycle operation and extended deployments
- 4-MB internal memory (over 200,000 samples)
- Beam angle 25° for near-boundary measurements
- Temperature sensor for automatic sound speed compensation

- Mounting plate for easy installation

Optional Features

- Internal flow calculations
- Multi-cell current profiling
- External battery pack for autonomous operation (alkaline batteries have capacity for 60 days continuous operation)
- Integrated pressure sensor for surface level measurement
- Integrated CTD
- Calculation of wave parameters such as significant wave height and peak period band

YSI 600LS Level Sonde

Conductivity	Range	0 to 100 mS/cm
	Resolution	.001 to .1 mS/cm
	Accuracy	+/- .5% of reading + mS/cm
Temperature	Range	-5 to +45 ° C
	Resolution	.01 ° C
	Accuracy	+/- .15 ° C
Vented Level	Range	0 to 30 ft
	Resolution	.001 ft
	Accuracy	0 to 10 ft, +/- .01ft
Salinity	Range	0 to 70 ppt
	Resolution	.01 ppt
	Accuracy	+/- of reading or .1 ppt, which ever is greater

INFINITIES USA

Water Level Pressure Sensor

The Pressure Water Level Data Logger electronically measures, using a built-in pressure sensor, and digitally records 3,906 water level readings. Any range is available up to 230 feet of water. The user can set the Data Logger to any time interval between recordings, from 1 recording every second to 1 recording per day or greater. When set to record 1 water level measurement per hour, the Data Logger, with integral pressure sensor, can store over 5 months of data before the Data Logger needs to be downloaded. Also, the Data Logger retains up to 31 data sets with different intervals allowing the user to change intervals and download the entire memory or just the memory since an interval was set. A contiguous dump feature allows the user to download only data since the user last downloaded the Data Logger.

The Data Logger's built-in pressure sensor is accurate to +/- 0.1% of the range. Any cable length is available with all sensors. Available pressure sensors are 2 psi (4.5 ft), 5 psi (11.5 ft), 15 psi (34.5 ft), 30 psi (69 ft), 50 psi (115 ft), and 100 psi (230 ft). Resolution is 0.01 inches. The user specifies cable length. The sensor compensates for changes in atmospheric pressure and can be field calibrated for the density of salt water or fresh water.

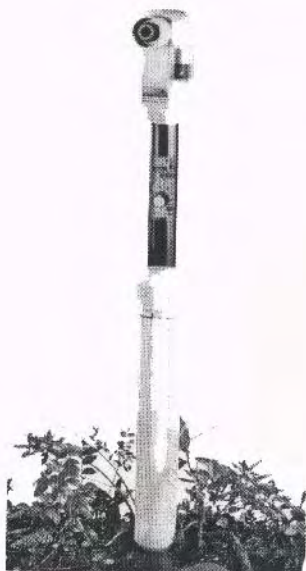
Pressure Water Level Data Loggers can reference any user-defined elevation, positive or negative.

Multi-year power is supplied to the Data Logger by four off-the-shelf AA alkaline batteries. Typical battery life is four years. Data is retained in memory in the absence of power

WL-SERIES PRODUCT SPECIFICATIONS			
	WL-20	WL-40	WL-80
Outside screen diameter	1.9"	3.5"	3.5"
Overall length	55.0"	66.0"	106.0"
Weight	7.0 lbs.	14.5 lbs.	23.0 lbs.
Resolution	0.1"	0.2"	0.4"
Sampling range	0-20"	0-40"	0-80"
Well screen slots	0.01" all models		
Accuracy	+/- 1% full scale all models		
Memory Type:	Non-volatile RAM, with 10 year minimum data retention		
Memory Capacity:	510 data points (0.5k), wrap-around memory		
Sampling Interval Range:	1 Reading/10 seconds to 1 reading/day		

Developing Technology for Environmental Science

[Return to RDS Product Guide](#)



How the WL-Series System Works (WL-20, 40 and 80)

Step 1

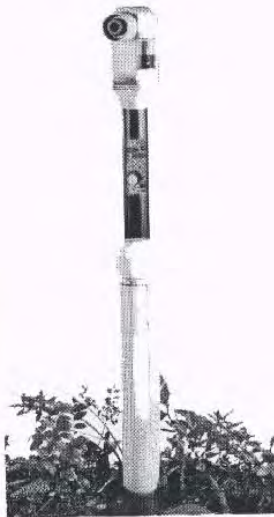
Collection of field data begins once installation and programming of the well has been completed. Simple keystrokes bring up prompted menu selections from the Hewlett-Packard calculator. Position the HP against well infrared optic port and press the appropriate keys to program or download data. Hold HP in place until prompted to release. Data transfer takes seconds.

Step 2

Once the data collection is accomplished, transfer the data to your PC. This is performed after the RDS translator software has been installed in your PC. By using the 4-9 pin connector, and following the instructions outlined in the Users Manual, the collected data can now be transferred to your PC in standard ASCII format. Data management is now possible.

Step 3

Import data files to personal software packages such as Quattro Pro, Excel, and Harvard Graphics to create bar graphs or hydrographs. The data can now be printed out for easy interpretation and inclusion into field reports or project and research documents.



Installation Procedures (WL-20, 40 and 80)

The installation of the WL-Series well is easily accomplished by using a standard hand auger with a 4" bucket for the 3 1/2" well screen found on the WL-40 and 80, or a mud auger for the 1 1/2" diameter well screen found on the WL-20.

We encourage you to follow published technical guidelines established by the WRP for the typical installation of monitoring wells, however it is not necessary for the proper performance of our products.

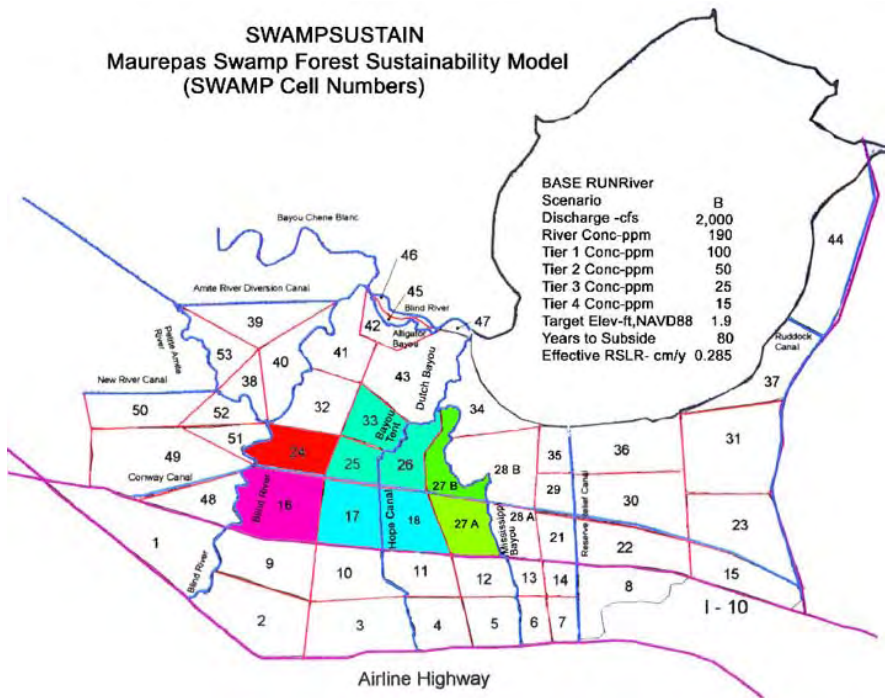
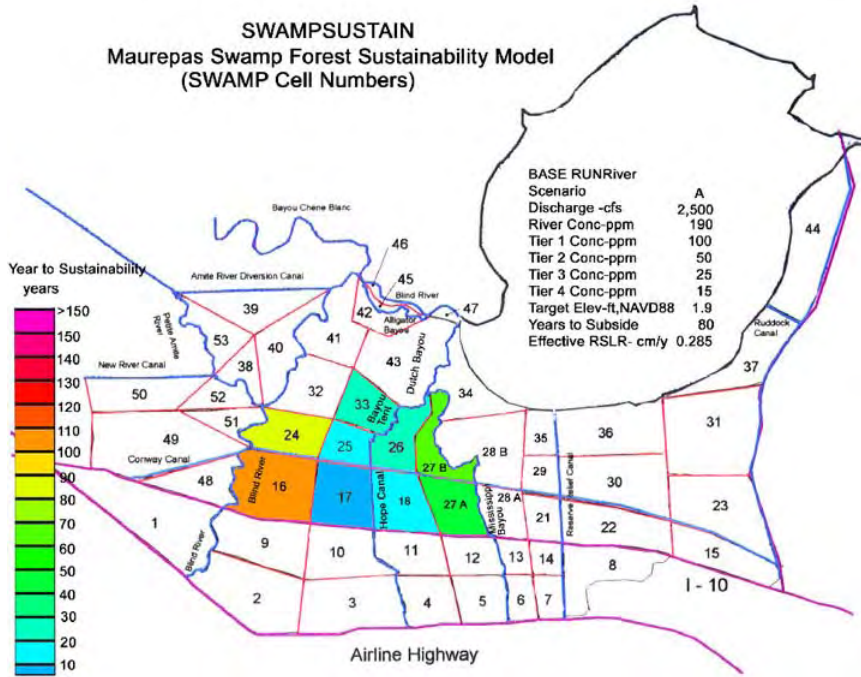
After the borehole has been established, insert the well down to the calibration mark located on the well screen and either backfill the annulus with a washed sand or use native material. It is recommended to seal off around the top of the well annulus with a bentonite clay or clayey native soils to prevent surface water infiltration that could cause erroneous readings.

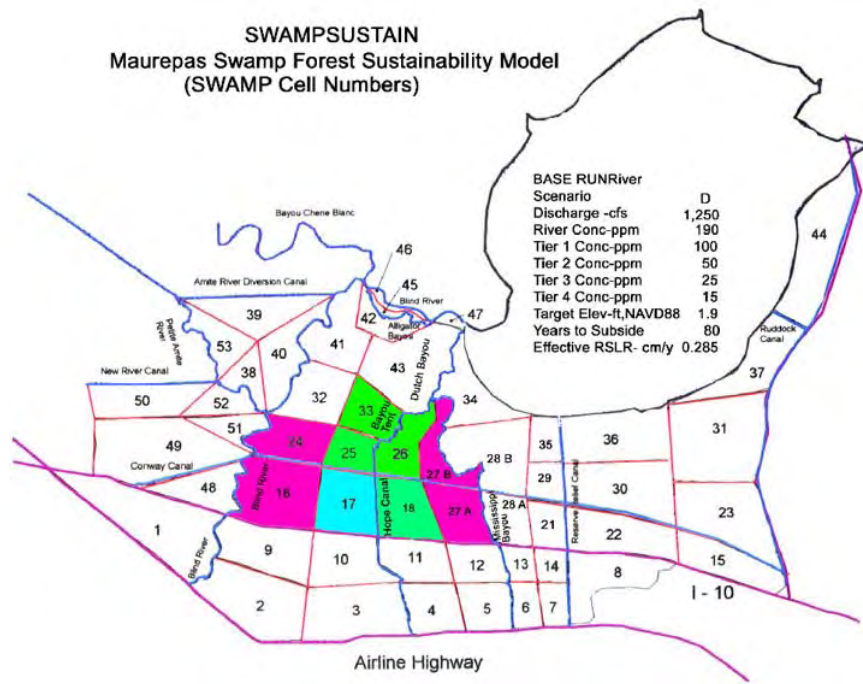
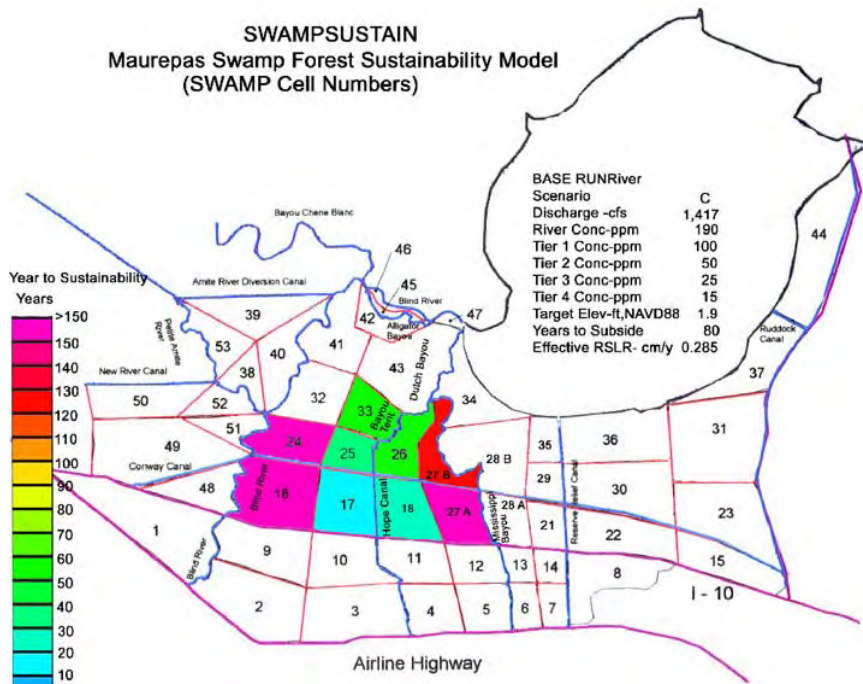
Install the well so the calibration mark is above expected flood elevations to insure complete data capture. The well will not record data if the water surface is above the calibration mark. However, should the well inadvertently become inundated, the battery compartment is protected with a foam seal and offers short term water protection.

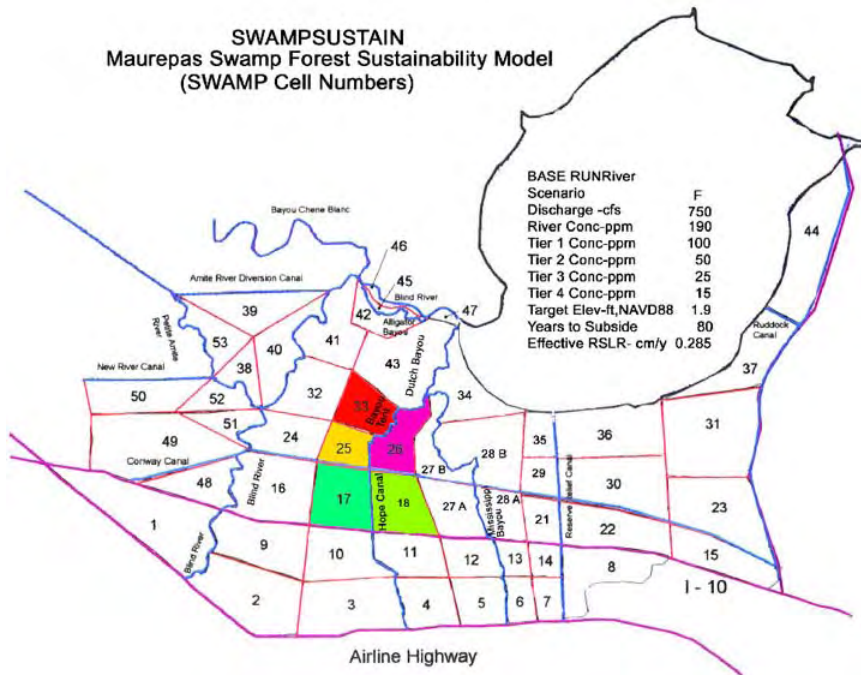
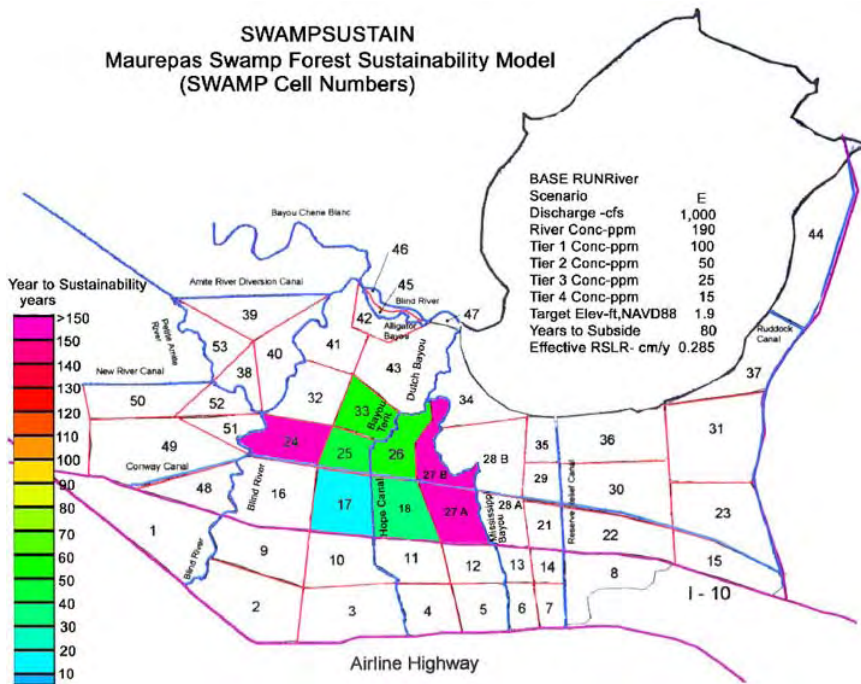
Confirm that the well is activated by downloading and reviewing the data on the HP and replace the vinyl cap to prevent inadvertent battery discharge. To prevent damage from vandalism we offer a canvas camouflage cover that helps hide the well from view. The cover does not offer much physical protection against vandalism, however it will add protection against ultraviolet light and precipitation.

APPENDIX - C

APPENDIX - D







SWAMPSUSTAIN
Maurepas Swamp Forest Sustainability Model
(SWAMP Cell Numbers)

